# The Impacts of Climate Change on The Tualatin River Basin Water Supply

## An Investigation into Projected Hydrologic and Management Impacts

Prepared by

**Richard N. Palmer, PhD, PE**
**Erin Clancy**
**Nathan T. VanRheenen**
**Matthew W. Wiley**
Department of Civil and Environmental Engineering
University of Washington
Box 352700
Seattle, WA 98195-2700

For

**Clean Water Services**
April 21, 2004

tAG
The Alpheus Group

# Executive Summary

This report addresses the potential future impacts of climate change on the Tualatin River Basin and the region's ability to meet current and future water demands. Although there is a growing preponderance of evidence that the earth's climate is changing, the exact type and magnitude of change that will occur in the future in relatively small river basins is not easily estimated. To address this issue, the report presents the results of a series of loosely-integrated models that track the impacts of climate change on precipitation and temperature, on streamflow, and finally, on water management.

## *Impacts on Temperature and Precipitation*

Using the average output of six General Circulation Models of global climate, it is estimated that average monthly temperatures will increase by as much as 2°F by 2040 and as much as 4°F by 2080. The increase in temperatures will be the most dramatic during the winter and summer months. Although average annual precipitation will increase in future decades, this will be due to increased precipitation in the winter months. Summer months, particularly the late summer, will become drier. This will stress the ability of the Tualatin system to meet water temperature standards and maintain instream flows. Figures ES1 and ES2 summarize the predicted impacts of climate change on temperature and precipitation, respectively.

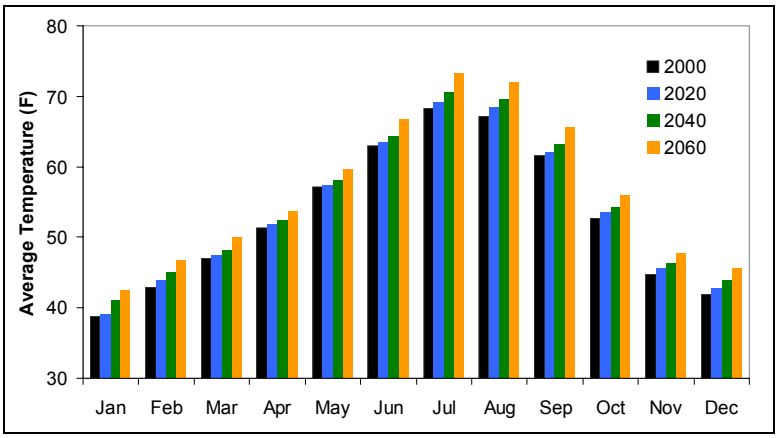


**Figure ES1 - Projected mean monthly temperature in the Scoggins area from 2000 to 2060.**

## *Impacts on Streamflow*

The changes in precipitation and temperature will significantly influence annual streamflow patterns. By 2040, the watershed's average annual runoff will be less than its historic average. In particular, summer streamflows will decrease by between 10 and 20%. The increase in annual and winter precipitation will be overshadowed by increases

in temperature. The increased temperature will increase evapotranspiration and result in much lower late-spring and summer flows. These changes will increase Hagg Lake's drawdown period and decrease the reliability with which future demands can be met. The impacts of climate change on streamflow are summarized in Figure ES3.

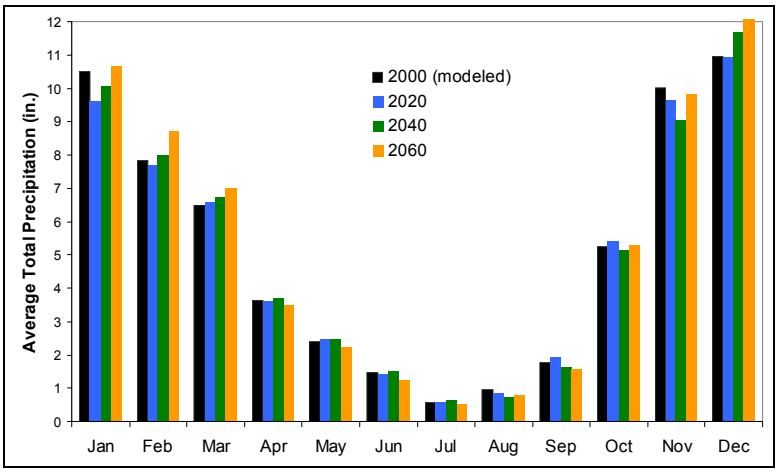


**Figure ES2 - Projected mean monthly Hagg Lake inflows from 2000-2060.**

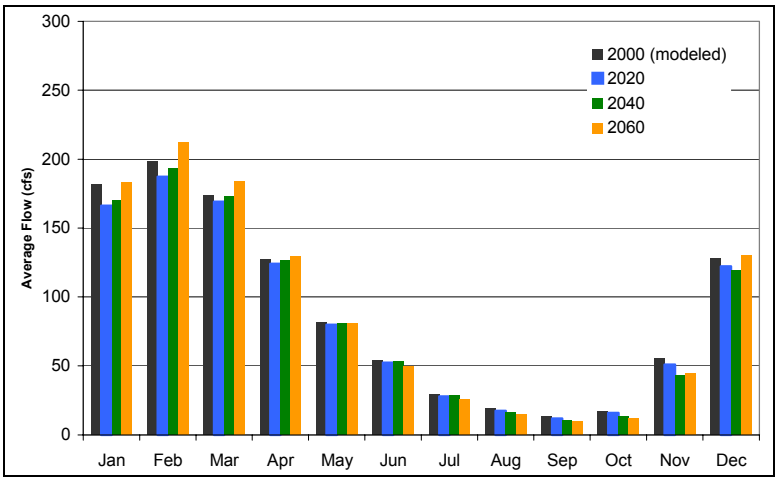


**Figure ES3 - Projected mean monthly Hagg Lake inflows from 2000-2060.**

## *Impacts on System Yield*

During future decades, climate change will consistently and significantly impact on the yield of the water supply system. The yield of the current system is expected to erode by approximately 1.5% per decade during the next forty years. This decrease in yield is relatively consistent for all levels of reliability, whether a 100% or 90% reliable yield is

chosen for analysis. This is particularly important as system demands are expected to increase in the future, and will surpass the system yield. Figures ES4 and ES5 summarize the impacts of climate change on system yield for the current water demands and future water demands, respectively.

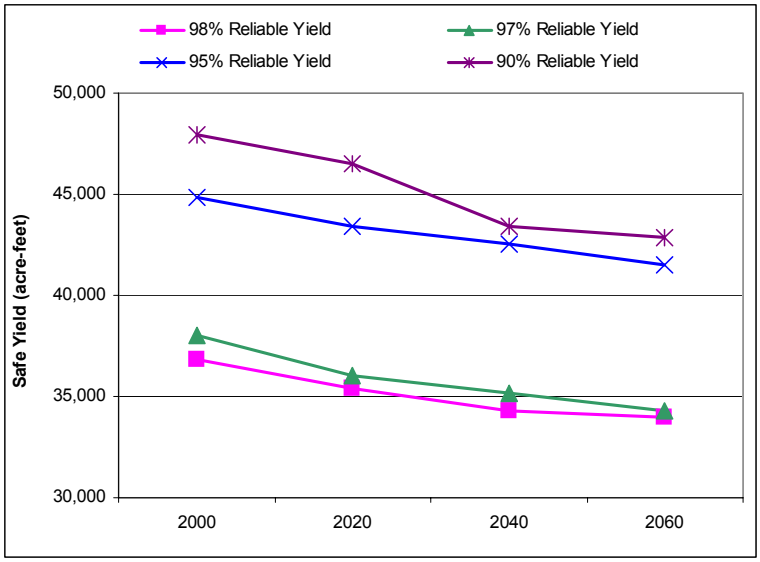


**Figure ES4 - Current Hagg Lake system yield for 2000, 2020, 2040, and 2060 climate periods at four levels of reliability for current demands.**

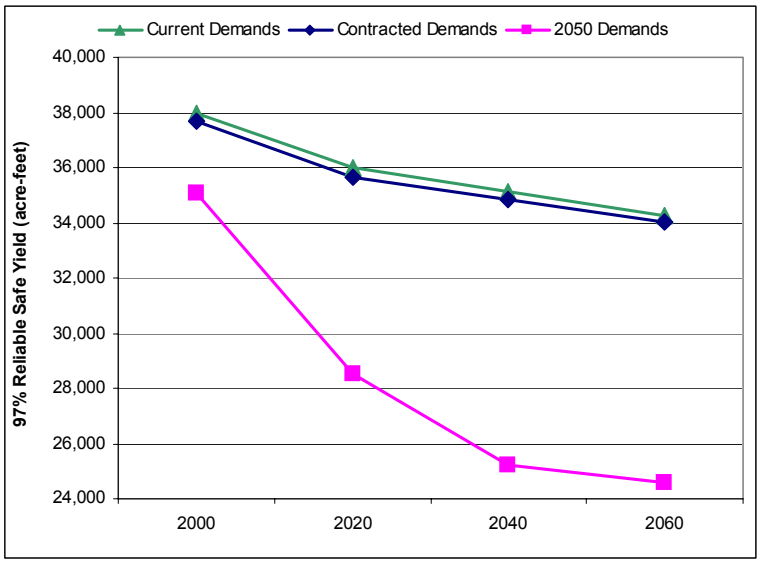


**Figure ES5 - Hagg Lake system yield for 2000, 2020, 2040, and 2060 climate periods for current, contracted, and forecasted 2050 demand scenarios.**

### *System Expansion Alternatives*

Two alternatives were evaluated for increasing system yield: raising the height of Scoggins Dam by 20 feet and raising it 40 feet. If climate change is not considered, these expansions increase the 97% reliable yield from 37,999 acre-ft per year at current levels of demand to 59,428 acre-feet (with the 20-foot expansion) to 73,342 acre-feet (with the 40-foot expansion) (Figures ES6 and ES7).

If climate change projections for 2040 are considered, the expansions will increase the 97% reliable yield from 35,142 acre-feet per year at current levels of demand to 55,713 acre-feet (with the 20 foot expansion) and to 70,628 acre-feet (with the 40 foot expansion), respectively.

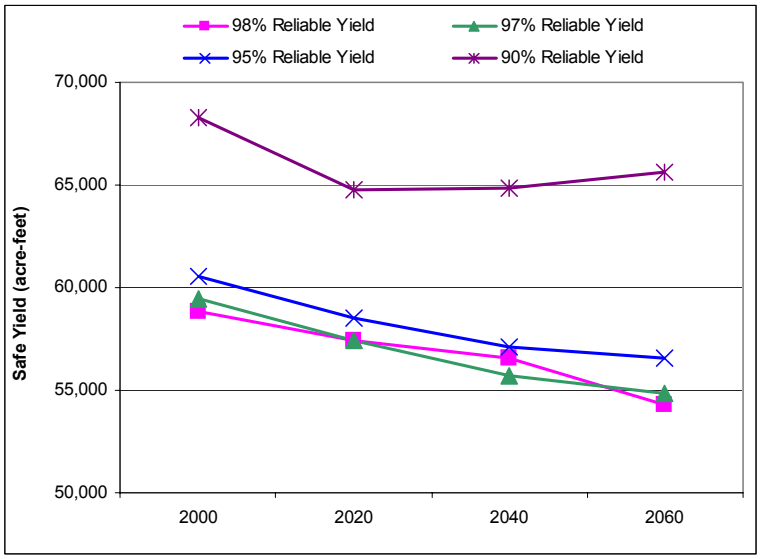


**Figure ES6 - Hagg Lake system safe yield with the 20-foot Scoggins Dam raise for 2000, 2020, 2040, and 2060 climate periods at four levels of reliability.**

The safe yield during the 2060 climate period is greater than the 2040 safe yield for all demand levels. This is due to changes in temperature and precipitation during the 2060 period that results in December-April runoff greater than during the 2000 period and annual volume greater than the 2020 and 2040 periods. Because both expanded systems provide sufficient capacity to begin storing spring runoff earlier without spilling, they are generally less susceptible to changes in runoff timing and volume. This is particularly true for the 40-foot expansion where earlier runoff and greater annual runoff volume in the 2060 period results in a greater safe yield than during the 2020 and 2040 periods (Figure ES7).

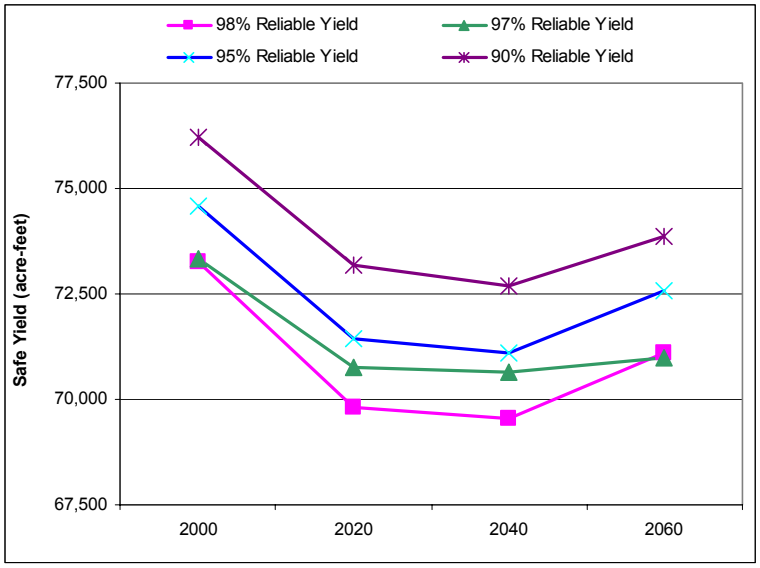


**Figure ES7 - Hagg Lake system safe yield with the 40-foot Scoggins Dam raise for 2000, 2020, 2040, and 2060 climate periods at four levels of reliability.**

### *Timing of System Expansion Alternatives*

If it is desirable to provide sufficient storage to attempt to meet future demands, expansion will be necessary. Without considering climate impacts, and using the 97% reliable yield as a standard, it will be necessary to expand the system by 20 feet by 2013 and to 40 feet by 2043 (Figure ES8). If the impacts of climate change are considered and an equal level of reliability is desired, the 20-foot expansion is needed by 2008 and the 40-foot expansion by 2035. This indicates that the impacts of climate change will increase the time by which the expansions are needed by five to eight years. In the simplest terms, climate change requires expansions of the current system sooner than if climate change did not occur.

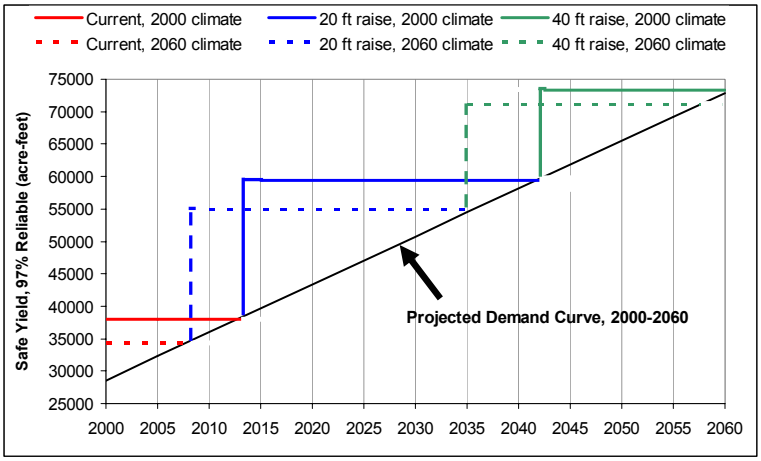


**Figure ES8 - Estimated reliable life span of the current Hagg Lake system and 20-foot and 40-foot Scoggins Dam raise alternatives given projected 2000-2060 demands for 2000, 2020, 2040, and 2060 climate periods.**

## *Nature of Droughts*

As the impacts of climate change are felt and as the system capacity is increased to meet larger demands, the Tualatin basin will encounter dramatically different types of droughts and reservoir operations. Currently, the system refills almost every year, with drawdown periods longer than a year being unusual. If the system attempts to meet increased demands in the future by significantly increasing its capacity, it is anticipated that system refill will become far less likely on an annual basis, multi-year draw-downs will be common, and the impacts of extended droughts may be much more significant. This will be a result of attempting to meet larger systems demands with smaller annual runoff. System management must adjust to deal with these changing characteristics. The development of a well-defined adaptive drought management plan will be essential.

# Table of Contents

**Executive Summary** ..... **ii**
**Table of Contents** ..... **1**
**List of Figures** ..... **3**
**List of Tables** ..... **5**
**1. Introduction** ..... **6**
**2. Tualatin River Basin Setting** ..... **8**
2.1. Hydrology ..... 8
2.2. Management ..... 9
**3. Models and Methods** ..... **13**
3.1. Climate Model ..... 14
3.2. Downscaling ..... 17
3.3. Hydrology Model ..... 24
3.4. Tualatin River Integrated Management Systems Model ..... 29
**4. Model Results—Local Impacts of Climate Change** ..... **39**
4.1. Temperature ..... 39
4.2. Precipitation ..... 42
4.3. Potential Evapotranspiration Function ..... 45
**5. Model Results—BASINS Hydrology Model** ..... **47**
5.1. Hagg Lake Inflows ..... 47
5.2. Distribution of Summer Flows ..... 49
5.3. Sensitivity Testing ..... 49
**6. Model Results - Tualatin River Integrated Management System Model** ..... **51**
6.1. Current System, Current Demands ..... 52
6.2. Current System, Future Demands ..... 52
6.3. Alternative – Raise Scoggins Dam 20 feet ..... 54
6.4. Alternative – Raise Scoggins Dam 40 feet ..... 56
6.5. Alternative Evaluation – Timing of Expansion ..... 58
6.6. Alternative Evaluation – Implications of Raising Scoggins Dam ..... 59
**7. Conclusions** ..... **60**
7.1. Impacts on Temperature and Precipitation ..... 60

7.2. Impacts on Streamflow ..... 60
7.3. Impacts on System Yield ..... 60
7.4. Nature of Droughts ..... 61
**8. References ..... 62**
**Appendix A ..... A1**
**Appendix B ..... A8**
**Appendix C ..... A16**

# List of Figures

Figure 1 - Map of the Tualatin River Basin. ..... 8

Figure 2 - Monthly total precipitation and mean temperature for water years 1984 and 1985. ..... 10

Figure 3 - Hagg Lake active storage during water years 1984 and 1985. ..... 10

Figure 4 - Monthly total precipitation and mean temperature for water years 2000 and 2001. ..... 11

Figure 5 - Hagg Lake active storage during water years 2000 and 2001. ..... 11

Figure 6 - The range of possible global carbon emission scenarios. The *y*-axis represents a ratio of total carbon in year *x* to the total carbon in the year 1990. (Reproduced from IPCC, 2001). ..... 21

Figure 7 - Subbasins in the Tualatin River watershed modeled in BASINS. ..... 25

Figure 8 - Hydrology model calibration procedure. ..... 26

Figure 9 - TRIMS Model schematic. ..... 30

Figure 10 - TRIMS control panel. ..... 35

Figure 11 - TRIMS control panel streamflow and demand selectors. ..... 36

Figure 12 - TRIMS control panel demand manipulator. ..... 37

Figure 13 - TRIMS control panel alternative selector. ..... 37

Figure 14 - Base case increases in mean monthly temperature between historic records and 2000 climate. ..... 40

Figure 15 - Increase in mean monthly temperature between 2000 climate and future climates through 2080. ..... 40

Figure 16 - HadCM3 (a) and PCM (b) predictions of mean monthly increase in temperature. ..... 41

Figure 17 - Projected mean monthly temperature in the Scoggins area from 2000 to 2060. ..... 42

Figure 18 - Ratio of historic precipitation to year 2000 climate precipitation. ..... 43

Figure 19 - Ratio of year 2000 climate precipitation to year 2010-2040 climate. ..... 43

Figure 20 - Ratio of year 2000 climate precipitation to year 2050-2080 climate ..... 43

Figure 21 - Projected mean monthly precipitation in the Hagg Lake area from 2000-2060. ..... 44

Figure 22 - Projected mean temperature and precipitation decadal variation from 2000-2060. ..... 44

Figure 23 - Linear regression of modeled versus observed potential evaporation. $R^2$ = 0.99..... 46

Figure 24 - Relative change in mean monthly Hagg Lake inflows from 2020-2060 based on inflows under the 2000 climate..... 48

Figure 25 - Projected mean monthly Hagg Lake inflows from 2000-2060..... 48

Figure 26 - July-August exceedance curves for mean flows at West Linn on the Tualatin River for 2000, 2020, 2040, and 2060 climate periods..... 49

Figure 27 - Logarithmic plot of mean Hagg Lake inflow under four scenarios: the base case (2000) climate, the 2060 climate, base case rainfall with 2060 temperatures, and base case temperatures with 2060 rainfall. ..... 50

Figure 28 - Current Hagg Lake system safe yield for 2000, 2020, 2040, and 2060 climate periods at four levels of reliability. ..... 52

Figure 29- Hagg Lake safe yield for 2000, 2020, 2040, and 2060 climate periods for current, contracted, and forecasted 2050 demand scenarios..... 53

Figure 30 - Hagg Lake system safe yield when Scoggins Dam is raised 20-feet for 2000, 2020, 2040, and 2060 climate periods at four levels of reliability. ..... 54

Figure 31 - Hagg Lake safe yield when Scoggins Dam is raised 20-feet for 2000, 2020, 2040, and 2060 climate periods for current, contracted, and forecasted 2050 demand scenarios..... 55

Figure 32 - Hagg Lake system safe yield when Scoggins Dam is raised 40-feet for 2000, 2020, 2040, and 2060 climate periods at different system reliabilities. ..... 56

Figure 33 - Hagg Lake safe yield when Scoggins Dam is raised 40-feet for 2000, 2020, 2040, and 2060 climate periods for current, contracted, and forecasted 2050 demand scenarios..... 57

Figure 34 - Estimated reliable life span of the current Hagg Lake system and 20-foot and 40-foot expansion alternatives given projected demands for 2000, 2020, 2040, and 2060 climate periods. ..... 58

Figure 35 - Maximum annual storage of the current Hagg Lake system and 20-foot and 40-foot Scoggins Dam raise alternatives operated at safe yield for the year-2000 climate period..... 59

# List of Tables

Table 1 – Streamflow gauging stations used to calibrate the BASINS model. ..... 27
Table 2 – Digital map layers used to set up the BASINS model. ..... 27
Table 3 – Precipitation gauging stations used to calibrate the BASINS model..... 28
Table 4 - Coefficients of determination for calibration and validation periods..... 29
Table 5 - Hagg Lake flood control space and maximum allowable storage (acre-feet). .. 32
Table 6 - Existing demands (Murdock, 2003). ..... 33
Table 7 - Contracted demands (Murdock, 2003). ..... 33
Table 8 - Forecasted 2050 demands (Murdock, 2003). ..... 34
Table 9 – TRIMS instream flow targets (cfs). ..... 35
Table 10 - TRIMS Model run summary. ..... 38
Table 11 - Monthly coefficients for PET, where PET = (coefficient) * (daily saturated water vapor density). ..... 45
Table 12 - Percent of demand satisfied for each of the demand scenarios in the current Hagg Lake system. ..... 53
Table 13 - Percent of demand satisfied for each of the demand scenarios when Scoggins Dam is raised 20-feet. ..... 55
Table 14 - Percent of demand satisfied for each of the demand scenarios when Scoggins Dam is raised 40-feet. ..... 57

# 1. Introduction

This report evaluates the potential impacts of global climate change on the hydrology and future water availability in the Tualatin River Basin. Historically, the yield of water supply systems has been calculated with the assumption that climate is not changing rapidly enough to impact yield. Based on this assumption, the largest challenges to evaluating yield was the paucity of continuous, long-term streamflow data and accurate water diversion data. Today, however, it is recognized that climate change is having a significant impact on our water resources.

Because of the potential impacts of climate change, it has become necessary to evaluate climate-impacted streamflows when estimating the sustainability of water supplies in the future. This study creates climate-corrected streamflows for water resources planning in the Tualatin River Basin by utilizing recognized climate change scenarios and a novel and freely-available hydrologic modeling tool to predict future climate-induced changes in water runoff and streamflows. These new streamflows are used in a water resources model that is able to predict the future yield of Tualatin River Basin water supplies.

As evidence confirming global climate change continues to grow, the potential impacts of these changes on water resources have become an area of particular concern (Frederick and Major, 1997; Gleick, 2000). In many parts of the world, including much of the United States, the demand for consumptive (water supply) and non-consumptive (navigation, hydroelectric power generation, instream flows) uses of fresh water is approaching the sustainable surface and groundwater sources. Current indicators, including recent findings from the Intergovernmental Panel on Climate Change (IPCC, 1996; IPCC, 2001), strongly suggest that water resources will respond to global warming in ways that will negatively impact both overall supplies and long-term reliability. These impacts will be experienced in a variety of ways, including increased temperatures, changed precipitation, and shifts in the historic hydrologic cycle.

The potential impact of climate change on water supplies in the Pacific Northwest has been of particular interest for nearly a decade (Payne et al., 2004; Hahn et al., 2001; Lettenmaier et al., 1999; Wood et al., 1997). Nash and Gleick's (1993) study of the Columbia River Basin predicts a 1-3% decrease in spring runoff for every degree Fahrenheit increase in temperature. Real potential evapotranspiration (PET) increases in this area were predicted by Lettenmaier et al. (1999) to be 3-4% per decade. However, in each of these cases, the basin being studied derived much of its late spring and early summer water from snowpack. This is not true for the Tualatin River Basin.

There is a significant potential impact of climate change on low-elevation, rain-driven watersheds in the Pacific Northwest, such as the Tualatin River Basin. Net climate change impacts on watersheds include the interactions of such factors as the magnitude of climate change, the physical setting, and degree of sustainable development. It is possible that small shifts in climate (precipitation and temperature) may result in significant hydrologic change. This is particularly true of watersheds that are at or near their sustainable level of use.

In a rain-driven watershed such as Tualatin, long-term changes in precipitation levels will impact the water budget. If winter precipitation increases and summer precipitation decreases, summer low flows and droughts will become more frequent even if total annual precipitation increases. There is evidence that a greater percentage of total rainfall is arriving during winter storms, rather than falling during moderate events that are more evenly distributed over the year (Karl and Knight, 1998). Increasing temperatures brought on by climate change will also directly impact soil moisture by altering plant metabolism and changing the ecological distribution of plant communities.

General Circulation Models (GCMs) have been developed to quantitatively assess the climate impacts of changes in atmospheric chemistry. Typically, these impacts are characterized as changes in $CO_2$, although most GCMs incorporate the interactions of other important greenhouse gases. By evaluating changes in atmospheric processes forecasts of future climate can be made, and in turn, forecasts can be made concerning future watershed hydrology and water supplies. Although great uncertainty persists in current understanding of climate change impacts at the watershed level, the vulnerability of an agriculture-reliant basin with a small, relatively isolated water supply system necessitates investigation of and long-range planning for the range of likely future water supply scenarios.

This study employs a suite of loosely-linked models to address the potential impacts of climate change in the Tualatin River Basin. These models simulate three components of this process: climate, hydrology, and water supply. This report describes the models that are used, the analysis process, and the results generated for the Tualatin River Basin water supply system. Section 2 describes the geography, climate, and water resources of the study area. Section 3 discusses the suite of models used to predict climate change impacts on hydrology and local water supply. Section 4 presents the expected decadal changes in temperature and precipitation in the basin, compares these differences to natural variability, and evaluates the accuracy of the method used to generate potential evapotranspiration from temperature. Section 5 presents and discusses the results generated by the hydrology model, the estimates of climate change impacts on streamflow in different seasons, and the relative contributions of temperature and precipitation to the overall effect. Section 6 presents and discusses results from the water resources model, the impact of climate change on safe yield, and the ability of two facility expansion alternatives to mitigate this impact. The final section summarizes the results of the three models, explains their significance to water resource management in the Tualatin River Basin, and offers recommendations for planning and management.

# 2. Tualatin River Basin Setting

## 2.1. Hydrology

The Tualatin River Basin is located in northwest Oregon and lies primarily in Washington County, although small portions lie in Yamhill, Tillamook, Clackamas, Columbia, and Multnomah Counties (Figure 1). The watershed has an area of 712 square miles and yields an average of 1 million acre-feet of water each year. Eight major tributaries (Wapato Creek, Scoggins Creek, Gales Creek, Dairy Creek, Rock Creek, McFee Creek, Chicken Creek, and Fanno Creek) provide flows to Tualatin River, which discharges into the Willamette River above Willamette Falls near West Linn.

Most of the watershed is between 100 and 300 feet above sea level. The Tualatin River has natural, geological falls at Ki-a-cut Falls, Haines Falls, Lee Falls, and Little Lee Falls before becoming less steep at 120 feet near Cherry Grove.

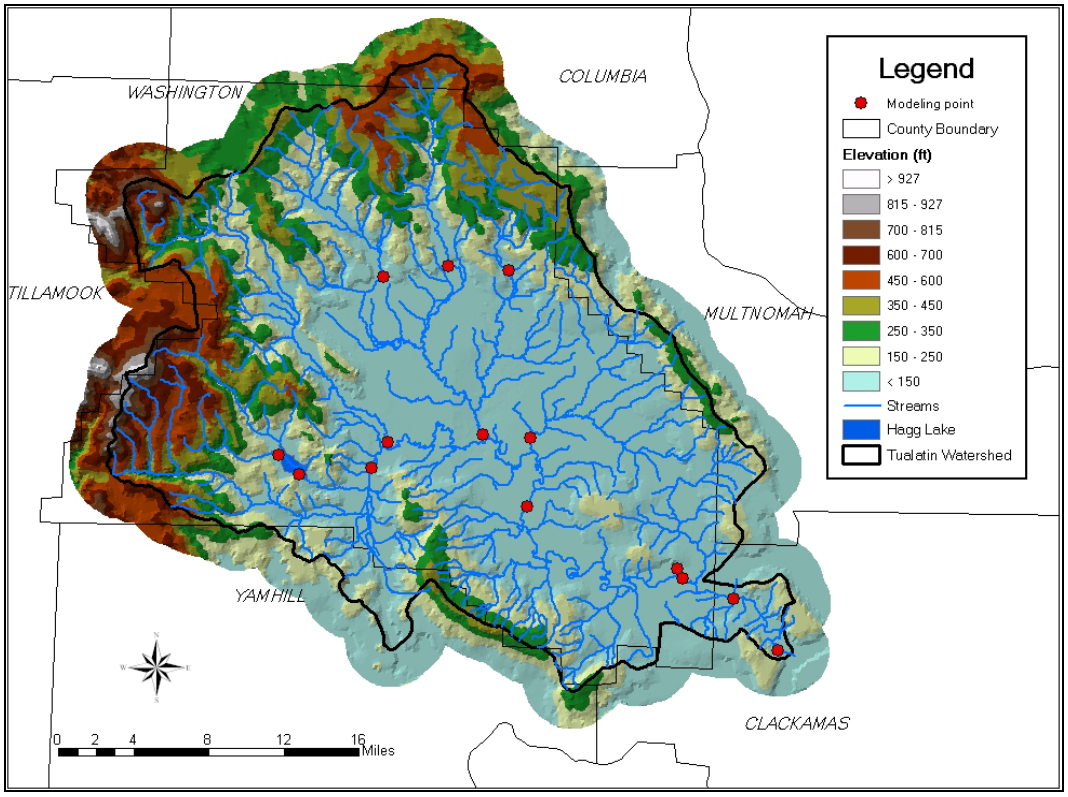


**Figure 1 - Map of the Tualatin River Basin.**

Average annual rainfall ranges from 37 to 110 inches across the basin, with most of the precipitation occurring between November and February. 85% of the total annual flow occurs between November and March, 12% during April and May, and only 3% from June through October. The lowest flows occur in August. The mild climate and low elevation prevent appreciable snow accumulation.

In its natural state, the Tualatin River Basin included large areas of wetlands. Most of these wetlands have since been converted to farmlands and urban development. Urban development has created thousands of acres of impervious surface that is now thought to limit infiltration and decrease summer base flow due to lower groundwater recharge.

The Tualatin's flow during summer is also reduced by irrigation and municipal withdrawals. Water rights on the Tualatin River date back to 1850. The river is now over appropriated during the summer season, with full water rights exceeding average flows. Appropriations also exist on Henry Hagg Lake and on the Tualatin River's tributaries. Although minimum streamflows have been established throughout the basin, they have priority dates of 1963 and 1993. Since streamflows are often insufficient to meet diversion rights established prior to that year (not only in the Tualatin River, but also in its tributaries), these regulations have historically not been enforced, but now are managed.

## 2.2. Management

The Tualatin River was unregulated until 1975. Construction of Scoggins Dam by the Bureau of Reclamation (BOR) on Scoggins Creek and the formation of Henry Hagg Lake provided storage for water to supplement the natural streamflow of the Tualatin River. Hagg Lake has 59,950 acre-foot reservoir of total storage, providing water for irrigation, municipal and industrial (M&I) needs, and environmental purposes. It is operated and maintained under BOR contract by the Tualatin Valley Irrigation District (TVID).

Peak storage in Hagg Lake occurs in April, shortly after the beginning of the irrigation season and the end of the refill period. Since drawdown ends in September and refill may not begin until November, lake levels are at their lowest in October. Hagg Lake refill timing and volume during the spring is largely determined by precipitation and temperature in the previous fall and winter. The 1984 and 1985 water years are characteristic of the typical "normal" year response. Since fall and winter precipitation was normal in both years (Figure 2), Hagg Lake quickly filled to the conservation storage maximum by April 1 and was not drafted below half of active storage during the summer (Figure 3). However, during dry years, as occurred during the 2001 water year, winter and spring precipitation that is lower than normal (Figure 4) results in only partial refill of Hagg Lake during the spring. As a result, summer storage decreases to precariously low levels (Figure 5).

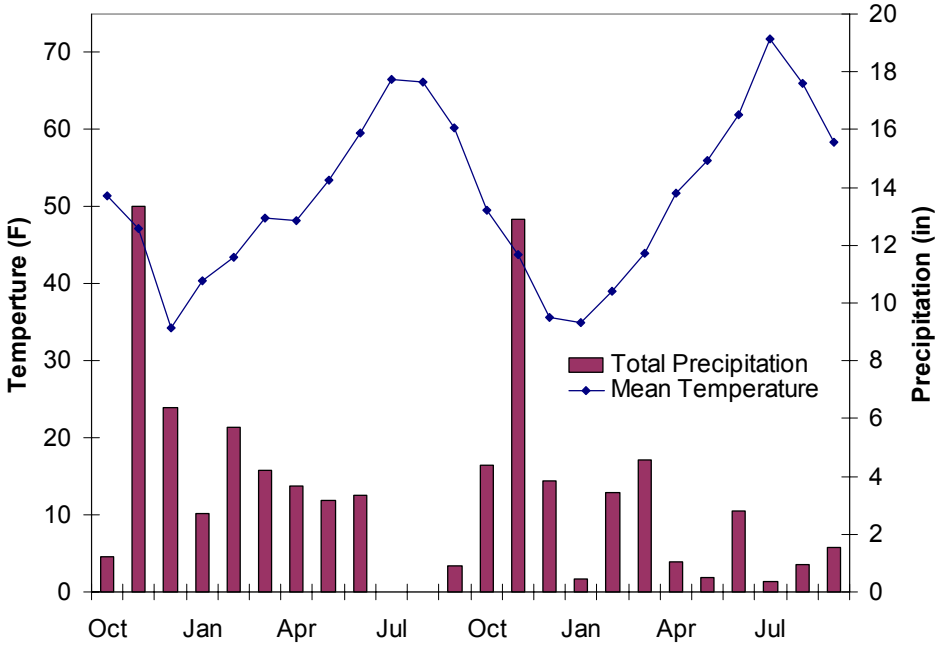


**Figure 2 - Monthly total precipitation and mean temperature for water years 1984 and 1985.**

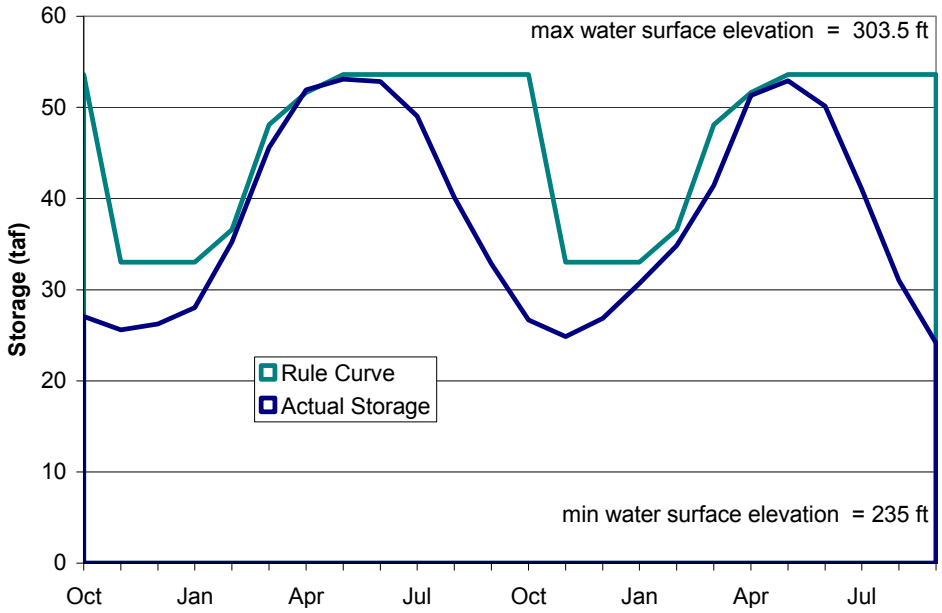


**Figure 3 - Hagg Lake active storage during water years 1984 and 1985.**

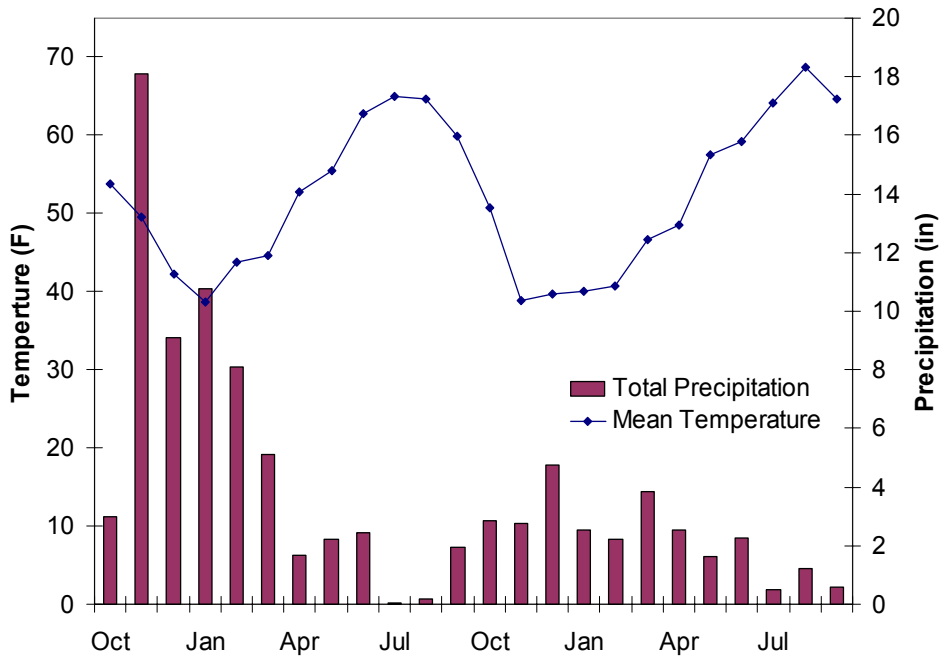


**Figure 4 - Monthly total precipitation and mean temperature for water years 2000 and 2001.**

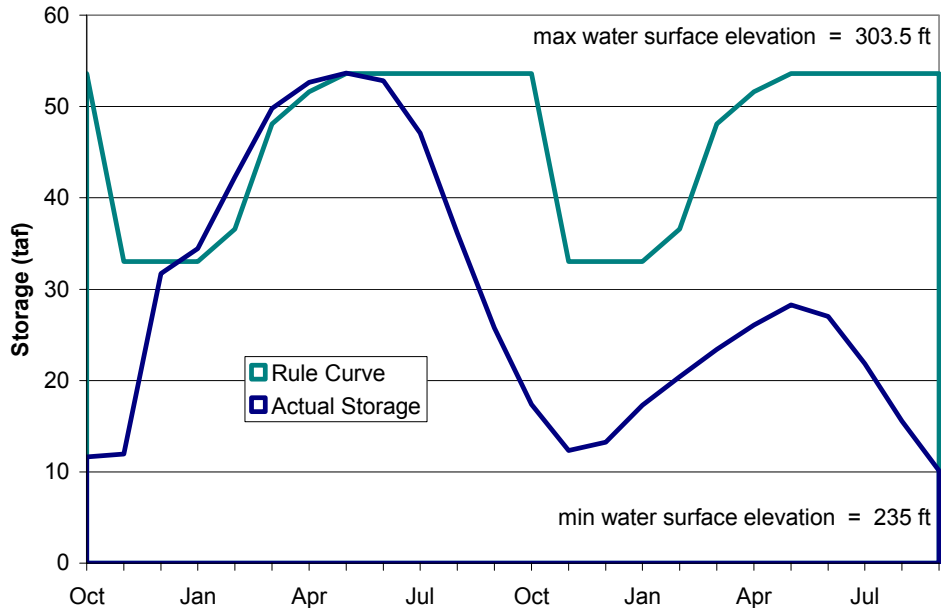


**Figure 5 - Hagg Lake active storage during water years 2000 and 2001.**

Like many reservoirs, Hagg Lake has multiple purposes. Scoggins Dam creates sufficient storage to provide flood control for a 50-year flood event. Hagg Lake serves as the main source of water supply in Washington County. Approximately 50% of the 53,640 acre-feet of active storage is devoted to agricultural use by TVID. Although there

are 17,235 acres of farmland currently assessed, only 17,000 can be served by the Tualatin Project at any one time. Each agricultural user can take up to 2.5 acre-feet per acre of land. When irrigation is not limited by water availability, TVID provides water to two golf courses. 14,000 acre-feet of the remaining active storage is reserved for M&I in Beaverton, Forest Grove, and Hillsboro. These cities also receive water from the Portland Water Bureau from the Bull Run system.

Hagg Lake's remaining water rights are for instream uses. Clean Water Services (CWS) helps maintain water quality, as well as instream flows for fish and wildlife habitat, by allowing controlled releases to flow through the Tualatin River to its mouth. CWS manages 12,618 acre-feet of stored water in Hagg Lake for river flow restoration purposes.

Hagg Lake is complemented by a smaller, non-Federal storage facility that transports released water into the Tualatin River from the Trask River, which is located outside the Tualatin River Basin. Barney Reservoir, formed by Eldon Mills Dam, is a 20,000 acre-foot reservoir that is operated by the city of Hillsboro on behalf of the Joint Barney Reservoir Ownership Commission, which represents TVWD, CWS, Beaverton, Hillsboro, and Forest Grove. Reservoir discharges are transported via an aqueduct into the Tualatin River near its headwaters. The primary use of the reservoir is to supplement M&I water supplies and provide instream flow for fish.

Lake Oswego is located in the city of Lake Oswego and diverts water directly from the Tualatin River at river-mile 6.7 to maintain lake levels for recreation. It is owned and managed by the Lake Oswego Corporation (LOC). A diversion dam located at river-mile 3.4 is used to raise the level of the Tualatin River and provide flows into the headgate. The LOC headgate, located 3 miles upstream, regulates the flows into a canal connected to Lake Oswego.

# 3. Models and Methods

Climate change impacts a basin's water supply in various ways. It may alter seasonal temperature and precipitation, shift the timing of streamflow runoff, and erode the ability of existing supplies to meet water needs. In this research, the dynamics of these interactions are captured by using a family of loosely-connected models to generate a forecast of future water supply in the Tualatin Basin.

The first models used to evaluate climate change are General Circulation Models (GCMs), which examine the impacts of increased greenhouse gases on long-term weather patterns. GCMs represent the complex physical processes occurring in the atmosphere. These models are typically run on supercomputers and are housed and maintained at a small number of national and international research centers. The output of these models includes statistical characterizations of several aspects of the weather, e.g. climate data in different regions of the world, over future periods of time. In this study, several GCMs are used to provide a forecast of the 21st century for an area of land including southwest Washington and most of Oregon. The trends in these forecasts are analyzed and then applied to the historical weather records in the Tualatin River Basin.

The second model used determines the impacts of climate change on regional hydrology. Rainfall/runoff models that translate climatological data into streamflow runoff have been used since the late 1960s. EPA's Better Assessment Science Integrating Point and Nonpoint Sources (BASINS) model was chosen as the most appropriate hydrology model for this study. An initial calibration of the BASINS model was made using topography, soil types, and ground cover and the average annual precipitation at different locations. A simulation using these equations and historical weather records produced values for water storage and streamflow at different spots in the basin. The model was calibrated by comparing these values to measured values and minimizing the difference between modeled values and those taken at gauging stations in the basin. Using the outputs of the GCMs for specific decades in the future, BASINS can be used to generate climate-impacted streamflows.

The third model used in this evaluation is a systems dynamics model of the water supply system. This model simulates the operation of the entire system and tracks flows throughout the river network. At stream confluence points, the water balance is simply the balance from the previous node plus incremental inflows less withdrawals. At reservoirs, storage and release must be characterized as well, based on the dimensions of the reservoir and the seasonal rule curves that have been adopted as official operating policy. This model can be used to calculate the amount of water that can be safely withdrawn from the system, given a particular set of incremental inflows from the simulations in BASINS and reservoir operating policies.

## 3.1. Climate Model

### 3.1.1. Introduction to General Circulation Models

General circulation models (GCMs) describe the global climate system, representing the complex dynamics of the atmosphere, oceans, and land with mathematical equations that balance mass and energy. By simulating interactions among sea ice, land surface, atmospheric chemistry, vegetation, and the oceans, they predict future climates, characterized by temperature, air pressure, and wind speed. Because these models are so computationally intensive, they can only be run on supercomputers at large research institutes. However, the results are made available to the general scientific community and have so far been used in more than 900 U.S. studies of climate change and its impacts on natural, social, and economic systems (Chalecki and Gleick, 1999).
Each research center that maintains a GCM has developed a unique approach to modeling these complex systems, differing in their levels of resolution and degree of specificity, approach to calculating the exchange of water between the atmosphere and the ocean, inclusion of different patterns of the influx of carbon dioxide into the atmosphere, and representations of other important processes. Hence, the 34 GCMs described by the Intergovernmental Panel on Climate Change produce a wide range of future climate predictions (IPCC, 2001). In addition to the different simulation models, there are also several different standard forcing scenarios, each representing a set of assumptions about population growth, economic and technological development, and sociopolitical globalization.

### 3.1.2. Elements of a General Circulation Model

Modeling involves a process of deciding the scope of what will be included in a model, the model's scale and/or granularity, and the interactions between model components. The most recent generation of GCMs are "coupled models" that include four principal components, each of which is created as an individual model capable of simulating processes in one domain—atmosphere, ocean, land surface, and sea ice. "Couplers" integrate these domains into one unified model by routing the flow of data between components.

A fundamental characteristic of any model is the scale at which it accurately depicts reality. Increasing model resolution often increases its computational demand exponentially. The level of detail for a general circulation model is defined by the number of layers it uses to model the atmosphere and the ocean and its spatial resolution (i.e., the size of the cells in its discretization of those layers). The highest resolution implemented in a GCM to date is 2.8º latitude x 2.8º longitude.

Like other models of complex natural systems, GCMs must be calibrated. Early GCMs did not accurately replicate the current climate and required correction factors called "flux adjustments" (IPCC, 1996). However, these adjustments were viewed as poor solutions in the calibration process because they introduced model uncertainties and violated the conservation of mass and energy. The newest generation of GCMs has eliminated the need for flux adjustment (IPCC, 2001).

After a model is developed and calibrated, it can be used to evaluate alternative scenarios. For climate models, these scenarios are known as "forcing functions." A forcing function represents a future emissions scenario. The purpose of these forcing functions is to estimate the rate at which carbon dioxide and other greenhouse gases will be introduced into the environment. With this information, the GCM calculates the impacts on the concentration and chemical composition of all atmospheric gases. First generation GCMs used the simple assumption of a steady-state atmosphere with some future fixed concentration of carbon dioxide. This approach addresses the consequences of increased levels of greenhouse gases but does not depict the transitional states of the atmosphere as the carbon dioxide level increases. To address this issue, new forcing scenarios were created to depict potential global economic growth and the associated production of greenhouse gases. The IS92a forcing scenario was the first attempt at predicting actual future emissions using established rates of economic and population growth and scientific projections of greenhouse gas emissions (Leggett et al., 1992).

Other scenarios have been created to represent plausible futures for those factors influencing greenhouse gas emissions (SRES, 2000). Of these 40 scenarios the six recommended by the SRES for common use (AIF1, A1T, A1B, A2, B1, and B2) have become the standard used by all GCMs for their forcing functions. Each of the six symbolizes a significantly different politico-economic future. Because of the great difficulty in forecasting global social and economic activities, it is inappropriate to assign likelihood of one story line relative to another (however, the recent downturn in the global economy has encouraged reevaluation of the best baseline scenarios). Although the different scenarios do create different climatic futures, it is important to note that during the next 40 years, the scenarios are basically similar. It is not until the years 2040 and beyond that the scenarios begin to diverge. This is due to the rather large "momentum" already contained in the direction of climate change, due to the generation of greenhouse gases since the industrial revolution.

In addition to all the available choices of GCM and forcing scenario, there are uncertainties related to how best to establish initial conditions in the model runs of the GCMs. This is very important, as small changes in initial conditions can create vastly different final states. To solve this dilemma, scientists create ensemble runs to illustrate plausible futures. The differences between results within a unimodal ensemble are the result of random oscillations in the model dynamics. Multimodal ensembles consist of runs of different GCMs. Differences between results within a multimodal ensemble are the result of biases within the individual models. Use of the ensemble average, rather than the individual GCM outputs, minimizes the effect of model bias on the final results.

### *3.1.3. Study Multimodal Ensemble*

In this study, six of the most commonly used GCMs were selected for analysis: CGCM2 (Flato and Boer, 2001), CSIRO mk2 (Gordon and O'Farrell, 1997), ECHAM4 (Roeckner et al., 1996), GFDL_R30 (Knutson et al., 1999), HadCM3 (Gordon et al., 2000), and DOE PCM (Washington et al., 2000). These models are the most extensively developed

and tested GCMs (Covey et al., 2000). Each has different strengths and weaknesses and none is clearly superior.

The Coupled General Circulation Model, 2nd generation, (CGCM2) was developed by the Canadian Centre of Climate Modeling and Analysis at the University of Victoria in British Columbia. It differs from the first generation in its more accurate representation of sea ice dynamics and ocean mixing. Resolution is 10 layers of 3.8º x 3.8º cells for the atmosphere and 29 layers of 1.8º x 1.8º cells for the ocean. The model's parameterization of atmosphere-land exchange processes is based on bucket hydrology, modified to incorporate multilayer soil temperatures. In the bucket method of hydrologic analysis, the land surface is divided into a grid, and each grid cell is assigned a water capacity. Each grid cell acts like a bucket in that it has a water budget computed by adding gains from snowmelt and precipitation and subtracting losses from sublimation and evaporation. For the scenario used in this study, CGCM2 predicts the second highest (out of the six ensemble GCMs) increase in global mean temperature by 2100 and the third lowest increase in precipitation (IPCC, 2001).

The Commonwealth Science and Industrial Research Organization in Victoria, Australia, created the CSIRO mk2 model. It uses 3.2º x 5.6º grid cells of a 9-layer atmosphere and a 21-layer ocean. The vegetation canopy is a single layer that can absorb or produce water vapor and heat. Precipitation is modeled as rain until it reaches the Earth's surface, at which point it is added to the snow budget if temperatures are below freezing. Soil temperature is tracked in three layers; soil moisture is tracked in two (Kowalczyk et al., 1994). This GCM is the best at reproducing current annual means of terrestrial snow cover and sea ice. On the downside, it relies on flux adjustments for water, momentum, and heat. CSIRO mk2 and CGCM2 were not able to accurately reproduce streamflow hydrographs in a study of Seattle climate impacts currently being completed in this research group (Wiley et al., 2004). Furthermore, CSIRO mk2 was unable to reproduce historic conditions at Seattle area weather stations. Of the models used in this study, CSIRO mk2 predicts the third highest global mean increases in both temperature and precipitation (IPCC, 2001).

The European Center for Medium Range Weather Forecasts, Hamburg, developed a weather forecasting model that was modified into a long-term climate model (ECHAM4) by researchers at the Max Planck Institute in Hamburg. ECHAM4 uses 2.8º x 2.8º grid cells of a 19-layer atmosphere and an 11-layer ocean. The model incorporates water and heat budgets for soil, ice-covered, and snow-covered land. Vegetative effects on land-atmosphere interactions are highly simplified, and heat and water flux adjustments are required. Of the six ensemble models, this one predicts the third lowest increase in temperature and the lowest increase in precipitation (IPCC, 2001).

GFDL R30 was developed by the Geophysical Fluid Dynamics Lab. GFDL R30 uses 14 atmosphere layers with 3.75º x 2.25º grid cells and 18 ocean layers with 1.875º x 2.25º grid cells. Hydrology is modeled using a bucket approach; albedo is computed as a function of snow depth. The model relies on flux adjustments for heat and water. In a study of Seattle climate impacts currently being completed, outputs from the ECHAM 4

and GFDL R30 model created good reproductions of streamflow hydrographs. Predictions for temperature increase are below average; predictions for precipitation increase are above average, but they vary more from year-to-year than in any of the other models (IPCC, 2001).

HadCM3 is one of a series of GCMs developed by the Hadley Centre for Climate Prediction, the division of the United Kingdom's National Meteorological Service that studies climate variability and change. Unlike other GCMs in the HadCM series, it does not rely on flux adjustment. It also includes a complex model of land surface processes, including 23 land cover classifications; four layers of soil where temperature, freezing, and melting are tracked; and a detailed evapotranspiration function that depends on temperature, vapor pressure, vegetation type, and ambient carbon dioxide concentrations (Cox et al., 1999). HadCM3 uses 19 layers of atmosphere with 2.5º x 3.75º grid cells and 20 layers of ocean with 1.25º x 1.25º grid cells. Its predictions for temperature change are average; its predictions for precipitation increase are below average (IPCC, 2001).

The Department Of Energy Parallel Climate Model (DOE PCM) incorporates state of the art algorithms for modeling ocean and sea ice processes and does not use flux adjustments. Land surface processes allow specification of vegetation and soil types at the sub-grid cell level. Resolution is 2.8º x 2.8º for 18 atmospheric layers. The resolution of the 32 oceanic layers increases from 0.67º x 0.67º near the poles to 0.5º x 0.67º near the equator. Its predictions of both temperature and precipitation increases are near the ensemble mean (IPCC, 2001).

## *3.2. Downscaling*

Using GCMs to predict climate change impacts at a regional level has limitations. The resolution at which the models operate is too coarse to include details affecting local weather patterns at the sub-continental scale. Orographic features such as mountains, other thermodynamically influential features (including large lakes or variations in vegetation), and distant climate anomalies such as El Niño, can significantly affect local weather patterns, yet are not represented by the current global-scale models. GCMs effectively reproduce global scale climactic variables; however, research has shown that daily precipitation values and historic trends are not reproduced well (Mearns et al., 1994). Using GCM climate predictions to assess regional changes requires results to be converted to a regional scale that preserves the trends present in the GCM data, but that also reproduces smaller scale weather phenomenon.

The scale of circulation and weather patterns is defined by the area over which these patterns occur. Global (or planetary) scale refers to patterns which cover an area greater than $10^7$ km$^2$ (~3.86 million mi$^2$); regional (sub-continental) scale covers from $10^7$ km$^2$ down to $10^4$ km$^2$ (3860 mi$^2$); local scale patterns are on a scale of less than $10^4$ km$^2$ (IPCC, 2001). Converting global data sets into meaningful regional and local information requires a downscaling process that preserves the trends and patterns in global climate present in the GCM data, while simultaneously incorporating local-scale

information about the spatial and temporal distribution of climate patterns available from the observed historic record. This process can be accomplished by one of several techniques, such as: High and Variable Resolution Atmospheric General Circulation Models (AGCM), Regional Climate Models (RCM), or statistical downscaling. The first two options are computationally intensive, which effectively limits their use in impact analysis studies to the creation of only one or two climate scenarios. Statistical methods have been shown to be as effective in reproducing local scale climate patterns as the dynamic modeling methods (Kidson and Thompson, 1998; Murphy, 1999). Because of their comparable performance, and the computational savings that allow for the incorporation of multiple GCM scenarios, statistical downscaling is the most commonly employed approach for assessments of climate change impacts on water resources.

### *3.2.1. Statistical Downscaling*

Statistical downscaling is a family of techniques for creating regional and local climate variables which are dependent upon global scale variables, but still maintain the observed variability and dependences which arise from local features. Statistical downscaling techniques differ substantially from RCN and high resolution AGCM in that they do not attempt to simulate physical atmospheric processes. Rather, they rely on empirical observation of relationships between climate variables and local phenomena. It is assumed that local weather is grossly dependent upon climatic variables, but may exhibit considerable deviations from regional norms. This relationship is captured through the development of a transfer function which relates the climate variables at different scales. Three additional assumptions which are implicit in any statistical downscaling approach are:

1) The global climate variables are being modeled realistically,
2) The observed empirical relationships which define the transfer functions are valid under all climate conditions, including climate change, and
3) The global variables used in the transfer function are capable of representing the climate change signal.

(IPCC, 2001)

Statistical downscaling techniques are very flexible. The approach, or combination of approaches, used for a particular study can be adapted and modified to best reproduce the weather of the region. It is not possible to demonstrate one downscaling to be superior to the others. The success of an approach is highly dependent upon the characteristics of the region to which it is applied. The best approach is to examine a variety of techniques and determine which will better reproduce the variability and patterns of the region in question (IPCC, 2001).

The benefits of statistical downscaling, as compared to physically-based downscaling techniques, are the relative speed and ease with which local climate variables can be derived. The accuracy of statistical downscaling relies on the accuracy of the input GCM data and the availability and accuracy of historic data from which downscaling

relationships can be developed. In areas with poor historic information, statistical techniques are not appropriate.

### *3.2.2. Downscaling Methodology*

There exist almost as many different downscaling techniques as there are individuals conducting research on the downscaling of climate model outputs. The process of selecting an appropriate method or methods should include several factors: accuracy of values generated at the desired scale, ease of implementation, and general acceptance by the scientific community.

The delta method (Smith and Tirpak, 1989; Lettenmaier and Gan, 1990) is a relatively direct approach to statistical downscaling. GCM-predicted climate variables are used to transform local weather patterns for use as input to a hydrology model. As input, the process requires a GCM-generated representation of both historic and future climate and an actual historic record of the weather which occurred in the area. The GCM representations are at a monthly time step and represent the values aggregated over a large area, typically 2º x 3º. Precipitation and temperature are averaged for each month over the modeled historic time period. Each month of the future climate is then compared to this modeled average value and a difference (also known as the perturbation or delta value) is taken between the predicted future value and the modeled historic average. This difference (in both temperature and precipitation) is then applied to an observed historic record from within the same grid cell from which the perturbation factor was acquired. The general formulas for deriving the perturbation values for precipitation and temperature are given as:

$$P_{future} = \frac{P_{GCM-future}}{P_{GCM-historic}} \cdot P_{historic} \qquad T_{future} = \left(T_{GCM-future} - T_{GCM-historic}\right) + T_{historic}$$

A month is then selected from the observed historic record and is altered so that the aggregated temperature and precipitation for the area match the $P_{future}$ and $T_{future}$ previously calculated.

There are several advantages to this method. First, the approach can be easily implemented. Second, because historic, observed daily values are used to generate the final downscaled values, local spatial and temporal variability are maintained and realistic weather sequences are generated. The disadvantage to this approach is that it limits future weather patterns to those roughly similar to historic. It is likely that a change in climate, such as an increase in monthly average temperature, will have additional effects on daily weather patterns that will not be captured by altering only the temperature and precipitation fields. Climate change effects of rain-day frequency and intensity are poorly captured; however, this method captures the historic climate variations and correlations better than other methods.

The delta approach allows for the creation of climate data sets that represent a steady-state climate condition as a given point in the future while also presenting a probabilistic estimate of future event frequency. A GCM simulation presents a single realization of potential future climate. The delta method takes a slice of time that defines future climate and expands it using historic records so that all the potential variability, as seen on that observed record, is also represented. For this study, steady-state representations of future climate are taken at 20-year intervals from the GCM-based year 2000 conditions through GCM 2060 conditions. The conditions for each period are defined by the 21 years centered on the year (e.g., year 2020 climate is defined by the GCM simulation of 2010-2030). The four steady state representations (2000, 2020 2040, and 2060) are evaluated for each of the six GCMs. The perturbation factors for each month are then averaged across the six GCMs to produce mean monthly ensemble estimates of the climate shifts in each future state. The GCM ensemble perturbation factors are then applied to observed meteorological station data from water years 1941-2002. The final product of the downscaling method is four sets of 62-year records, each representative of potential historic variability and future climate conditions.

### *3.2.3. Uncertainty*

The prediction of climate change impacts on water resource systems relies on a series of models. Each model in the series relies upon simplifying assumptions and contributes an element of uncertainty to the final results. In a series of models each successive model is input with the results from the preceding model. This creates a "cascade of uncertainty" in which each successive step propagates and potentially amplifies the uncertainty from the previous step. The degree of uncertainty can be quantified at some stages, but only estimated qualitatively for others. The degree of uncertainty created by each step in the modeling process is explored below with a discussion of the steps which can be taken to reduce the overall uncertainty of the impact assessment.

### *3.2.4. Uncertainty in the Forcing Scenario*

It is generally assumed that the primary cause of the observed change in global climate is anthropogenic emissions of greenhouse gases. The rate of future emissions is dependent upon complex variables, such as technological development, demographic shifts, and socio-economic forces, all of which contain a high degree of uncertainty (SRES, 2000). Possibilities for future emissions are proposed by the IPCC in the Special Report on Emission Scenarios. This report presents 40 emission scenarios in six distinct families of future development patterns and is intended to cover the range of future possibilities. Figure 6 shows the range of the emission scenarios in terms of global carbon dioxide emitted. All scenarios are considered equally likely and no occurrence probabilities are assigned (SRES, 2000). Every GCM modeling run is based on a future emission scenario. The scenarios are equally probable, yet the results from the different scenarios may differ dramatically. The choice of one emission scenario over another is the first source of uncertainty in climate change impact assessments.

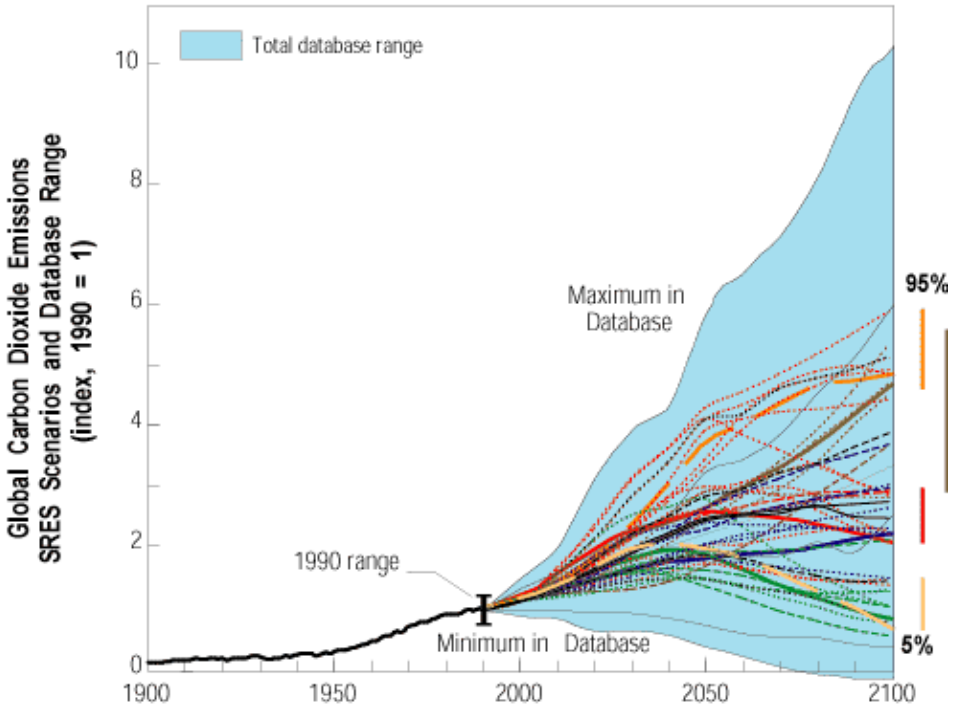


**Figure 6 - The range of possible global carbon emission scenarios. The *y*-axis represents a ratio of total carbon in year *x* to the total carbon in the year 1990. (Reproduced from IPCC, 2001)**

A reasonable method for addressing the uncertainty associated with the prediction of future greenhouse gas emission patterns is to model climate patterns multiple times using multiple emission scenarios which cover the entire range of reasonable future possibilities. This approach has the advantage of addressing a wide range of possibilities, thereby reducing the probability of not modeling the "correct" future. The disadvantage of this technique is that by covering such a wide range of possibilities little insight is gained in terms of the likely impacts to water resource systems. As the range of possibilities examined increases, it becomes more difficult to determine appropriate mitigation strategies.

### *3.2.5. Uncertainty in GCM Output*

At the global scale there is significant agreement among GCM projections of trends in tropospheric variables such as air temperature and geopotential height. Derived climactic variables such as precipitation, relative humidity and cloud cover, show much less agreement and are in general only modeled moderately well. Land surface processes at the regional scale show even greater divergence with little consensus for projected changes in soil moisture content or runoff (IPCC, 2001).

The level of uncertainty in GCM outputs cannot be determined quantitatively and is essentially unknown; however, by using the range of predictions available from all

current generation GCMs, it is possible to determine a lower bound to the uncertainty (Wood et al., 1997).

To reduce the level of uncertainty being propagated from the GCM output to the chosen downscaling technique, it is recommended that the more consistent tropospheric variables (e.g. temperature, geopotential height) be given greater weight in the downscaling methodology than derived variables such as precipitation (IPCC, 2001). However, the inclusion of more GCM output variables as predictors in a downscaling technique has been shown to improve the downscaled precipitation predictions. Several studies (Charles et al., 1999; Hewitson and Crane, 1996) have found improved accuracy in downscaled simulations of present day conditions by the addition of measures of atmospheric moisture content in addition to general circulation variables. Therefore, derived variables, while containing greater uncertainty, are still of value when applied to downscaling techniques.

Giorgi and Mearns (2002) propose a method to quantify the uncertainty present in predictions of climate variables generated by GCMs. This method relies on the availability of multiple climate models running the same emissions scenarios. The method uses a weighted average of the models to generate an ensemble mean. Model results that fall closer to the mean and better reproduce historic values are termed more 'reliable' and given a higher value in the averaging process. The standard deviation of the collection of models away from the ensemble mean represents a quantified measure of uncertainty. The GCM ensemble mean generated by this process can then be used to drive impact studies, thereby providing GCM output that can be considered as having a greater reliability and a quantified level of uncertainty.

### *3.2.6. Uncertainty in Downscaling*

The downscaling techniques discussed in previous sections each have unique sources of uncertainty. High resolution GCMs and RCMs are subject to the same uncertainties as global-scale GCMs. The incomplete knowledge of atmospheric physics and the uncertain effects generated by the use of GCM variables, such as boundary conditions, result in an inevitable and non-quantifiable bias in RCM and HRGCM output (Wood et al., 1997). The additional burden of the intense computational requirements of these downscaling techniques has resulted in a preference for the statistical/empirical downscaling techniques; these latter techniques have received much more attention in the scientific literature and will be the subject of the remainder of this discussion.

A multitude of different downscaling techniques have been proposed. Most reproduce current regional phenomena with a good degree of accuracy, and most are capable of generating plausible values for regional phenomena using a climate change scenario. However, all downscaling techniques suffer from the same degree of uncertainty because the basic assumptions of statistical downscaling are not verifiable (IPCC, 2001). Wood et al. (1997) describe the downscaling step as "among the least quantifiable links" in the chain of models used for assessing climate change impacts. Wilby et al. (1998) performed a comparison of six different downscaling techniques, applied to the same data

set, and demonstrated significant variability in the prediction of daily precipitation. The implication to be had is that the selection of modeling techniques can have an equal or larger effect on predicted impacts of climate change than the predicted change itself.

### *3.2.7. Uncertainty in Hydrologic Modeling*

The primary source of uncertainty in the use of hydrologic models to predict the impacts of climate change arises from the implicit assumption that parameters used in model development under current climate conditions remain valid under conditions of climate change. Efforts to quantify the uncertainty in the hydrologic modeling step resulted in the conclusion that errors due to the above assumption are modest when compared to natural variability and when compared to uncertainty from the GCMs (Wood et al., 1997).

### *3.2.8. Uncertainty in Systems Management Models*

Water resources systems management models have traditionally been developed for either the planning of a system or the provision of operational guidelines for the system. Because of this, it is difficult to operate these models in a manner conducive to the prediction of climate change impacts. Operational models are constrained by capricious political and social forces that make the application of these models to future demand scenarios difficult (Wood et al., 1997; Palmer and Hahn, 2002). The comparison of results from system management models driven by observed data and simulated data from the same time period can provide some insight to the degree of bias generated by the use of simulated data fields; however, this exercise must be qualified by the recognition of the frequent paucity and often questionable accuracy of observed data (IPCC, 2001).

### *3.2.9. Implications of Uncertainty on Long Range Planning*

The strategies required for anticipating and preparing for climate change and its effects on water resource systems are as varied as the systems themselves. Lettenmaier et al. (1999) found that the application of identical climate change scenarios to different systems resulted in quite different impacts. Systems with large supplies of groundwater or currently unused storage volumes have a built-in buffering capacity that can mitigate potential climate change impacts. Systems that are highly allocated or have several (often conflicting) purposes face potentially dramatic declines in performance with even modest changes in climate.

A comprehensive study that characterizes all the sources of uncertainties that can affect long term planning in water resources has yet to be performed. Wood et al. (1997) determined that the relative magnitude of the uncertainties from GCM output and downscaling methods were greater than the other sources of uncertainty when the planning efforts attempted a predictive approach (i.e., attempting to determine stream flows and storage volumes at some point in the future).

The alternative to the predictive approach is to perform a sensitivity analysis of the system to determine the potential impacts of climate change. The sensitivity approach yields a more qualitative understanding of how a system is likely to respond to climate change. With the sensitivity approach the uncertainties associated with GCM output and downscaling methods become much less significant than those associated with demand forecasts and system operations (Wood et al., 1997).

Uncertainty exists at every level of analysis and in every data source. The degree to which this uncertainty affects the outcome of an impact evaluation varies widely. It is important to recognize that many of the same uncertainties exist in the traditional, historic record based water resource system evaluations. These uncertainties are not necessarily significant enough to mask the underlying trends or scale of impacts, but simply obscure our ability to identify the exact magnitude and timing of future events.

## 3.3. Hydrology Model

### 3.3.1. Modeling Environment

A calibrated watershed model is required to evaluate the impacts of climate change on water supply. For this study, the EPS's Better Assessment Science Integrating Point and Nonpoint Sources (BASINS) model is used to model the Tualatin watershed. BASINS includes four main components: meteorological data preparation, digital map assembly, model development, and illustration of model results. These components are based on software that has previously been used independently. The BASINS package links these models together with improved interfaces, streamlining the flow of information (USEPA, 2001).

Meteorological data in BASINS is stored in WDM (Watershed Data Management) files. These files are small databases that provide an efficient format for cataloguing and storing time-series data. Included in the BASINS package is a tool called WDMUtil, which allows data to be written to WDM files and then listed, edited, and summarized.

The creation of a BASINS hydrology model requires overlapping a variety of map layers in ArcView GIS: the stream network, land use, soils, and topography. Once the layers have been organized, an area of analysis (the watershed) is outlined and selected. The software extracts hydraulic characteristics from the physiographic data contained in the map layers and automatically creates a model of the flow of water over the land, through the ground, and within stream channels. In addition to an HSPF (Hydrologic Simulation Program Fortran) hydrology model, this process creates useful displays of the watershed's geography.

The EPA recommends HSPF as the most accurate and appropriate model available for long-term simulation of watershed hydrology or water quality. In HSPF, a watershed's water quantity and quality processes are continuously simulated using equations from the Stanford Watershed Model. HSPF is a lumped-element model; each element (reach, reservoir, or land segment) is characterized by a set of measured and calibrated

parameters. These parameters are incorporated into the functions that calculate an element's water budget. Within an element, the water budget is based on inflows, outflows, and storages in several zones. The zones divide flow into surface flow, interflow, and groundwater flow. The rate at which water flows laterally to an adjacent element, percolates vertically to a lower zone, or evaporates is partially determined by its zone.

The results of the HSPF simulation can be statistically analyzed and graphically displayed in a program called GenScn. This application facilitates comparative analysis of streamflow under several scenarios and in multiple locations. It can also be used to quickly change an input time series before re-running a scenario.

### *3.3.2. Model of the Tualatin Watershed*

For the modeling process, the Tualatin Watershed was divided into nine areas grouped by subbasin. The distributed Tualatin River Basin network is shown in Figure 7. Each area was individually calibrated following the process shown in Figure 8. The paucity of both continuous hydrologic data and documentation of the quantities of diversions presented a challenge in this calibration. Table 1 presents the gauging stations in the basin, the longest continuous period recorded on each gage, and the streams that catch the runoff recorded at each gage.

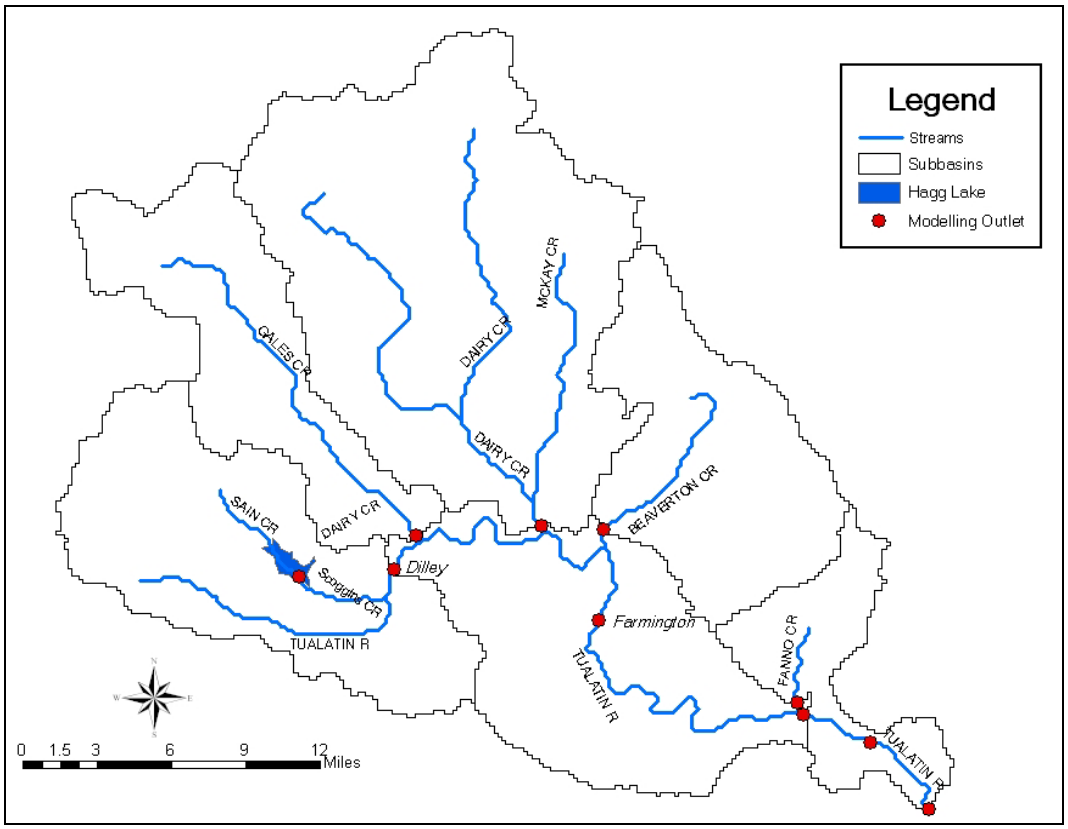


**Figure 7 - Subbasins in the Tualatin River watershed modeled in BASINS.**

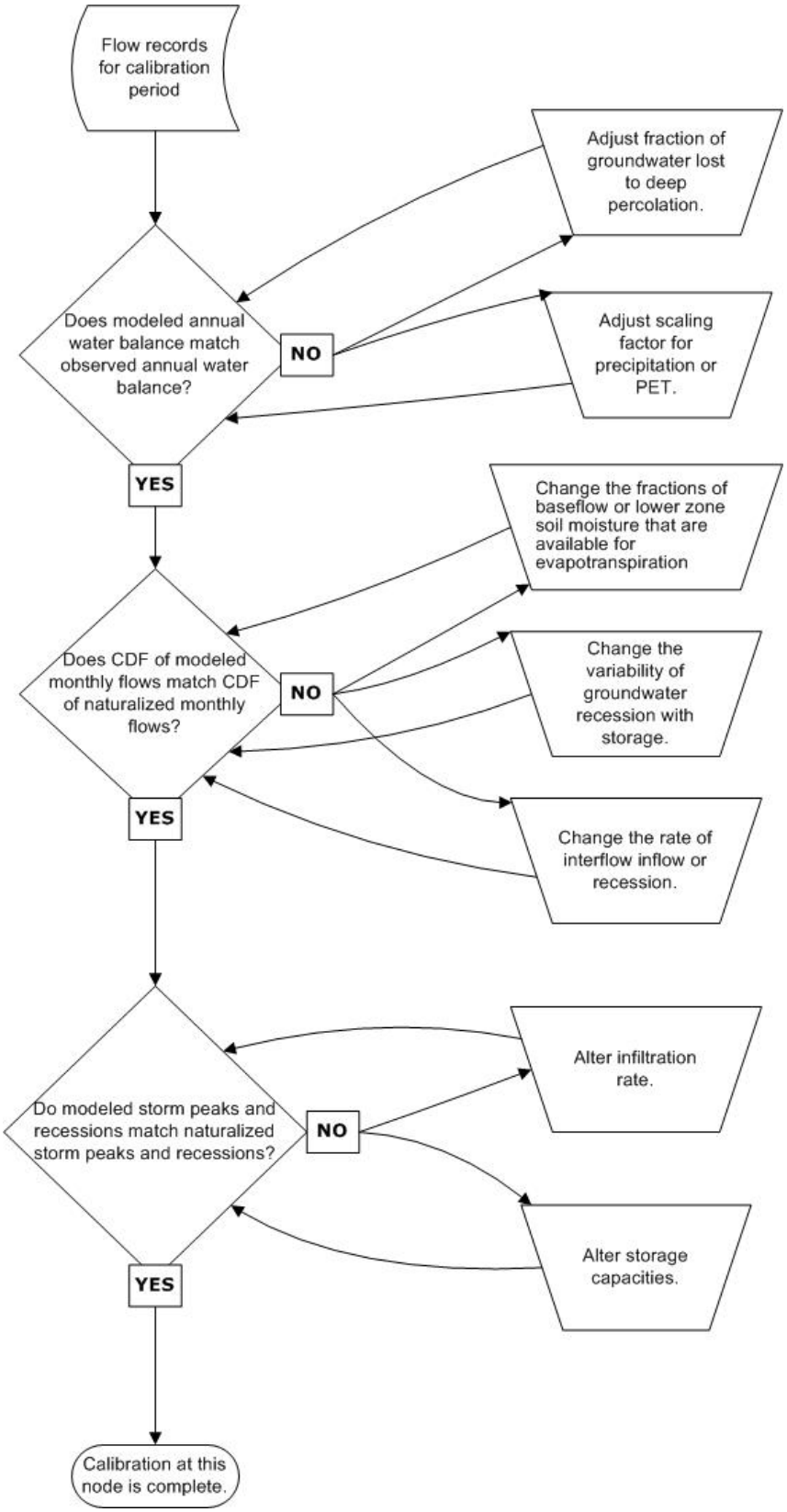


**Figure 8 - Hydrology model calibration procedure.**

As mentioned previously, setting up a BASINS model requires four digital map layers. Cartographic data for the Tualatin River watershed came from the sources shown in Table 2

**Table 1 – Streamflow gauging stations used to calibrate the BASINS model.**

| Gauging Station | Longest Period of Record | Stream; Upstream tributaries |
|---|---|---|
| USGS 14205500 | 1940-1951 | Dairy |
| USGS 14204500 | 1940-1956 | Gales |
| Bureau | 1940-2003 | Scoggins; Sain |
| Watermaster 14206450 | 1994-2002 (summers only) | North Rock; Holcomb, Bethany, Dawson, Abbey, Bannister, Bronson, Cedar Mill, Willow, Turner, Johnson, Beaverton, Golf, Reedville, Hall, Erickson |
| USGS 14207500 | 1928-1987 | Lower Tualatin; Christensen, Cross, Gordon, Hedges, Nyberg, South Rock, Saum |
| USGS 14206950 | 1993-1996 | Fanno; Sylvan, Ivey, Woods, Ash, Summer, Hiteon, Red Rock, Krueger, Ball, Derry Dell |

**Table 2 – Digital map layers used to set up the BASINS model.**

| Required Map Layer | Source | Theme Name |
|---|---|---|
| Streams | USEPA | Reach File, V1 |
| Land Use | USGS | GIRAS |
| Soils | USDA-NRCS | State Soil |
| Topography | USGS | DEM (CU) |

ArcGIS maps obtained from Clean Water Services provided both the geographic boundary of the basin and a digital delineation of the subbasins and streamsheds it contains.

Hagg Lake was modeled simply as an area in the basin where the land use is 100% "water." Land in a calibration area that drained to a point below the gauging station was assumed to have the same parameter values as the rest of the area.

Five stations provided precipitation records (Table 3). Areas within the basin were calibrated using rainfall from a station included within their boundary or to the nearest station for which rainfall data was available during the calibration historical period. Potential evapotranspiration data recorded at the Portland Airport station were used for the entire basin. Scaling factors for both precipitation and evapotranspiration were assigned to each calibration area, based on its average annual rainfall and water balance.

**Table 3 – Precipitation gauging stations used to calibrate the BASINS model.**

| Station Owner, Gage ID | Station Location, Duration | Calibration Period | Validation Period |
|---|---|---|---|
| USGS, 14205500 | Timber, 1934-1976 | 1942-1945 | 1946-1949 |
| USGS, 14204500 | Glenwood, 1948-2003 | 1940-1945 | 1951-1955 |
| BOR, SCOO | Scoggins, 1972-1985 | 1940-1945 | 1961-1965 |
| Watermaster, 14206450 | Beaverton, 1973-2002 | 1995-1997 | 1999-2001 |
| USGS, 14207500 | Beaverton, 1973-2002 | 1940-1945 | 1957-1961 |
| USGS, 14206950 | Beaverton, 1973-2002 | 1993-1996 | 2000-2001 |

Parameters characterizing pervious land use were adjusted in three stages of calibration. First, annual water balance was calibrated by adjusting the fraction of groundwater lost to deep percolation and the scaling factors for precipitation and potential evapotranspiration. Second, the cumulative distribution of monthly flows was calibrated by changing the rate of interflow inflow and recession, groundwater recession variability, and the fractions of base flow and lower zone soil moisture that are available for evapotranspiration. Finally, modeled storm peaks and recessions were compared to historical records by altering storage capacities and the infiltration rate.

After calibration, mean monthly modeled flows at each node were compared to observed monthly average flows, to find the coefficient of determination (often referred to as $r^2$). If it were possible to model the flows perfectly, the coefficient of determination would be 1.0. In this study, $r^2$ was greater than 0.9 in most cases. On Rock Creek and Gales Creek, this value was lower. Unmeasured diversions may have caused significant discrepancy between natural and measured streamflows. To remedy this, a term representing an estimate of actual withdrawals was added to the flows in these creeks during summer months. This term was chosen as that which maximized the goodness-of-fit with modeled flows and did not exceed the total amount of water rights that had been issued on the creek before the end of the period calibrated over. On Rock Creek, the naturalization term used was 19.1 cfs; on Gales Creek, this term was 14.6 cfs.

Coefficients of determination for the calibration and validation periods in each of the modeled subbasins are shown in Table 4.

The calibration of Rock Creek was still relatively poor, probably because gage data was only available for summer months when flows are impacted by diversions and when gauging is least accurate. For small flows, the stage-discharge function is sensitive to changes in the shape of the channel bed's surface. This creates error when stream stage is used to measure discharge. Also, very low flows create the opportunity for water to meander away from the gage, causing it to miss some of the water that is actually in the stream.

**Table 4 - Coefficients of determination for calibration and validation periods.**

| Stream | Calibration Coefficient of Determination | Validation Coefficient of Determination |
|---|---|---|
| Tualatin | 0.92 | 0.93 |
| Fanno | 0.95 | 0.84 |
| Rock | 0.71 | 0.97 |
| Dairy | 0.92 | 0.95 |
| Gales | 0.90 | 0.82 |
| Scoggins | 0.94 | 0.96 |

Modeled flows are shown graphed with measured or corrected flows in Appendix B.

## *3.4. Tualatin River Integrated Management Systems Model*

### *3.4.1. General Overview*

The Tualatin River Integrated Management Systems (TRIMS) model is a monthly-time-step water resources model that incorporates the major components and operational features of the Tualatin River Basin. The TRIMS model simulates the storage and movement of water throughout the basin for current and projected operational policies. TRIMS is a comprehensive model, with its domain ranging from the headwaters of Scoggins Creek above Henry Hagg Lake to the mouth of the Tualatin River, and including the major tributaries of the system (Upper Tualatin River, Gales Creek, Rock Creek, Dairy Creek, and Fanno Creek). TRIMS also includes Barney Reservoir. Although located outside the basin, Barney's releases are exported via an aqueduct to the Upper Tualatin River. The TRIMS model schematic is shown in Figure 9.

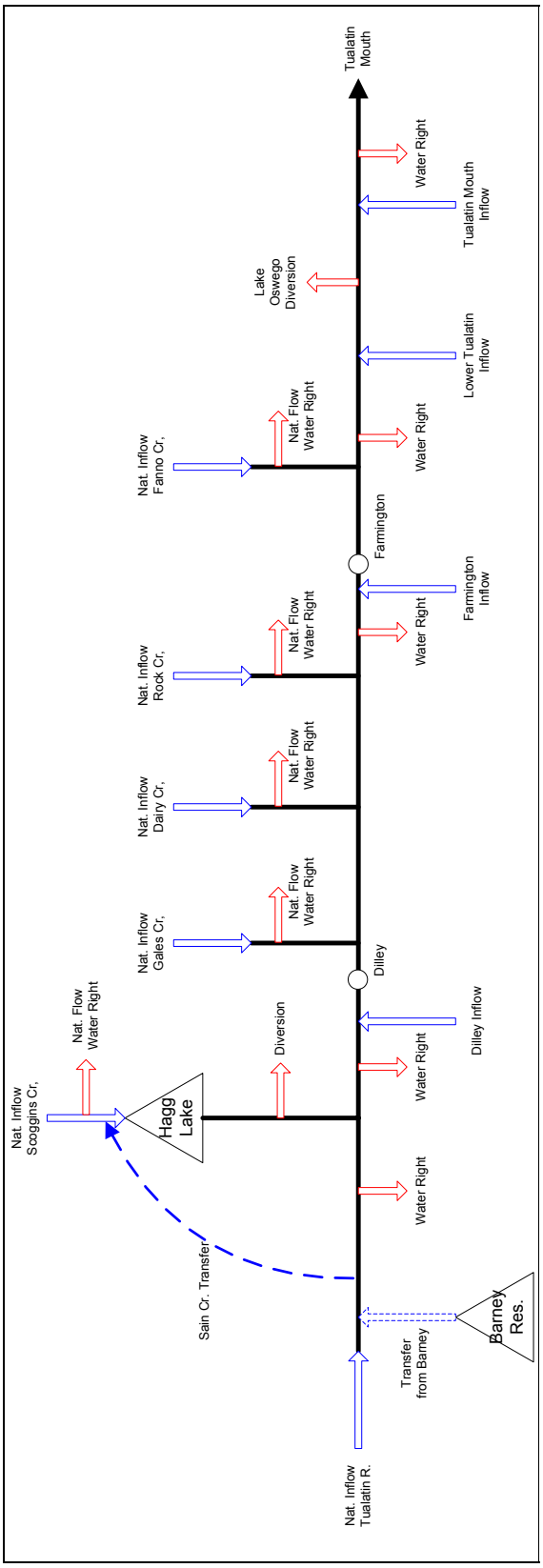


**Figure 9 - TRIMS Model schematic.**

The streamflows generated by the BASINS model are aggregated from daily to monthly values and used as inputs to TRIMS. The model contains seasonally varying reservoir release rule curves and flow targets that determine the amount of water stored in and released from Hagg Lake and Barney Reservoir. TRIMS also models surface water demands and water rights at each node in the system. TRIMS accurately simulates the flow of water throughout the water transmission system and calculates both current and future system safe yields and reliabilities given various operating policies and infrastructure alternatives.

### *3.4.2. Motivation for Developing TRIMS*

TRIMS is a flexible, dynamic simulation model that evaluates a wide range of water supply alternatives under different inflow scenarios. Specific questions of interest addressed by TRIMS include:

1. What is the safe yield of the current Hagg Lake water supply?
2. What is the safe yield of the Hagg Lake if its elevation is raised 20 feet?
3. What is the safe yield of the Hagg Lake if its elevation is raised 40 feet?
4. Will future climate change impact the safe yield of the system?
5. Will foreseeable future demands become unsustainable?
6. Will structural changes be required to ensure water supply sustainability?

### *3.4.3. Software*

The Stella® modeling environment (High Performance Systems, Inc.) was selected as the most appropriate systems dynamic modeling tool for developing TRIMS. Stella® is arguably the most popular and efficient simulation tool currently available for constructing graphical models and has been widely used by water resources planners and others for more than a decade (e.g., Keyes and Palmer, 1993; Palmer and Hahn, 2002; VanRheenen et al., 2004).

### *3.4.4. TRIMS Key Assumptions*

Several key assumptions have been incorporated into the formulation of TRIMS and in the evaluation of its results, including:

1. Safe yield is defined here as the maximum quantity of water that can be supplied, given a specified sequence of streamflows and demands. If a larger quantity than the safe yield is extracted from a system, then it will be unable to meet all demands and this inability is termed a failure. Using TRIMS, the first, second, third, and sixth failure years and corresponding safe yields were identified
2. Water rights are met at 50% of the full right or less. This assumption is based on personal communication with Tom VanderPlaat of CWS (VanderPlaat, 2003).
3. Hagg Lake demand scenarios developed by MWH are appropriate for this study.

4. Barney Reservoir releases that enter the Tualatin system are modeled as the mean monthly release from 2000-2003.
5. In all runs, instream flow targets are met prior to making releases to meet demands.

### *3.4.5. Operating Rules*

The active storage of Hagg Lake is 53,640 acre-feet. The U.S. Army Corps of Engineers' official flood control rule defines the maximum volume of water that can be stored in Hagg Lake from November through April. Table 5 shows the flood space reservation and maximum allowable contents for Hagg Lake. Also shown are storage rule curves for the structural options under consideration.

**Table 5 - Hagg Lake flood control space and maximum allowable storage (acre-feet).**

| Month | Flood Volume | Current Total Storage | 20 ft Raise, Total Storage | 40 ft Raise, Total Storage |
|---|---|---|---|---|
| Oct | 0 | 59950 | 86518 | 114766 |
| Nov | 20560 | 39390 | 65958 | 94206 |
| Dec | 20560 | 39390 | 65958 | 94206 |
| Jan | 20560 | 39390 | 65958 | 94206 |
| Feb | 17000 | 42950 | 69518 | 97766 |
| Mar | 5500 | 54450 | 81018 | 109266 |
| Apr | 2000 | 57950 | 84518 | 112766 |
| May | 0 | 59950 | 86518 | 114766 |
| Jun | 0 | 59950 | 86518 | 114766 |
| Jul | 0 | 59950 | 86518 | 114766 |
| Aug | 0 | 59950 | 86518 | 114766 |
| Sep | 0 | 59950 | 86518 | 114766 |

Barney Reservoir is analogous to Hagg Lake in that they have similar drawdown and refill periods. Since Barney has only been operating in its current storage capacity of 20,000 acre-feet for three years, firm release rules have not been established. To remedy this, historical mean monthly releases from Barney Reservoir are used in TRIMS.

### *3.4.6. Demands*

Demands and demand management strategies used in TRIMS simulations were adapted from previous studies in the basin (Murdock, 2003) and from personal communication with CWS personnel (VanderPlaat, 2003). Monthly demands on Hagg Lake were estimated by MWH Consultants (Murdock, 2003) for TVID, M&I, and Lake Oswego at existing, contracted, and forecasted year-2050 levels. These demands are shown in Tables 6-8. Because CWS demands are non-consumptive and are modeled differently

from other uses, they are not included with the other tabulations of demand. They are summarized in Section 3.4.7.

**Table 6 - Existing demands (Murdock, 2003).**

| | TVID | | M & I | | Lake Oswego | | Total | |
|---|---|---|---|---|---|---|---|---|
| | acre feet | cfs | acre feet | cfs | acre feet | cfs | acre feet | cfs |
| Oct | 945 | 15.4 | 1114 | 18.1 | 18 | 0.3 | 2077 | 33.8 |
| Nov | 39 | 0.7 | 222 | 3.7 | 0 | 0.0 | 261 | 4.4 |
| Dec | 0 | 0.0 | 0 | 0.0 | 0 | 0.0 | 0 | 0.0 |
| Jan | 0 | 0.0 | 0 | 0.0 | 0 | 0.0 | 0 | 0.0 |
| Feb | 0 | 0.0 | 0 | 0.0 | 0 | 0.0 | 0 | 0.0 |
| Mar | 0 | 0.0 | 0 | 0.0 | 0 | 0.0 | 0 | 0.0 |
| Apr | 73 | 1.2 | 0 | 0.0 | 0 | 0.0 | 73 | 1.2 |
| May | 29 | 0.5 | 0 | 0.0 | 0 | 0.0 | 29 | 0.5 |
| Jun | 1338 | 22.5 | 867 | 14.6 | 11 | 0.2 | 2216 | 37.2 |
| Jul | 6284 | 102.2 | 2362 | 38.4 | 182 | 3.0 | 8828 | 143.6 |
| Aug | 7184 | 116.8 | 2651 | 43.1 | 172 | 2.8 | 10007 | 162.7 |
| Sep | 3179 | 53.4 | 2284 | 38.4 | 117 | 2.0 | 5580 | 93.8 |
| **Total** | **19071** | | **9500** | | **500** | | **29071** | |

**Table 7 - Contracted demands (Murdock, 2003).**

| | TVID | | M & I | | Lake Oswego | | Total | |
|---|---|---|---|---|---|---|---|---|
| | acre feet | cfs | acre feet | cfs | acre feet | cfs | acre feet | cfs |
| Oct | 1339 | 21.8 | 1583 | 25.7 | 18 | 0.3 | 2940 | 47.8 |
| Nov | 55 | 0.9 | 315 | 5.3 | 0 | 0.0 | 370 | 6.2 |
| Dec | 0 | 0.0 | 0 | 0.0 | 0 | 0.0 | 0 | 0.0 |
| Jan | 0 | 0.0 | 0 | 0.0 | 0 | 0.0 | 0 | 0.0 |
| Feb | 0 | 0.0 | 0 | 0.0 | 0 | 0.0 | 0 | 0.0 |
| Mar | 0 | 0.0 | 0 | 0.0 | 0 | 0.0 | 0 | 0.0 |
| Apr | 104 | 1.7 | 0 | 0.0 | 0 | 0.0 | 104 | 1.7 |
| May | 41 | 0.7 | 0 | 0.0 | 0 | 0.0 | 41 | 0.7 |
| Jun | 1895 | 31.8 | 1232 | 20.7 | 11 | 0.2 | 3138 | 52.7 |
| Jul | 8904 | 144.8 | 3357 | 54.6 | 182 | 3.0 | 12443 | 202.4 |
| Aug | 10179 | 165.5 | 3767 | 61.3 | 172 | 2.8 | 14118 | 229.6 |
| Sep | 4505 | 75.7 | 3246 | 54.6 | 117 | 2.0 | 7868 | 132.2 |
| **Total** | **27022** | | **13500** | | **500** | | **41022** | |

**Table 8 - Forecasted 2050 demands (Murdock, 2003).**

| | TVID | | M & I | | Lake Oswego | | Total | |
|---|---|---|---|---|---|---|---|---|
| | acre feet | cfs | acre feet | cfs | acre feet | cfs | acre feet | cfs |
| Oct | 1339 | 21.8 | 4514 | 73.4 | 18 | 0.3 | 5871 | 95.5 |
| Nov | 55 | 0.9 | 899 | 15.1 | 0 | 0.0 | 954 | 16.0 |
| Dec | 0 | 0.0 | 0 | 0.0 | 0 | 0.0 | 0 | 0.0 |
| Jan | 0 | 0.0 | 0 | 0.0 | 0 | 0.0 | 0 | 0.0 |
| Feb | 0 | 0.0 | 0 | 0.0 | 0 | 0.0 | 0 | 0.0 |
| Mar | 0 | 0.0 | 0 | 0.0 | 0 | 0.0 | 0 | 0.0 |
| Apr | 104 | 1.7 | 0 | 0.0 | 0 | 0.0 | 104 | 1.7 |
| May | 41 | 0.7 | 0 | 0.0 | 0 | 0.0 | 41 | 0.7 |
| Jun | 1895 | 31.8 | 3513 | 59.0 | 11 | 0.2 | 5419 | 91.1 |
| Jul | 8904 | 144.8 | 9573 | 155.7 | 182 | 3.0 | 18659 | 303.5 |
| Aug | 10179 | 165.5 | 10743 | 174.7 | 172 | 2.8 | 21094 | 343.1 |
| Sep | 4505 | 75.7 | 9258 | 155.6 | 117 | 2.0 | 13880 | 233.3 |
| **Total** | **27022** | | **38500** | | **500** | | **66022** | |

### *3.4.7. Instream Flow Requirements*

TRIMS includes instream flow requirements in Scoggins Creek below Hagg Lake and in the Tualatin River at Farmington (Table 9) (USBR, 2002). The target in Scoggins Creek is modeled as a monthly minimum release requirement from Hagg Lake. The target at Farmington is met by a combination of Hagg Lake releases and natural flows less demands from upstream tributaries and Tualatin River incremental inflows. In the current and contracted demand scenarios, up to 12,618 af may be released annually from Hagg Lake to assist in meeting the flow target at Farmington. In the 2050 demand scenario, up to 27,618 af may be released annually. These maximum annual release values are consistent with the MWH draft report (MWH, 2003). As noted elsewhere, instream flow demands are given first priority, ensuring that water is provided for these targets before other types of demands are met.

**Table 9 – TRIMS instream flow targets (cfs).**

| Month | Below Hagg Lake | Farmington |
|---|---|---|
| Oct | 20 | 180 |
| Nov | 20 | 180 |
| Dec | 10 | 0 |
| Jan | 10 | 0 |
| Feb | 10 | 0 |
| Mar | 10 | 0 |
| Apr | 10 | 0 |
| May | 10 | 0 |
| Jun | 10 | 120 |
| Jul | 10 | 120 |
| Aug | 10 | 180 |
| Sep | 10 | 180 |

### *3.4.8. TRIMS Interface and Operation*

A user interface was developed for TRIMS to facilitate rapid and efficient operation of the model. The interface allows exploration of a range of operating alternatives and the testing of the impacts of various streamflows. The principal interface panel is shown in Figure 10.

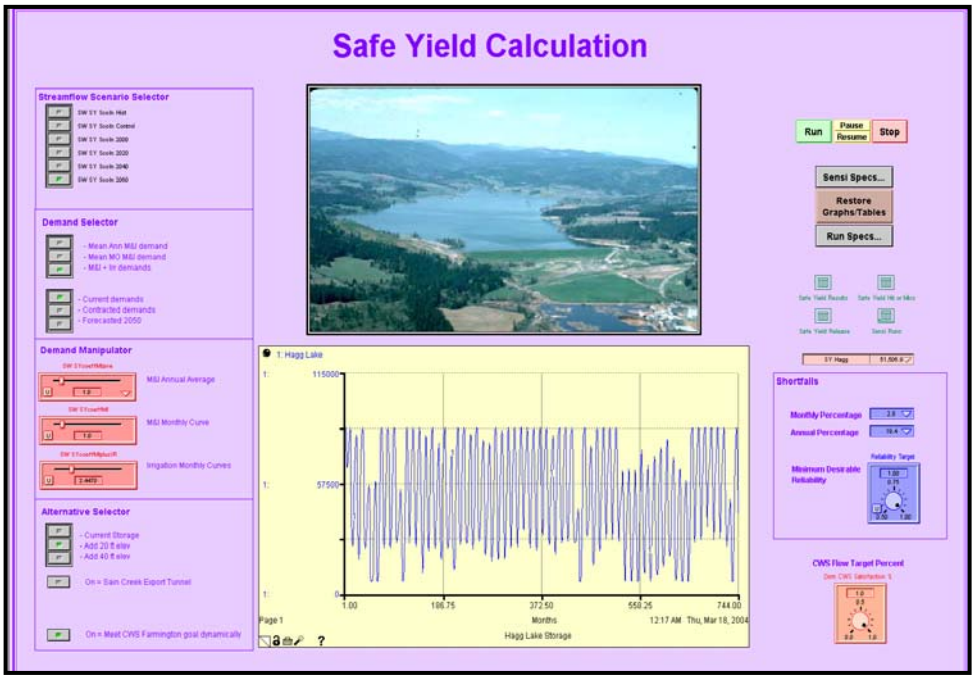


**Figure 10 - TRIMS control panel.**

To execute the model, the user must identify various model assumptions:

1. Select the streamflow scenario (Figure 11).
2. Select the demand type and the demand calculation method to be used (Figure 10).
3. The "Demand Manipulator" determines the factor by which the demand selected in step 2 will be multiplied (Figure 12). To calculate the system yield, this value is increased until the system fails. This process has been automated with the use of Stella's sensitivity feature.
4. Select the structural alternative to be used for the run in the "Alternative Selector" (Figure 13). The user may choose to run TRIMS at the current storage or with either the 20 foot or 40 foot dam elevation expansions. Each of the storage alternatives may also be run with or without the Sain Creek Tunnel activated from January to April.

Once these selections have been made, a run of TRIMS may be performed.

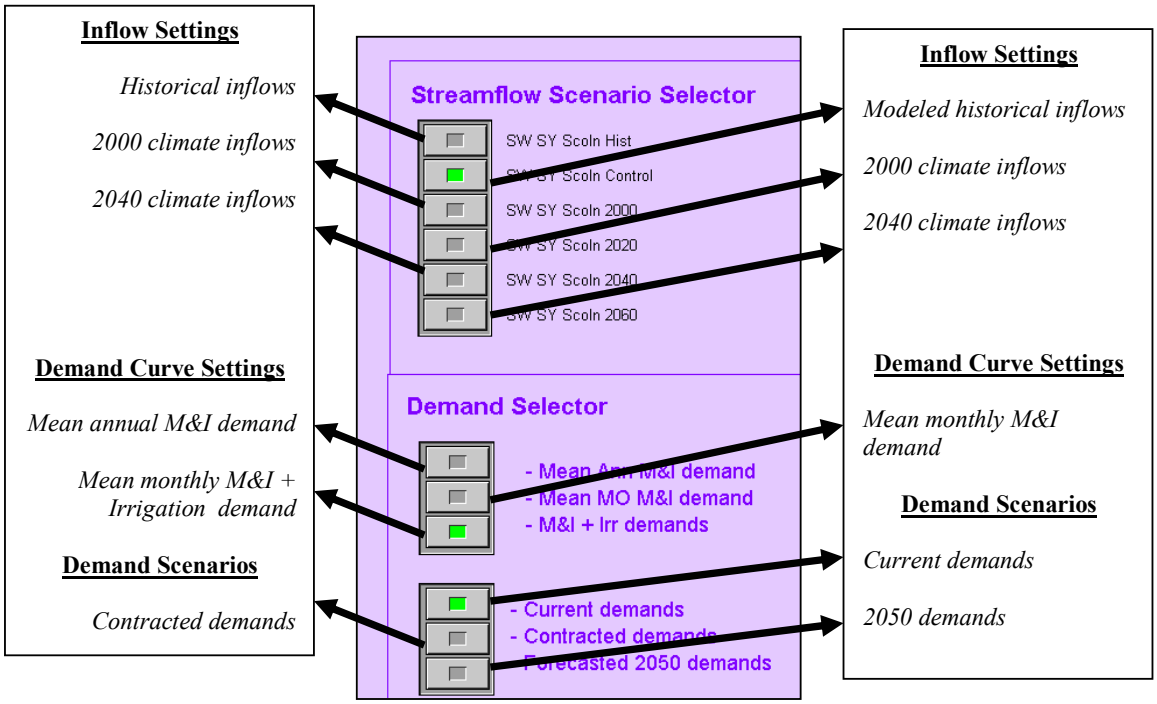


**Figure 11 - TRIMS control panel streamflow and demand selectors.**

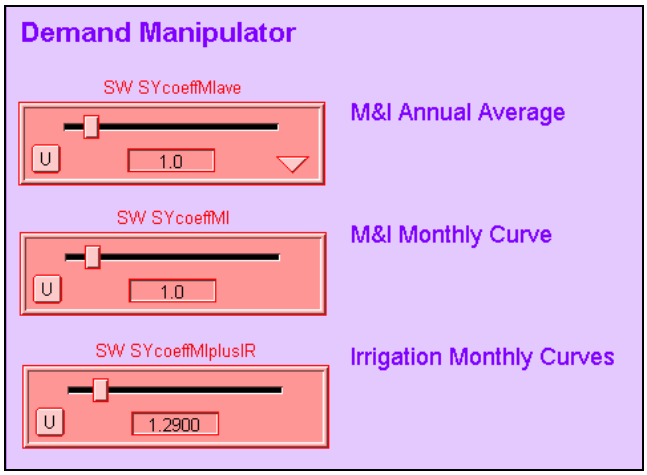


**Figure 12 - TRIMS control panel demand manipulator.**

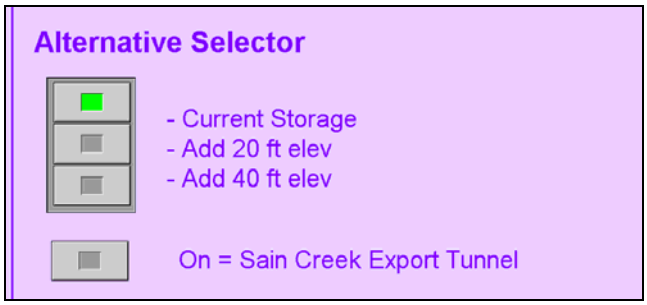


**Figure 13 - TRIMS control panel alternative selector.**

### *3.4.9. TRIMS Model Runs*

The TRIMS model was run for twelve different demand and structural alternative combinations with five climate-impacted streamflow scenarios.

- Year-2000 level of climate change
- Year-2020 level of climate change
- Year-2040 level of climate change
- Year-2060 level of climate change

The complete listing of runs performed, with demand, structural alternatives, and Farmington target percentage settings are shown in Table 10.

**Table 10 - TRIMS Model run summary.**

| Demand Scenario | Fish Target Percentage | Expansion Alternatives | | |
|---|---|---|---|---|
| | | Current | 20 ft | 40 ft |
| Current | 100 | X | | |
| Current | 100 | | X | |
| Current | 100 | | | X |
| Contracted | 100 | X | | |
| Contracted | 100 | | X | |
| Contracted | 100 | | | X |
| 2050 | 100 | X | | |
| 2050 | 100 | | X | |
| 2050 | 100 | | | X |

# 4. Model Results—Local Impacts of Climate Change

The resolution at which even the most recent GCMs operate is too coarse to directly predict localized climate conditions. Thermodynamically influential features such as mountains, lakes, and rivers have significant effects on local weather, but are not represented in GCMs. Assessing regional change requires extracting decadal changes from GCM output and casting them onto a finer scale of spatial complexity. Downscaling techniques allow us to preserve both the trends forecasted by GCMs and the small-scale phenomena recorded at weather stations.

This study incorporates the perturbation method of downscaling, an approach that has been successfully used in other climate impacts studies (Lettenmaier et al., 1999; Lettenmaier and Gan, 1990; Smith and Tirpak, 1989). This approach rests on two facts:

1. GCMs do not reliably reproduce exact values of observed meteorological variables, but are able to reliably reproduce observed changes in those variables (Mote et al., 1999).
2. Pacific Northwest weather is regionally coherent (Mote et al., 1999).

As discussed in Section 3.1.3, six of the most commonly used GCMs (CGCM2, CSIRO mk2, ECHAM4, GFDL_R30, HadCM3, and DOE PCM) were selected for analysis. The climate signals generated by these models were averaged over the specified decades to get an ensemble average for the evaluation.

## *4.1. Temperature*

In the perturbation method, average monthly temperatures from the historical record are compared to GCM temperatures. These temperatures are monthly averages aggregated over a large geographic area (the same size as a GCM grid cell). The arithmetic difference between historical averages and GCM forecasts is referred to as the temperature signal. Because GCMs are not able to perfectly reproduce current conditions and because some climate change has already occurred during the 20$^{th}$ century, differences between the historic record and GCM predictions for the year 2000 period (1990-2010; also referred to as the "control") are nonzero.

The year 2000 climate is warmer than the historic record in each month of the year (Figure 14). From April – September, the 2000 climate is about 1º F than historic. Figure 15 shows consistent temperature increases, with the signals for all twelve months in each decade stronger than those for the previous one (with the exception of January 2020). Although temperature increases are predicted year-round, they are largest in the summer (except in 2010) and smallest in the spring. Beginning in 2050, each decade is about 1º F warmer than the last. However, interannual variability (even given a stable climate) is much greater than the shifts caused by an altered climate. Therefore, it is not unusual for average temperatures during a specific month to be lower than they were the previous month, and year-to-year differences will often be larger than 1º F.

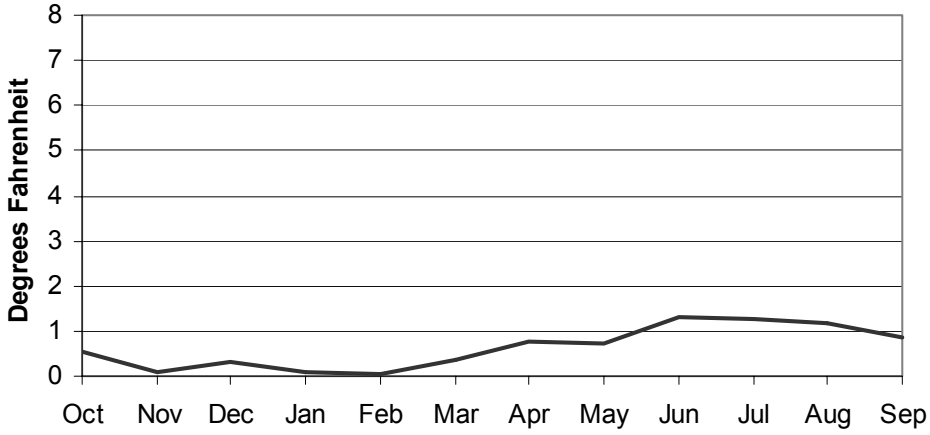


**Figure 14 - Base case increases in mean monthly temperature between historic records and 2000 climate.**

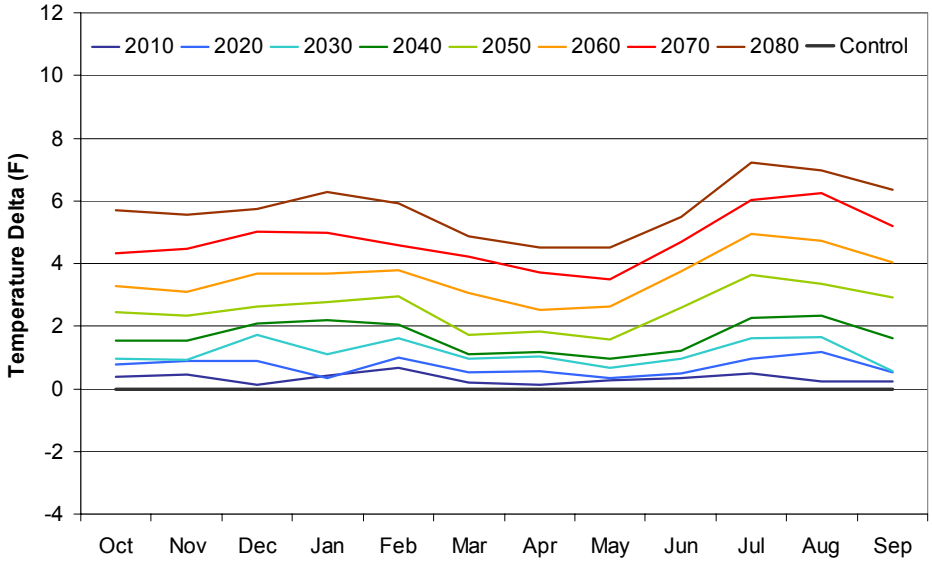


**Figure 15 - Increase in mean monthly temperature between 2000 climate and future climates through 2080.**

Figure 16 shows temperature changes from 2010-2080 from the year 2000 control climate for two of the four GCMs used in the analysis. Since mean monthly temperatures for a given year are calculated by averaging the forecasts produced by four different GCMs over a 20-year period centered on the given year, considerable variability is present between models. The Hadley Center CM3 model predicts monthly temperature changes of 3-11º F by 2080 (Figure 16a), whereas the Parallel Climate Model predicts changes of 2-5º F by 2080 (Figure 16b).

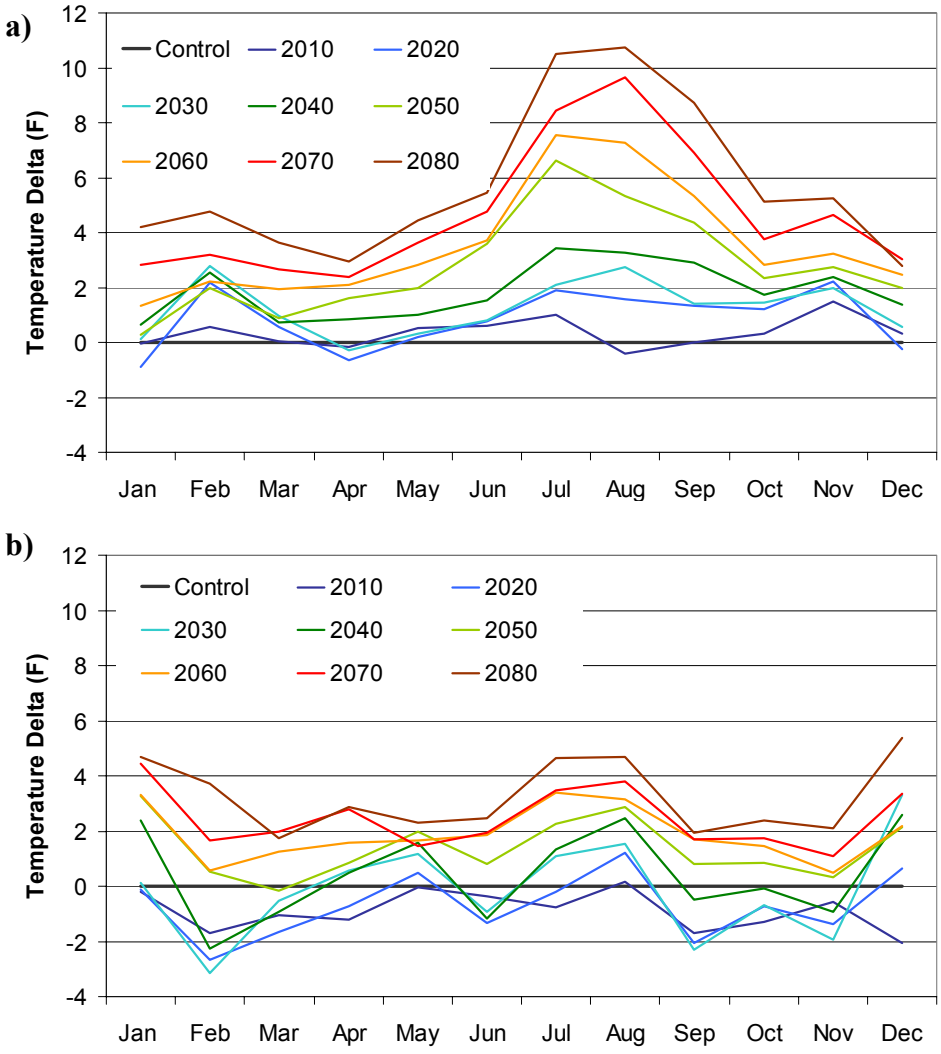


**Figure 16 - HadCM3 (a) and PCM (b) predictions of mean monthly increase in temperature.**

In the area of Hagg Lake, projected mean monthly temperatures show a similarly increasing trend from 2000-2060 (Figure 17). On average, July is the warmest month and January is the coolest month. For most months, the change that occurs from 2040-2060 is nearly as much or greater than the change occurring from 2000-2040.

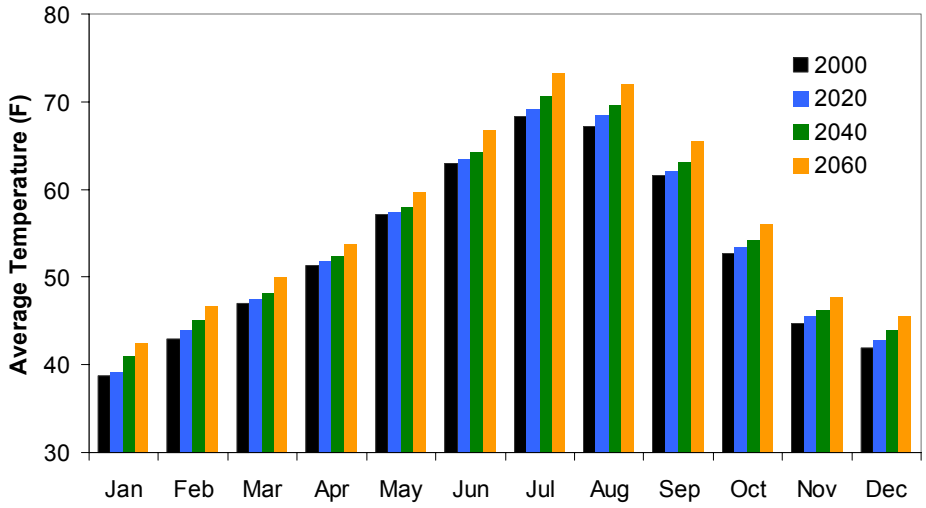


**Figure 17 - Projected mean monthly temperature in the Scoggins area from 2000 to 2060.**

## *4.2. Precipitation*

It is recognized that the precipitation signal provided by climate models is less certain than the temperature signal. GCMs are less effective at producing regional precipitation than they are at producing regional temperature because the physics involved in determining precipitation are more complex.

With the perturbation method, a period's monthly precipitation signals are the average ratio between the temperatures in that period and the temperatures in the control period. For example, a precipitation signal of 1.0 indicates that there is no expected change in average precipitation for a given month. Figure 18 shows the difference in precipitation between the historic records and the year 2000 climate. In general, winters are slighter wetter and summers are slightly drier than historic. June and July show the greatest variation from historic and are 80-90% drier in the year 2000 climate.

Monthly precipitation patterns from 2010-2040 are similar to that of the 2000 climate, the only exception being in August which gets progressively drier through 2040 (Figure 19). From 2050 though 2080, winters get progressively wetter and summers get progressively drier than the year 2000 climate (Figure 20). This precipitation trend is consistent in the area of Hagg Lake (Figure 21).

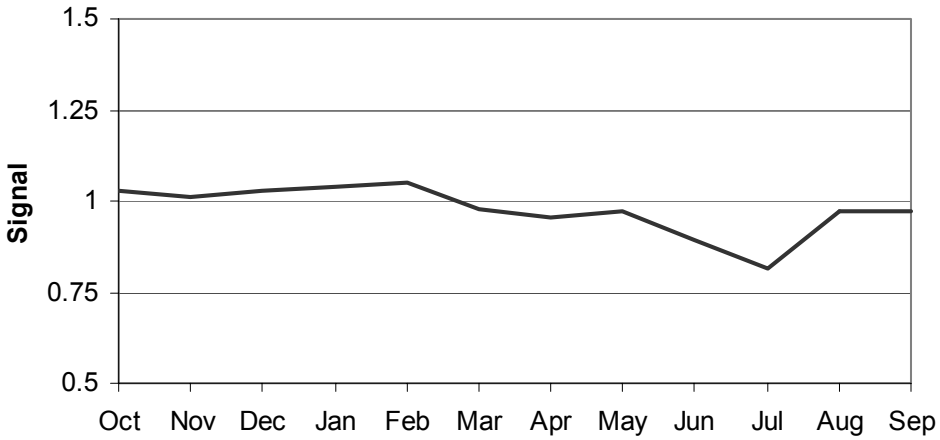


**Figure 18 - Ratio of historic precipitation to year 2000 climate precipitation.**

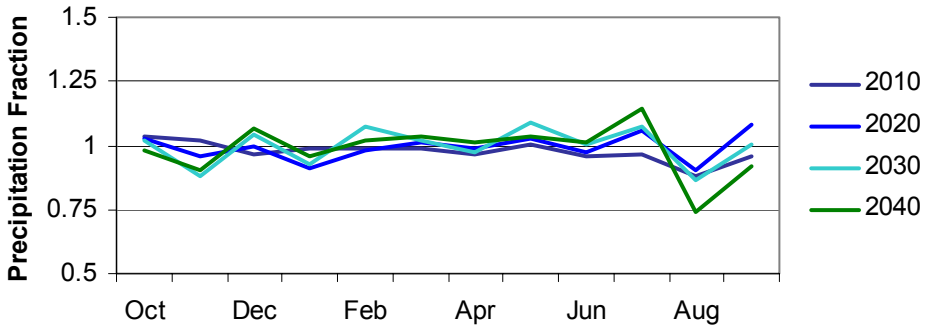


**Figure 19 - Ratio of year 2000 climate precipitation to year 2010-2040 climate.**

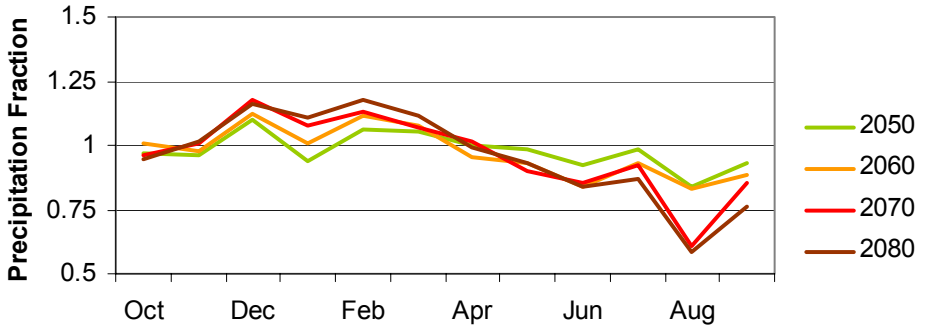


**Figure 20 - Ratio of year 2000 climate precipitation to year 2050-2080 climate**

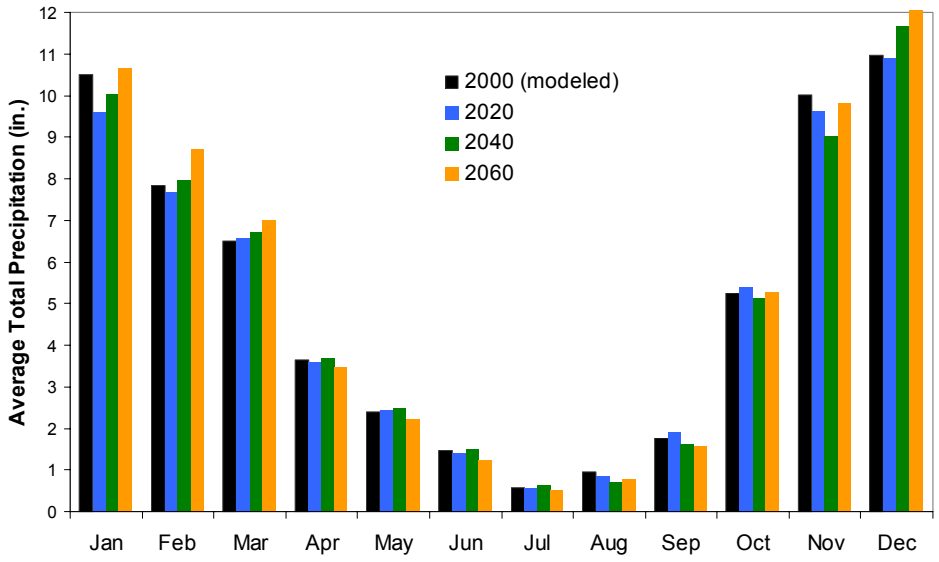


**Figure 21 - Projected mean monthly precipitation in the Hagg Lake area from 2000-2060.**

Although there is a trend toward wetter winters, drier summers, and hotter temperatures year-round, it is assumed that daily and annual variability will be preserved. Figure 22 illustrates the relative values and the variance of mean temperature and precipitation in the basin. The figure indicates that the temperature is forecasted to increase steadily, the trend in precipitation is less clearly defined, and there is considerable variability in both values.

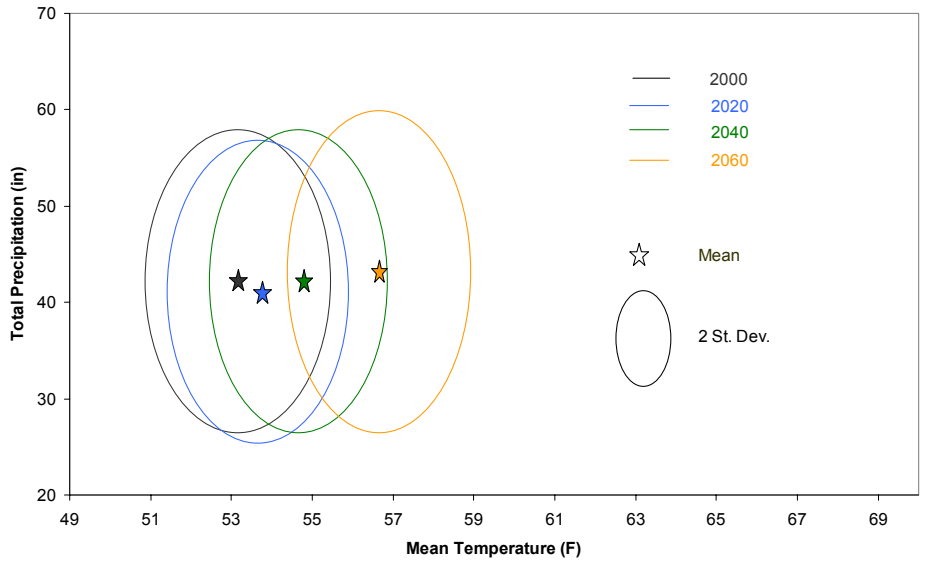


**Figure 22 - Projected mean temperature and precipitation decadal variation from 2000-2060.**

## 4.3. Potential Evapotranspiration Function

Potential evapotranspiration (PET) is the maximum amount of water that could, were it available, be lost from soil to the air (through evaporation) or to plant metabolism (through transpiration). Evapotranspiration is typically not measured. Actual evaporation is calculated inside the BASINS model, as a function of PET and available soil moisture.

Because GCM predictions are stated in terms of precipitation and temperature, it was necessary to convert temperature outputs to PET inputs. The conversion from temperature to PET was also required for creating a 69-year base weather sequence for the hydrology model, using weather stations that recorded temperature, rather than the PET time-series that the model uses. A modified Hamon method (Hamon, 1961) was used in coordination with variable monthly coefficients (Table 11) to predict PET from Portland Airport weather station temperature measurements. The predictive equation is:

PET = (monthly coefficient) * (daily saturated water vapor density).

Coefficients were selected such that they produced the best possible fit between modeled and observed PET at the Portland Airport weather station. Correlation analysis yielded R-square = 0.99 (Figure 21), validating the predictive equation.

It was assumed that the monthly coefficients derived for this location would also be appropriate for locations in Washington County.

**Table 11 - Monthly coefficients for PET, where PET = (coefficient) * (daily saturated water vapor density).**

| Month | Coefficient |
|---|---|
| January | 0.020 |
| February | 0.029 |
| March | 0.045 |
| April | 0.064 |
| May | 0.099 |
| June | 0.135 |
| July | 0.153 |
| August | 0.130 |
| September | 0.083 |
| October | 0.047 |
| November | 0.027 |
| December | 0.020 |

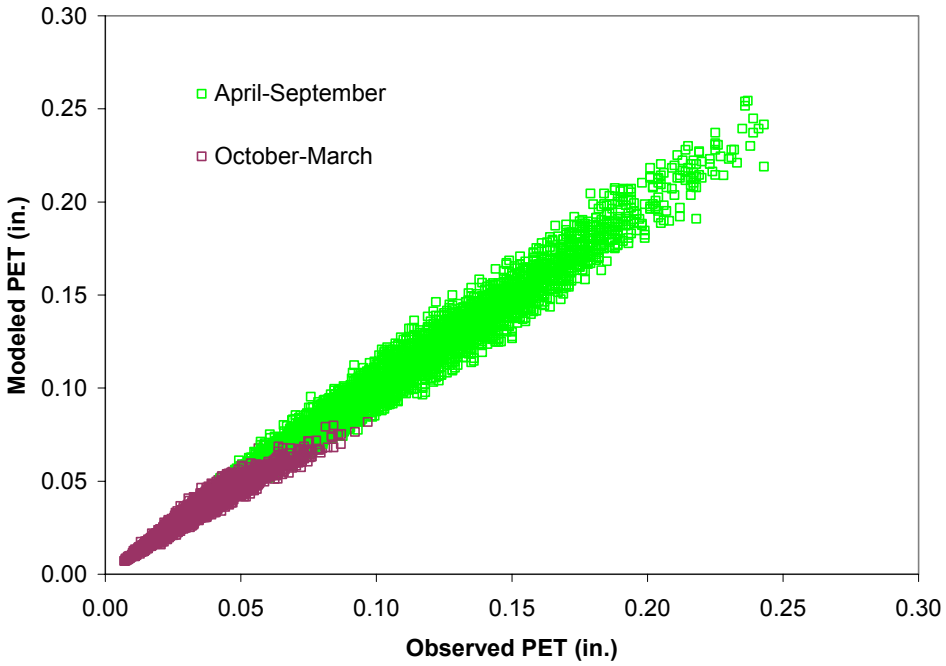


**Figure 23 - Linear regression of modeled versus observed potential evaporation. $R^2 = 0.99$.**

# 5. Model Results—BASINS Hydrology Model

An accurate hydrology model is required to evaluate the impacts of climate change. As noted previously, the EPA's BASINS hydrology model was chosen because it is user-friendly, well-documented, and widely applied.

BASINS transforms the climate-impacted meteorological data into likely streamflow scenarios in the watershed. As described in the previous section, four decadal weather timeseries were generated to represent average climate conditions during progressive 21-year periods. Each period contains the same short-term fluctuations and interannual variability as the historical record, but the means are shifted by different amounts as prescribed by the climate change model.

## *5.1. Hagg Lake Inflows*

Although climate change is expected to impact streamflows throughout the Tualatin River Basin, inflows into Henry Hagg Lake are of particular concern, as supply from this reservoir currently meets the needs of many users. Figure 24 shows the relative impacts of climate change on predicted reservoir inflows for three future periods, years 2020, 2040, and 2060, as compared to the year 2000 climate.

In the 2020 period (2010-2030), Hagg Lake inflows will decrease by less than 10%, with reductions greatest between August and January. Although total annual inflows may increase after 2020, summer inflows to the reservoir are expected to progressively decline. By the 2040 and 2060 periods, the decrease in summer flows (July-Oct) is significant and is expected to decline by more than 15% in the 2040 period and more than 20% in the 2060 period. While winter and spring inflows under 2020 and 2040 climates are lower than in the 2000 climate, it is interesting to note that February-April flows under the 2060 climate are greater than under the 2000 climate. Furthermore, the relative decrease of inflow from June-October occurs earlier and is greater than with the other modeled climate periods. This trend is shown in both Figure 24 and Figure 25.

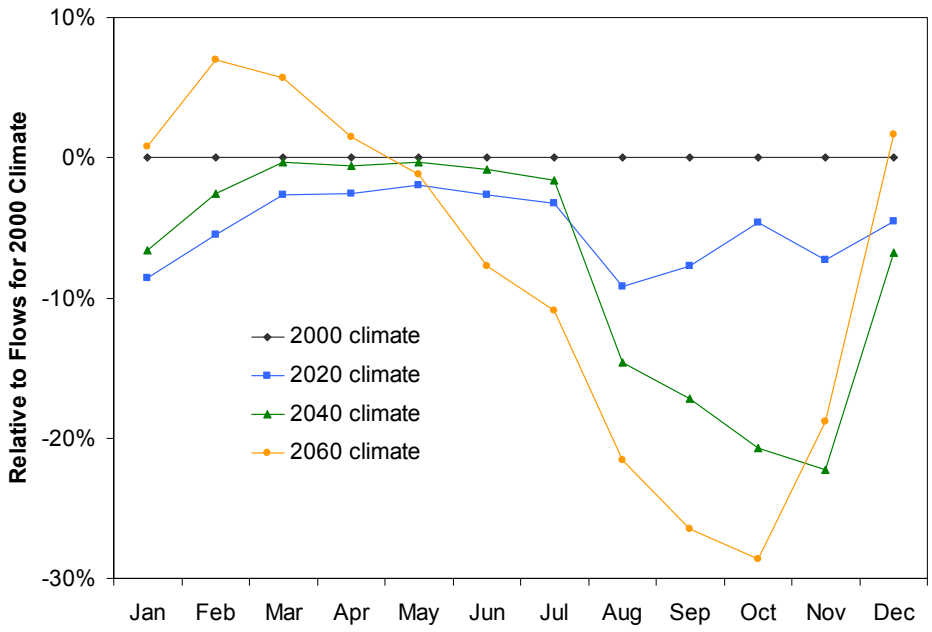


**Figure 24 - Relative change in mean monthly Hagg Lake inflows from 2020-2060 based on inflows under the 2000 climate.**

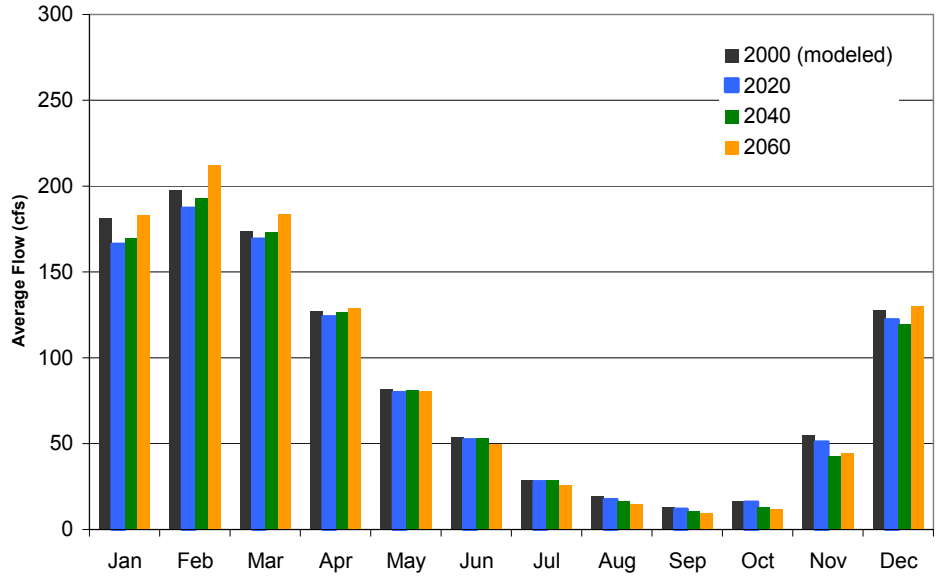


**Figure 25 - Projected mean monthly Hagg Lake inflows from 2000-2060.**

## 5.2. Distribution of Summer Flows

Although average flows are important in water resources management, the distribution of flows in high and low-flow years is also important. This information can be presented conveniently in exceedance curves, such as that shown in Figure 26. Appendix A contains exceedance curves for each node of the stream network modeled in BASINS. These curves show the expected probability that average flow past a certain point is greater than a specified level. Conversely, they show the average flow level that is expected to be met for a specified season.

Figure 26 and the other figures in Appendix A clearly show significant shifts in streamflow distribution. For the summer season, an average flow (50%) of 350 cfs in 2000 will occur only 45% of the time in 2020, 30% of the time in 2040, and 18% of the time in 2060.

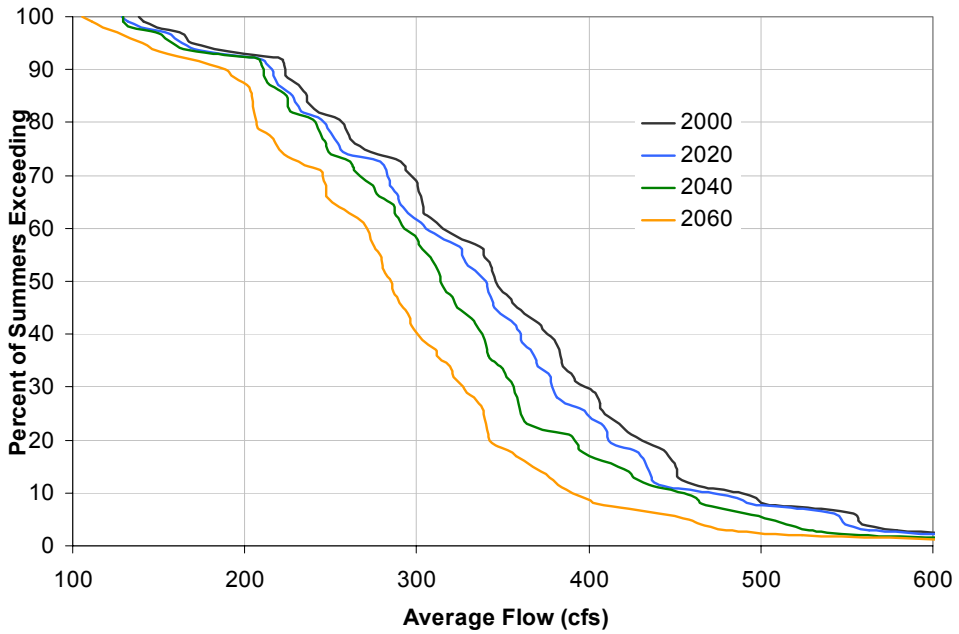


**Figure 26 - July-August exceedance curves for mean flows at West Linn on the Tualatin River for 2000, 2020, 2040, and 2060 climate periods.**

## 5.3. Sensitivity Testing

A sensitivity analysis was performed to test the separate effects of temperature change and precipitation change on streamflow. This was done to confirm that each meteorological change produced a reasonable hydrologic effect, to investigate the relative importance of the two types of meteorological change, and to help in assessing our belief that the hydrologic changes forecasted will actually occur. Specifically, it may be more likely that streamflow changes caused by increased temperatures (which GCMs predict

with a high degree of confidence) will actually occur than changes caused by altered patterns of precipitation (which GCMs predict less dependably).

The sensitivity analysis involved running the hydrology model with two sets of "hybrid climate" inputs. The first set was a combination of base case (year 2000) precipitation and perturbed (2060) PET; the second set was a combination of base case PET and perturbed precipitation. The output streamflows were compared to those produced using the regular set of base case inputs and the regular set of 2060 inputs. Differences in Hagg Lake inflow among the four runs were representative of differences across the basin.

The relative effects of temperature and precipitation on streamflows can be best shown using logarithmic plots. Figure 27 shows that May-November 2060 climate inflows are smaller than base case inflows due to the combined effects of lower rainfall and higher temperature. Although both types of changes in the climate have qualitatively similar impacts during the summer, it is worth noting that higher temperatures alone cause flows to deviate further from the base case than reduced rainfall alone does. From December-April the influence of warmer temperatures is mild and barely mediates the higher flows caused by increased rainfall.

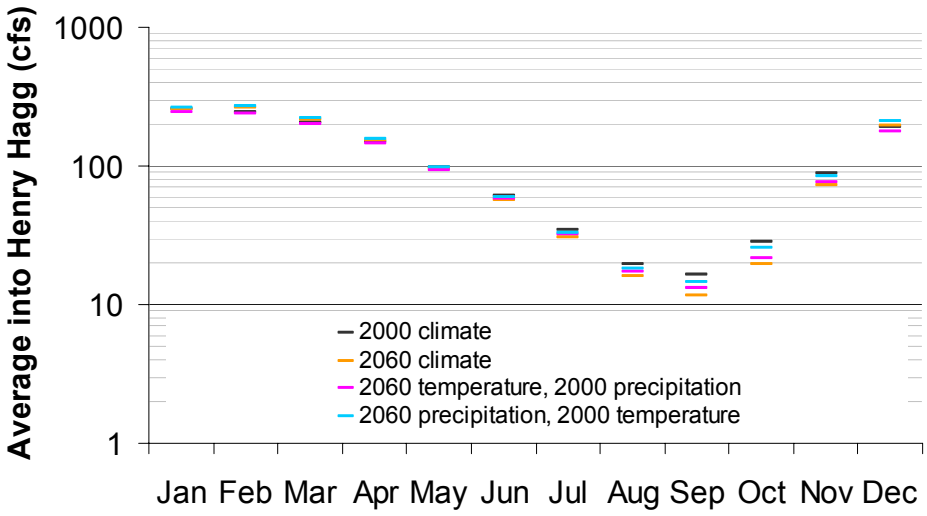


**Figure 27 - Logarithmic plot of mean Hagg Lake inflow under four scenarios: the base case (2000) climate, the 2060 climate, base case rainfall with 2060 temperatures, and base case temperatures with 2060 rainfall.**

# 6. Model Results - Tualatin River Integrated Management System Model

Safe yield is the maximum volume of water that can be withdrawn from a water resources system while still meeting all demands and instream flow requirements. Safe yield implies a system operation that is sustainable. For modest sized reservoir systems in the Pacific Northwest, this is characterized as the system refilling each year. In the case of Hagg Lake, a system failure occurs when the reservoir is drafted below active storage levels and available water supply is less than water demanded. Safe yield was calculated at four different reliability levels for each of the runs shown in Table 10:

- 98% reliable – the system fails once in the 62-year record
- 97% reliable – the system fails twice in the 62-year record
- 95% reliable – the system fails three times in the 62-year record
- 90% reliable – the system fails six times in the 62- record

Unless otherwise noted, the term "safe yield" in this report will refer to the safe yield at 97% reliability. All safe yield results are reported in Appendix C. Summaries of key results and trends are provided in sections 6.1-6.4.

## 6.1. Current System, Current Demands

The safe yield of Hagg Lake during the 2000 climate period is 37,999 acre-feet per year. Between the years 2000 and 2060, it is expected that this safe yield will decrease 1.6 % per decade (to 34,285 acre-ft in 2060) due to the impacts of climate change. This is due primarily to the decreased flows that can be expected in Scoggins Creek. The safe yield of Hagg Lake from 2000-2060 are shown at 98%, 97%, 95%, and 90% reliability in Figure 28.


**Figure 28 - Current Hagg Lake system safe yield for 2000, 2020, 2040, and 2060 climate periods at four levels of reliability.**

## 6.2. Current System, Future Demands

The safe yield of Hagg Lake decreases from current levels when contracted and forecasted 2050 demands are used (Figure 29). During the 2060 climate period the safe yield of the system with 2050 demands decreases by 28% relative to current demands, decreasing from 34,285 acre-ft to 24,571 acre-ft. The reason for this precipitous decrease is that the Montgomery-Watson 2050 demand scenarios permits Hagg Lake to release an additional 15,000 acre-ft annually to meet the Farmington flow target. In the absence of this additional Hagg Lake allocation, it is expected that the safe yield of the 2050 demand run would be similar to that of the contracted demand.

Furthermore, the percentage of annual demand that is met in each demand scenario changes with the predicted change in climate from year-2000 to year-2060. The annual

current M&I and irrigation demand is 28,571 acre-feet. At 97% reliability, 133% (37,999 acre-feet) of this amount can be met in the 2000 climate, decreasing to 120% (34,285 acre-feet) in the 2060 climate. The annual contracted M&I and irrigation demand is 40,522 acre-feet. At 97% reliability, 93% (37,685 acre-feet) of this amount can be met in the 2000 climate, decreasing to 84% (34,038 acre-feet) in the 2060 climate. The annual forecasted 2050 M&I and irrigation demand is 65,522 acre-feet. At 97% reliability, only 54% (35,054 acre-feet) of this amount can be met in the 2000 climate, decreasing to 38% (24,571 acre-feet) in the 2060 climate. These findings are shown in Table 12.

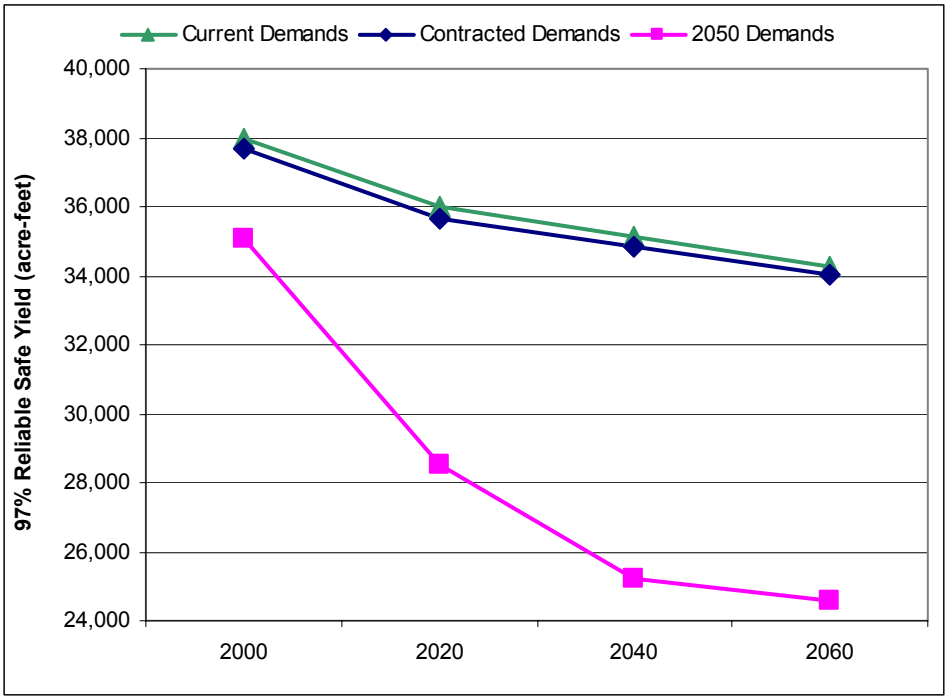


**Figure 29- Hagg Lake safe yield for 2000, 2020, 2040, and 2060 climate periods for current, contracted, and forecasted 2050 demand scenarios.**

**Table 12 - Percent of demand satisfied for each of the demand scenarios in the current Hagg Lake system.**

| | Percent of Demand Satisfied | | |
|---|---|---|---|
| **Scenario** | **Current** | **Contracted** | **2050** |
| 2000 | 133% | 93% | 54% |
| 2020 | 126% | 88% | 44% |
| 2040 | 123% | 86% | 39% |
| 2060 | 120% | 84% | 38% |

## 6.3. Alternative – Raise Scoggins Dam 20 feet

The safe yield of Hagg Lake when Scoggins Dam is raised 20 feet during the 2000 climate period is 59,428 acre-feet per year. At current levels of demand it is expected that this safe yield will decrease 1.3% per decade to 54,856 acre-feet in 2060. The safe yield of Hagg Lake from 2000-2060 at 98%, 97%, 95%, and 90% reliability are shown in Figure 30.

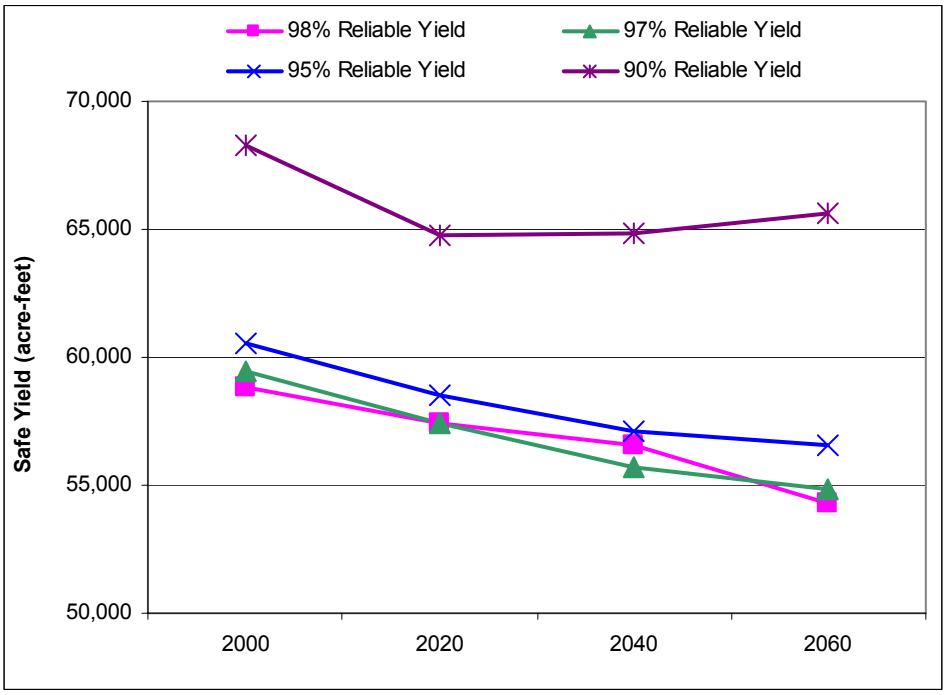


**Figure 30 - Hagg Lake system safe yield when Scoggins Dam is raised 20-feet for 2000, 2020, 2040, and 2060 climate periods at four levels of reliability.**

The safe yield of the expanded Hagg Lake increases slightly when contracted and forecasted 2050 demands are used (Figure 31). The negative impact of the 2050 demand scenario seen in the current Hagg Lake system (Figure 29) does not occur in the expanded system. When the storage capacity is increased, the increased availability of water allows for more water to be released to meet the flow target at Farmington.

The increased availability of water in the 20-foot expansion alternative greatly increases the percentage of annual demand that is met in each climate change scenario from demands met in the current Hagg Lake system. The current annual M&I and irrigation demand is 28,571 acre-feet. At 97% reliability, 208% (59,428 acre-feet) of this amount can be met in the 2000 climate, decreasing to 192% (54,856 acre-feet) in the 2060 climate. The annual contracted M&I and irrigation demand is 40,522 acre-feet. At 97% reliability, 146% (59,162 acre-feet) of this amount can be met in the 2000 climate,

decreasing to 135% (54,705 acre-feet) in the 2060 climate. The annual forecasted 2050 M&I and irrigation demand is 65,522 acre-feet. At 97% reliability, 91% (59,625 acre-feet) of this amount can be met in the 2000 climate, decreasing to 83% (54,383 acre-feet) in the 2060 climate. These findings are shown in Table 13.

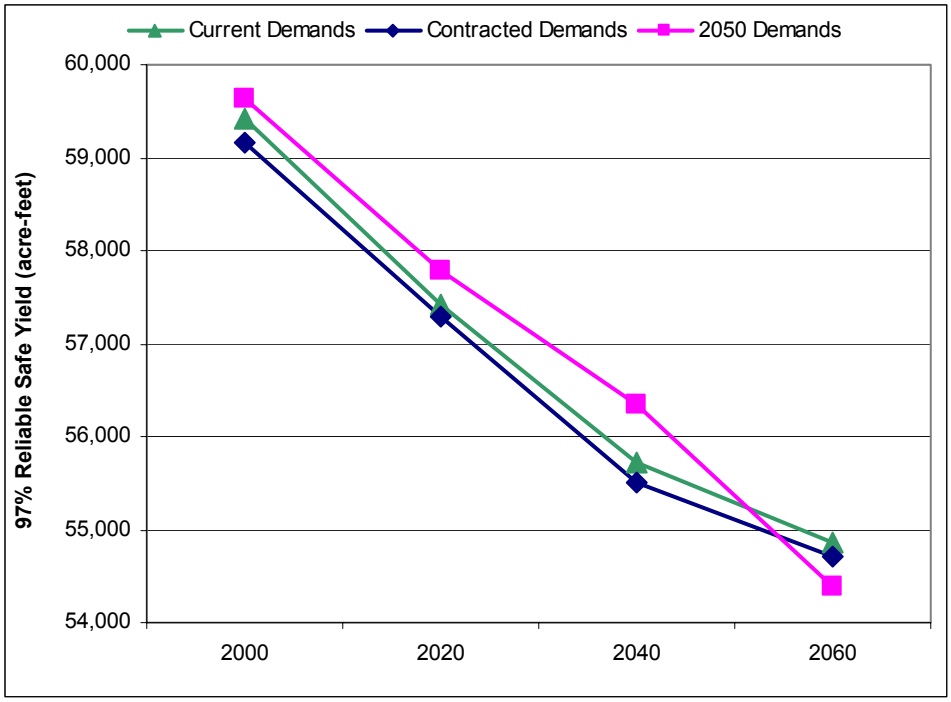


**Figure 31 - Hagg Lake safe yield when Scoggins Dam is raised 20-feet for 2000, 2020, 2040, and 2060 climate periods for current, contracted, and forecasted 2050 demand scenarios.**

**Table 13 - Percent of demand satisfied for each of the demand scenarios when Scoggins Dam is raised 20-feet.**

| | Percent of Demand Satisfied | | |
|---|---|---|---|
| **Scenario** | **Current** | **Contracted** | **2050** |
| 2000 | 208% | 146% | 91% |
| 2020 | 201% | 141% | 88% |
| 2040 | 195% | 137% | 86% |
| 2060 | 192% | 135% | 83% |

## 6.4. Alternative – Raise Scoggins Dam 40 feet

The safe yield of Hagg Lake when Scoggins Dam is raised 40 feet is 73,342 acre-feet per year during the 2000 climate period. At current levels of demand it is expected that this safe yield will decrease 0.5% per decade to 70,970 acre-feet in 2060. The safe yield of Hagg Lake from 2000-2060 at 98%, 97%, 95%, and 90% reliability are shown in Figure 32.

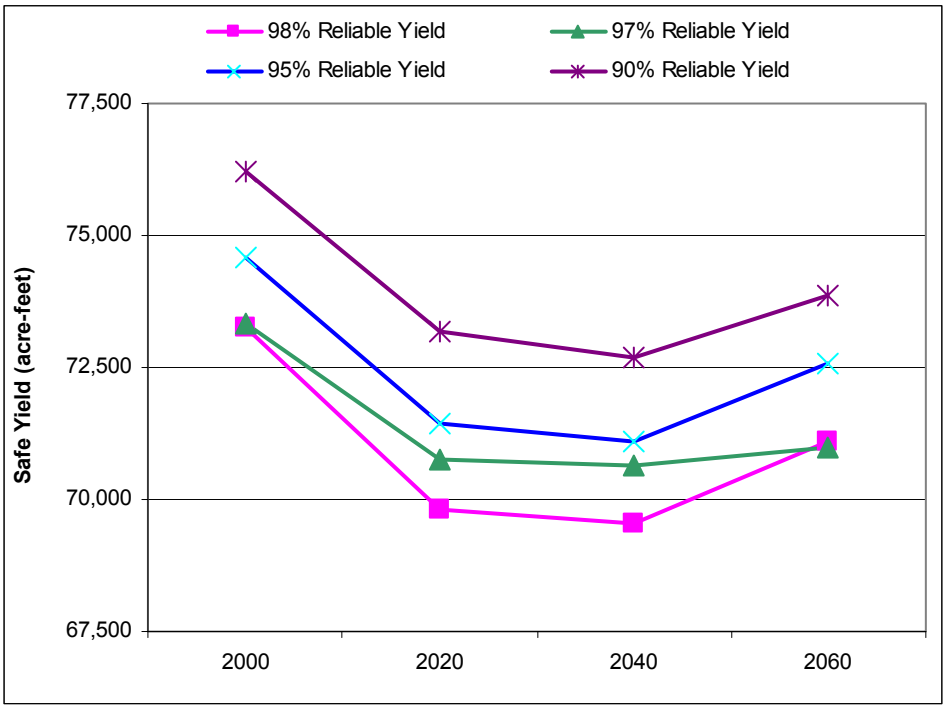


**Figure 32 - Hagg Lake system safe yield when Scoggins Dam is raised 40-feet for 2000, 2020, 2040, and 2060 climate periods at different system reliabilities.**

The increased availability of stored water in the 40-foot expansion alternative increases the percentage of annual demand that is met in each climate change scenario relative to the current system. As a result, overall safe yield of the 40-foot expansion alternative increases slightly when contracted and forecasted 2050 demands are used (Figure 33).

The safe yield during the 2060 climate period is greater than the 2040 safe yield for all demand levels. This is due to changes in temperature and precipitation during the 2060 period that results in December-April runoff greater than during the 2000 period and annual volume greater than the 2020 and 2040 periods. Because both expanded systems provide sufficient capacity to begin storing spring runoff earlier without spilling, they are generally less susceptible to changes in runoff timing and volume. This is particularly true for the 40-foot expansion where earlier runoff and greater annual runoff volume in the 2060 period results in a greater safe yield than during the 2020 and 2040 periods.

The annual current M&I and irrigation demand is 28,571 acre-feet. At 97% reliability, 257% (73,342 acre-feet) of this amount can be met in the 2000 climate, decreasing to 248% (70,970 acre-feet) in the 2060 climate. The annual contracted M&I and irrigation demand is 40,522 acre-feet. At 97% reliability, 181% (73,345 acre-feet) of this amount can be met in the 2000 climate, decreasing to 176% (71,116 acre-feet) in the 2060 climate. The annual forecasted 2050 M&I and irrigation demand is 65,522 acre-feet. At 97% reliability, 113% (73,974 acre-feet) of this amount can be met in the 2000 climate, decreasing to 111% (72,533 acre-feet) in the 2060 climate. These findings are shown in Table 14.

Only the 40-foot expansion alternative reliably provides enough water to meet at least 100% of 2050 demand under the year-2060 climate change scenario.

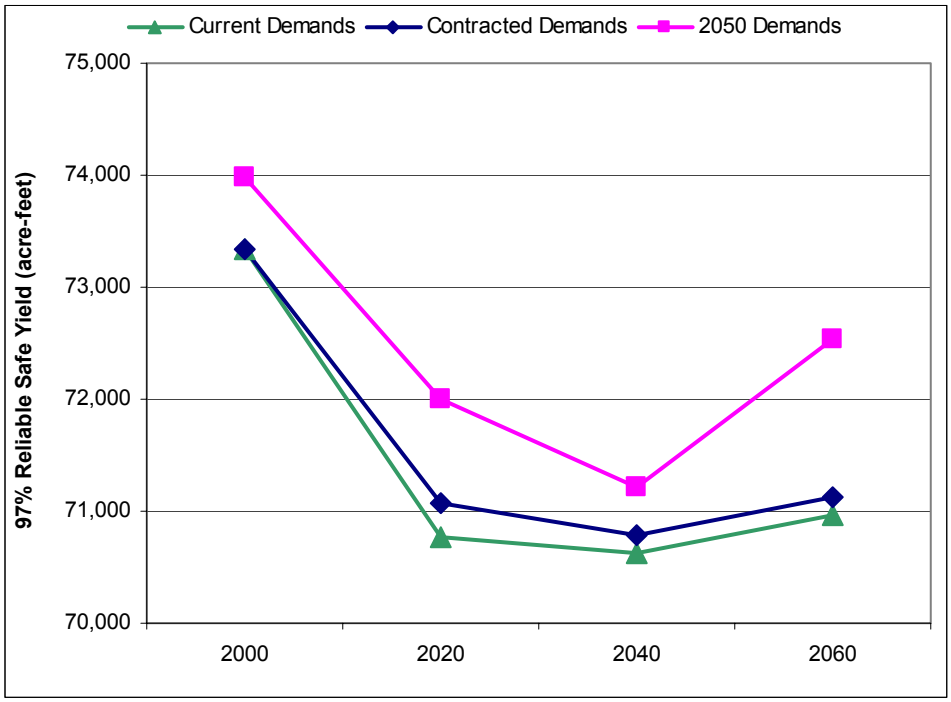


**Figure 33 - Hagg Lake safe yield when Scoggins Dam is raised 40-feet for 2000, 2020, 2040, and 2060 climate periods for current, contracted, and forecasted 2050 demand scenarios.**

**Table 14 - Percent of demand satisfied for each of the demand scenarios when Scoggins Dam is raised 40-feet.**

| | Percent of Demand Satisfied | | |
|---|---|---|---|
| **Scenario** | **Current** | **Contracted** | **2050** |
| 2000 | 257% | 181% | 113% |
| 2020 | 248% | 175% | 110% |
| 2040 | 247% | 175% | 109% |
| 2060 | 248% | 176% | 111% |

## 6.5. Alternative Evaluation – Timing of Expansion

Given projected increases in water supply demand from Hagg Lake through year 2050, it is evident that Hagg Lake will need to be expanded if the projected demands are to be met reliably in the future. Figure 34 shows the point in the future at which system modification will be required to ensure that safe yield is greater than demand (assuming linear demand growth from 2000-2060). Without the effects of climate change, the system will require modification at the following periods to ensure that safe yield exceeds total demand:

- 2013 – Current system safe yield falls below full demand
- 2043 – Safe yield of raising Scoggins Dam 20-feet falls below full demand
- 2060 (approx.) – Safe yield of raising Scoggins Dam 40-feet equals full demand

The impacts of 60 years of climate change (year-2000 to year-2060) suggest that expansion alternatives must be implemented approximately five to eight years earlier than indicated above:

- 2008 – Current system safe yield falls below full demand
- 2035 – Safe yield of raising Scoggins Dam 20-feet falls below full demand
- 2057 – Safe yield of raising Scoggins Dam 40-feet equals full demand

The clear implication is that raising Scoggins Dam 40-feet ensures that the system would be reliable for approximately 60 years. However, this alternative does not come without risk, as is discussed in the next section.

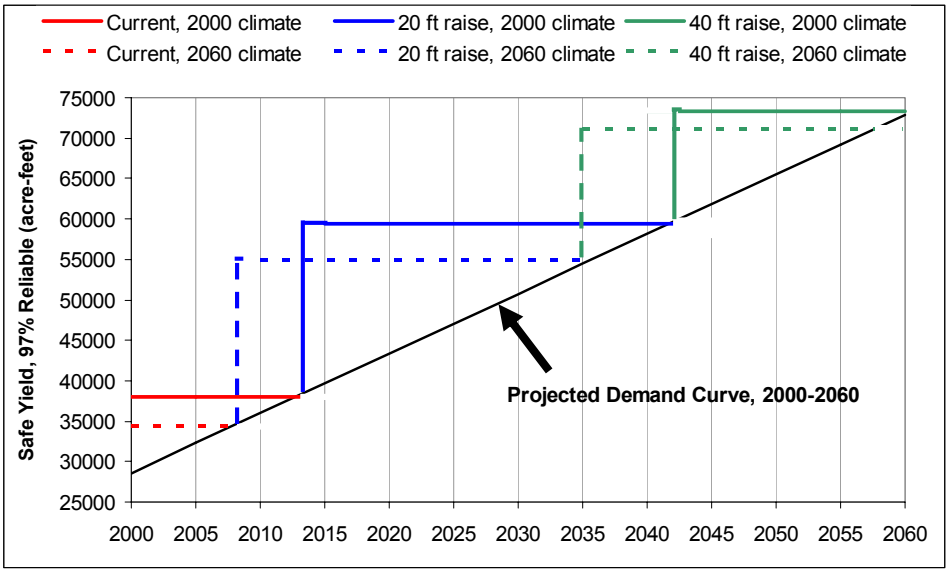


**Figure 34 - Estimated reliable life span of the current Hagg Lake system and 20-foot and 40-foot expansion alternatives given projected demands for 2000, 2020, 2040, and 2060 climate periods.**

## 6.6. Alternative Evaluation – Implications of Raising Scoggins Dam

In the current Hagg Lake system, it is expected that the reservoir will refill annually. This refill results from both the annual water demands being less than annual streamflows and from the inflow to capacity ratio being much greater than one. As shown in Figure 35, when operated at its safe yield, the reservoir refilled completely in 55 of 62 modeled years (89%) and had only one multi-year drought event (i.e., the reservoir did not refill to full capacity) from 1944-1945.

When Scoggins Dam is raised, the ability to successfully refill each year, and in years following single-year drought events, decreases substantially. For the 20-foot expansion, the reservoir refills completely in 53 of 62 modeled years (85%). As in the current system, the only multi-year drought event occurs from 1944-1945.

The storage characteristics of the 40-foot Scoggins Dam raise alternative are significantly different. Whereas the 20-foot expansion refilled to full capacity in 85% of the years, the 40-foot expansion does so only 42% of the time (26 of 62 years). Furthermore, there are six multi-year drought events during the 62-year period: 1944-1950, 1957-1958, 1962-1963, 1977-1981, 1984-1995, and 2001-2002.

The implication is that although the 40-foot expansion provides for increased opportunity to store water, there is a limit to its effectiveness. When raised 40-feet, the inflow to storage curve of the reservoir now decreases by more than half. Expanding the reservoir capacity has not only changed the amount of water that is available, but it has also changed the character of the system. Whereas a single drought year in the current system is unlikely to be followed by a second drought year, this is very likely in the expanded system. In fact, it is likely that the drought will continue for more than two years.

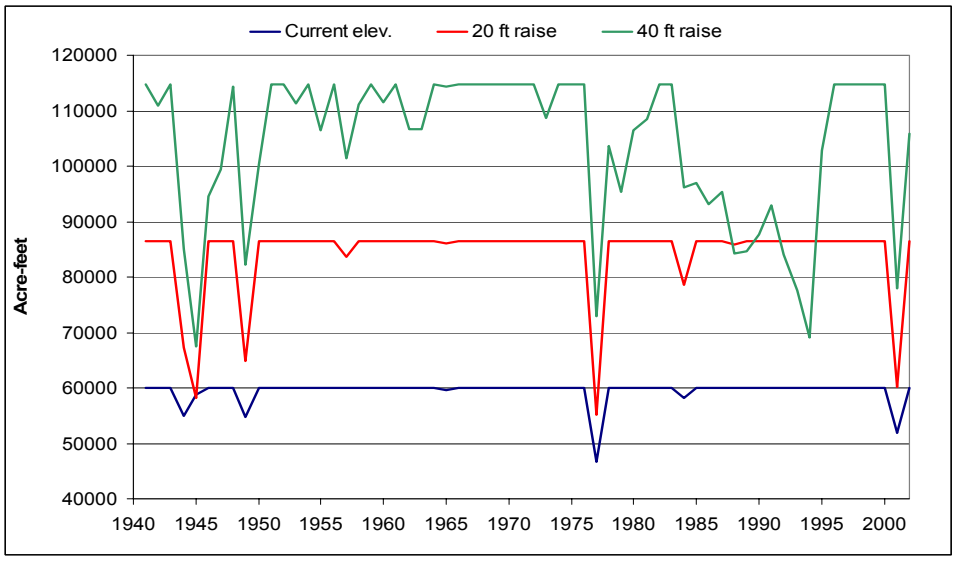


**Figure 35 - Maximum annual storage of the current Hagg Lake system and 20-foot and 40-foot Scoggins Dam raise alternatives operated at safe yield for the year-2000 climate period.**

# 7. Conclusions

This report addresses the potential future impacts of climate change on the Tualatin River Basin and the region's ability to meet current and future water demands. Although there is a growing preponderance of evidence that the earth's climate is changing, the precise nature and magnitude of change that will occur in the future in relatively small river basins is not easily estimated. To address this issue, this report presents the results of a series of loosely-integrated models that track the impacts of climate change on precipitation and temperature, streamflow, and water management.

## *7.1. Impacts on Temperature and Precipitation*

Using the average output of six General Circulation Models of global climate, it is estimated that average monthly temperatures will increased by as much as 2° F by 2040 and as much as 4° F by 2080. The increase in temperatures will be the most dramatic during the winter and summer months. Although average annual precipitation will increase in future decades, this will be due to increased precipitation in the winter months. Summer months, particularly the late summer, will become drier. This will stress the ability of the Tualatin system to meet water temperature standards and maintain instream flows.

## *7.2. Impacts on Streamflow*

The changes in precipitation and temperature will significantly influence annual streamflow patterns. By 2040, the watershed's average annual runoff will be less than its historic average. In particular, summer streamflows will decrease between ten and twenty percent. The increase in annual and winter precipitation will be overshadowed by increases in temperature. The increased temperature will increase evapotranspiration and result in much lower late-spring and summer flows. These changes will increase the duration of Hagg Lake's drawdown period, which will decrease the reliability of meeting future demands.

## *7.3. Impacts on System Yield*

During future decades, climate change will consistently and significantly impact the yield of the water supply system. The yield of the current system is expected to erode by approximately 1.5% per decade during the next forty years. This decrease in yield is relatively consistent for all levels of reliability, whether a 100% or 90% reliable yield is chosen for analysis. This is particularly important as system demands are expected to increase in the future, eventually surpassing the system yield.

### *7.3.1. System Expansion Alternatives*

Two alternatives were evaluated for increasing system yield: raising the height of Scoggins Dam by 20 feet and raising it 40 feet. If climate change is not considered, these expansions increase the 97% reliable yield from 37,999 acre-feet per year at current

levels of demand to 59,428 acre-feet (with the 20-foot expansion) to 73,342 acre-feet (with the 40-foot expansion).

If climate change projections for 2040 are considered, the expansions will increase the 97% reliable yield from 35,142 acre-feet per year at current levels of demand to 55,713 acre-feet (with the 20-foot expansion) and to 70,628 acre-feet (with the 40-foot expansion), respectively.

### *7.3.2. Timing of System Expansion Alternatives*

If it is desirable to provide sufficient storage to attempt to meet future demands, expansion will be necessary. Without considering climate impacts, and using the 97% reliable yield as a standard, it will be necessary to expand the system by 20 feet by 2013 and to 40 feet by 2043. If the impacts of climate change are considered and an equal level of reliability is desired, the 20-foot expansion is needed by 2008 and the 40-foot expansion is needed by 2035. This indicates that the impacts of climate change will increase the time by which the expansions are needed by five to eight years. In the simplest terms, climate change requires expansions of the current system sooner than if climate change did not occur.

## *7.4. Nature of Droughts*

As the impacts of climate change are felt and as the system capacity is increased to meet larger demands, the Tualatin basin will encounter dramatically different types of droughts and reservoir operations. Currently, the system refills almost every year, with drawdown periods longer than a year being unusual. If the system attempts to meet increased demands in the future by significantly increasing its capacity, it is anticipated that system refill will become far less likely on an annual basis, multi-year draw-downs will be common, and the impacts of extended droughts may be much more significant. This will be a result of attempting to meet larger systems demands with smaller annual runoff. System management must adjust to deal with these changing characteristics. The development of a well-defined adaptive drought management plan will be essential.

# 8. References


Alexandersson, H., Schmith, T., Iden, K., and Tuomenvirta, H. (2000). "Trends in storms in NW Europe derived from an updated pressure data set." *Climate Research*, 14, 71-73.

Angel, J.R. and Isard, S.A (1998). "The frequency and intensity of Great Lake cyclones." *Journal of Climate*, 11, 61-71.

Barnola, J.M., Anklin, M., Porcheron, J., Raynaud, D., Schwander, and Stauffer, B. (1995). "$CO_2$ evolution during the last millennium as recorded by Antarctic and Greenland ice." *Tellus Series B-Chemical and Physical Meteorology*, 47, 264-272.

Chalecki, E.L. and Gleick, P.H. (1999). "A Framework of Ordered Climate Effects on Water Resources: A Comprehensive Bibliography." *Journal of the American Water Resource Association*, 25(6), 1657-1665.

Charles, S.P., Bates, B.C., Whetton, P.H., and Hughes, J.P. (1999). "Validation of downscaling models for changed climate conditions: Case study of Southwestern Australia." *Climate Research*, 12, 1-14.

Covey, C., Achuta-Rao, K.M., Cubasch, U., Jones, P., Lambert, S.J., Mann, M.E., Phillips, T.J., and Taylor, K.E. (2000). "An overview of results from the Coupled Model Intercomparison Project (CMIP)." *Global and Planetary Change,* 30.

Cox, P.M., Betts, R.A., Bunton, C.B., Essery, R.L.H., Rowntree, P.R., Smith, J. (1999). "The impact of new land surface physics on the GCM simulation of climate and climate sensitivity." *Climate Dynamics*, 15(3), 183-203.

Etheridge, D.M., Steele, L.P., Langenfelds, R.L., Francey, R.J., Barnola, J.M., and Morgan, V.I. (1996). "Natural and anthropogenic changes in atmospheric $CO_2$ over the last 1000 years from air in Antarctic ice and fern". *Journal of Geophysical Research - Atmosphere*, 101, 4115-4128.

Frederick, K.D., and Major, D.C. (1997). "Climate change and water resources." *Climatic Change*, 37, 7-23

Flato, G.M. and Boer, G.J. (2001). "Warming asymmetry in climate change simulations." *Geophysical Research Letters*, 28, 195-198.

Giorgi, F. and Mearns, L.O. (2002). "Calculation of average, uncertainty range, and reliability of regional climate changes from AOGCM simulations via the 'Reliability Ensemble Averaging' (REA) method." *Journal of Climate*, 15, 1141-1158.

Gleick, P. H. (2000). *Water: The potential consequences of climate variability and change for the water resources of the United States*, Report of the Water Sector Assessment Team of the National Assessment of the Potential Consequences of Climate Variability and Change, Pacific Institute, Berkeley, CA.

Gordon, C., Cooper, C., Senior, C.A., Banks, H.T., Gregory, J.M., Johns, T.C., Mitchell, J.F.B., and Wood, R.A. (2000). "The simulation of SST, sea ice extents and ocean heat transports in a version of the Hadley Centre coupled model without flux adjustments." *Climate Dynamics*, 16, 147-168.

Gordon, H.B. and O'Farrell, S.P. (1997). "Transient climate change in the CSIRO coupled model with dynamic sea ice." *Monthly Weather Review*, 125, 875-907.

Graham, N.E. and Diaz, H.F. (2001). "Evidence for intensification of North Pacific winter cyclones since 1948." *Bulletin of the American Meteorological Society*, 82(9), 1869-1893.

Hahn, M.A., Palmer, R.N., Hamlet, A.F., and Storck, P. (2001). "A preliminary analysis of the impacts of climate change on the reliability of the Seattle water supply." *Proceedings of the World Water and Environmental Resources Congress*. Orlando, Florida, May.

Hamon, R.W. (1961). "Estimating potential evapotranspiration," *ASCE Proceedings*, 87, HY3, 107-120.

Hewitson, B.C. and Crane, R.G. (1996). "Climate downscaling: techniques and applications." *Climate Research*, 7, 85-95.

Intergovernmental Panel on Climate Change (IPCC). (1996). *Climate Change 1995: The Science of climate Change: Contribution of Working Group I to the Second Assessment Report of the Intergovernmental Panel on Climate Change*. J.T. Houghton, L.G. Meira Filho, B.A. Callander, N. Harris, A. Kattenberg, and K. Maskell (eds.), Cambridge University Press: Cambridge.

Intergovernmental Panel on Climate Change (IPCC). (2001). *Climate Change 2001, The Scientific Basis," The Contribution of Working Group I to the Third Assessment Report of the Intergovernmental Panel on Climate Change*. F. Joos, A. Rohas-Ramirez, J.M.R. Stone, J. Zillman (eds.), Cambridge University Press: Cambridge.

Karl, T.R. and Knight, R.W. (1998). "Secular trends of precipitation amount, frequency and intensity in the United States." *Bulletin of the American Meteorological Society*, 79, 321-241.

Keyes, A.M. and Palmer, R.N. (1993). "The role of object-oriented simulation models in the drought preparedness studies." *Proceedings of the 20th Annual National Conference, Water Resources Planning and Management Division of ASCE*, Seattle, WA, 479-482.

Kidson, J.W. and Thompson, C. S. (1998). "A comparison of statistical and model-based downscaling techniques for estimating local climate variations." *Journal of Climate*, 11(4), 735-753.

Knutson, T.R., Delworh, T.L., Dixon, K.W., and Stouffer, R.J. (1999). "Model assessment of regional surface temperature trends (1949-1997)." *Journal of Geophysical. Research*, 104, 30981-30996.

Kowalczyk, E.A., Garratt, J.R., and Krummel, P.B. (1994). *Implementation of a Soil-Canopy Scheme into the CSIRO GCM*. CSIRO Division of Atmospheric Research: Victoria, Australia.

Lambert, S.J. (1996). "Intense extratopical Northern Hemisphere winter cyclone events: 1189-1991." *Journal of Geophysical Research*, 101, 21319-21325.

Leggett, J.A., Pepper, W.J., and Swart, R.J. (1992). "Emissions scenarios for the IPCC: An update." pp. 69-95 in *Climate Change 1992*. J.T. Houghton, B.A. Callander and S.K. Varney (eds.). Cambridge University Press: Cambridge.

Lettenmaier, D.P. and Gan, T-Y. (1990). "Hydrologic sensitivities of the Sacramento-San Joaquin River Basin, California, to global warming," *Water Resources Research*, 26, 69-86.

Lettenmaier, D.P., Wood, A.W., Palmer, R.N., Wood, E.F., and Stakiv, E.Z. (1999). "Water Resources implications of Global Warming: A U.S. regional perspective," *Climatic Change*, 43, 537-579.

Mann, M.E., Bradley, R.S., and Hughes, M.K. (1999). "Northern Hemisphere temperatures during the past millennium: Inferences, uncertainties, and limitations." *Geophysical Research Letters*, 26, 759-762.

Mearns, L.O., Georgi, F., McDaniel, L., and Shields, C. (1994). "Analysis of daily variability of precipitation in a nested regional climate mode: comparison with observations and doubled CO2 results." *Global and Planetary Change*, 10, 55-78.

Mote, P., Canning, D., Fluharty, D., Francis, R., Franklin, J., Hamlet, A., Hershman, M., Holmberg, M., Gray-Ideker, K., Keeton, W.S., Lettenmaier, D., Leung, R., Mantua, N., Miles, E., Noble, B., Parandvash, H., Peterson, D.W., Snover, A., and Willard, S. (1999). *Impacts of Climate Variability and Change, Pacific Northwest*. National Atmospheric and Oceanic Administration, Office of Global Programs, and JISAO/SMA Climate Impacts Group, Seattle, WA.

Murdock, R. (2003). *Water Supply Feasibility Study, Techical Memorandum – Tualatin River Water Balance Model: Documentation and Results (Draft)*, Prepared by Montgomery-Watson for Clean Water Services, November 10.

Murphy, J. (1997). "An evaluation of statistical and dynamical techniques for downscaling local climate." *Journal of Climate*, 12, 8, 2256-2284.

Nash, L.L. and Gleick, P.H. (1993). *The Colorado River Basin and Climatic Change*. EPA230-R-93-009. U.S. Environmental Protection Agency, Washington D.C.

Palmer, R.N., and Hahn, M. (2002). *The Impacts of Climate Change on Portland's Water Supply: An Investigation of Potential Hydrologic and Management Impacts on the Bull Run System*. Report to the Portland Water Bureau, Portland, Oregon.

Payne, J.T., Wood, A.W., Hamlet, A.F., Palmer, R.N. and Lettenmaier, D.P. (2004). "Mitigating the effects of climate change on the water resources of the Columbia River basin." *Climatic Change*, 62(1-3), 233-256.

Roeckner, E., Arpe, K., Bengtsson, L., Christoph, M., Claussen, M., Dümenil, L., Esch, M., Giorgetta, M., Schlese, U., and Schulzweida, U. (1996). *The atmospheric general circulation model ECHAM4: Model description and simulation of present-day climate*. MPI Report No. 218, Max-Planck-Institut für Meteorologie: Hamburg, Germany.

Schneider, S.H., Gleick, P.H., and Mearns, L.O. (1990). "Prospects for Climate Change," pp. 41-73 in *Climate Change and U.S. Water Resources*, P.E. Waggoner (ed.), John Wiley and Sons: New York.

Siegenthaler, U., Friedli, H., Loetscher, H., Moor, E., Neftel, A., Oeschger, H. and Stauffer, B. (1988). "Stable-isotope ratios and concentration of $CO_2$ in air from polar ice cores." *Annals of Glaciology*, 10, 1-6.

Smith J.B. and Tirpak, D.A. (eds.). (1989). *The potential effects of global climate change on the United States*, Office of Policy, Planning, and Evaluation, U.S. Environmental Protection Agency.

SRES. (2000). *SRES 2000, Special Report on Emissions Scenarios, A Special Report of Working Group III of the Intergovernmental Panel on Climate Change*, Nakicenovic, Nebojsa and Swart, Rob (eds.), Cambridge University Press: New York.

United States Bureau of Reclamation (USBOR). (2002). *Tualatin Project, Oregon: Facilities and Operation and Maintenance*, U.S. Department of the Interior, Lower Columbia Area Office, Portland, Oregon.

United States Environmental Protection Agency (USEPA). (2001). *Better Assessment Science Integrating point and Nonpoint Sources: BASINS 3.0 User's Manual*, Office of Water, EPA-823-B-01-001.

VanderPlaat, T. (2003). Personal email communication on October 9.

VanRheenen, N.T., Wood, A.W., Palmer, R.N., and Lettenmaier, D.P. (2004). "Potential implications of PCM climate change scenarios for Sacramento - San Joaquin River Basin hydrology and water resources." *Climatic Change*, 62(1-3), 257-281.

Washington, W.M., Weatherly, J.W., Meehl, G.A., Semtner, A.J., Bettge, T.W., Craig, A.P., Strand, W.G., Arblaster, J., Wayland, V.B., James, R., and Zhang, Y. (2000). "Parallel climate model (PCM) control and transient simulations." *Climate Dynamics*, 16, 755-774.

Wilby, R.L., Wigley, M.L., Conway, D., Jones, P.D., Hewitson, B.C., Main, J., and Wilks, D.S. (1998). "Statistical downscaling of general circulation model output: A comparison of methods." *Water Resources Research*, 34(11), 2998-3008.

Wiley, M.W., Palmer, R.N., and Kame'enui, A.E. (2004). *Developing Analysis Techniques to Incorporate Climate Change Information into Seattle's Long Range Water Supply Planning.* Draft report to the City of Seattle Public Utilities Department, Seattle, Washington. University of Washington, Department of Civil and Environmental Engineering.

Wood, A.W., Lettenmaier, D.P., and Palmer, R.N. (1997). "Assessing climate change implications for water resource planning." *Climatic Change*, 37, 203-228.

# Appendix A

**Table 1** – Percentage of years in the 63 year modeling period that July-October year-2000 mean monthly flow is met during different climate periods.

| Location | Percentage of years when July-October year-2000 median average flow is met | | |
|---|---|---|---|
| | **2020 climate** | **2040 climate** | **2060 climate** |
| Tualatin at West Linn | 45 | 35 | 19 |
| Scoggins Creek below Hagg Lake | 45 | 36 | 19 |
| Tualatin River at Dilley | 48 | 42 | 31 |
| Mouth of Dairy Creek | 47 | 37 | 19 |
| Mouth of Rock Creek | 46 | 36 | 31 |
| Tualatin River at Highway 10 | 44 | 32 | 18 |
| Tualatin River after confluence with Fanno Creek | 45 | 35 | 19 |
| Tualatin River directly south of Lake Oswego | 45 | 35 | 19 |
| Mouth of Gales Creek | 46 | 44 | 35 |
| Mouth of Fanno Creek | 45 | 34 | 31 |

**Table 2** – Percentage of years in the 63 year modeling period that July-October flows are less than the year-2000 10-year low flow.

| Location | Percentage of years when July-October flows are less than year-2000 10-year low flows | | |
|---|---|---|---|
| | **2020 climate** | **2040 climate** | **2060 climate** |
| Tualatin at West Linn | 14 | 15 | 26 |
| Scoggins Creek below Hagg Lake | 18 | 18 | 23 |
| Tualatin River at Dilley | 11 | 12 | 16 |
| Mouth of Dairy Creek | 15 | 16 | 22 |
| Mouth of Rock Creek | 10 | 13 | 17 |
| Tualatin River at Highway 10 | 13 | 14 | 25 |
| Tualatin River after confluence with Fanno Creek | 14 | 16 | 26 |
| Tualatin River directly south of Lake Oswego | 14 | 15 | 26 |
| Mouth of Gales Creek | 14 | 13 | 16 |
| Mouth of Fanno Creek | 11 | 12 | 19 |

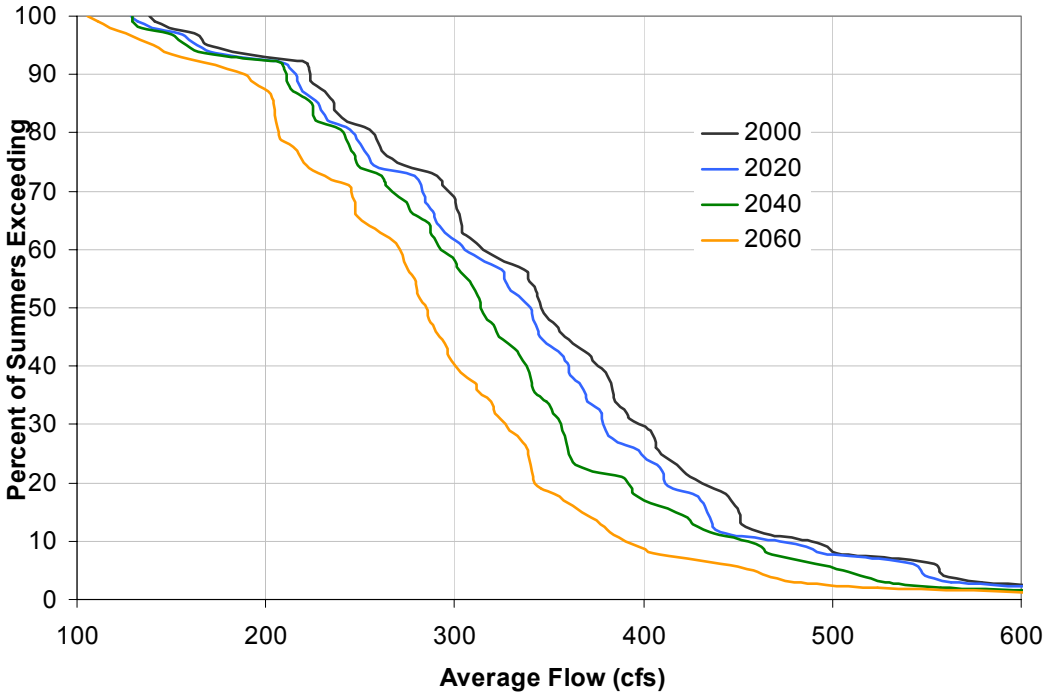


**Figure 1** – July-October exceedance curves of mean flows at West Linn on the Tualatin River for 2000, 2020, 2040, and 2060 climate periods.

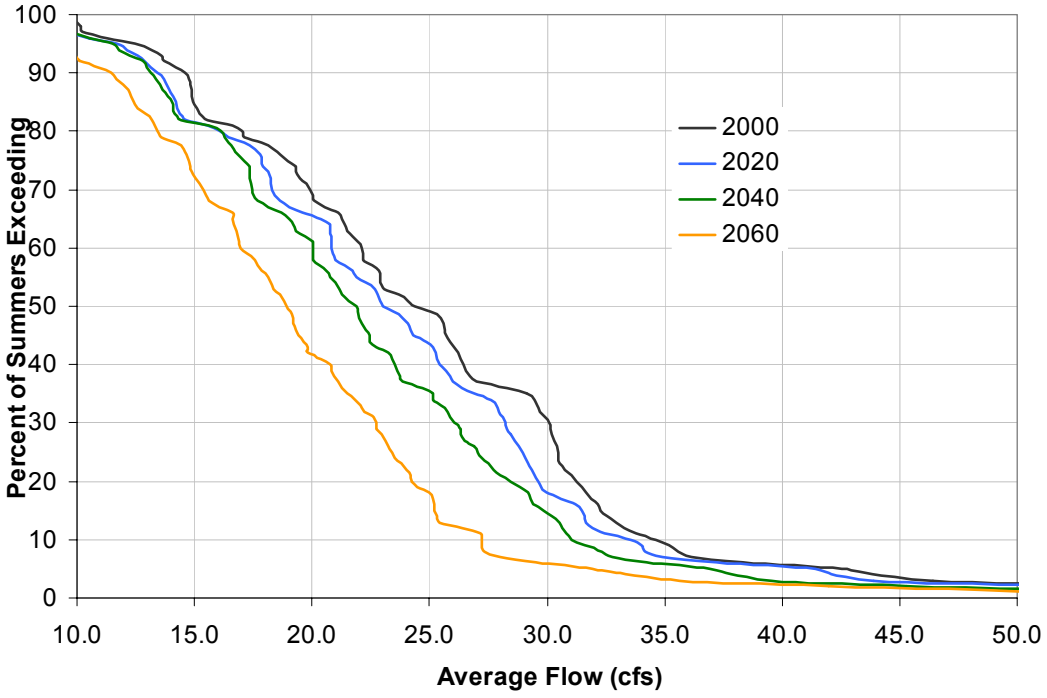


**Figure 2** – July-October exceedance curves of mean flows below Hagg Lake on Scoggins Creek for 2000, 2020, 2040, and 2060 climate periods.

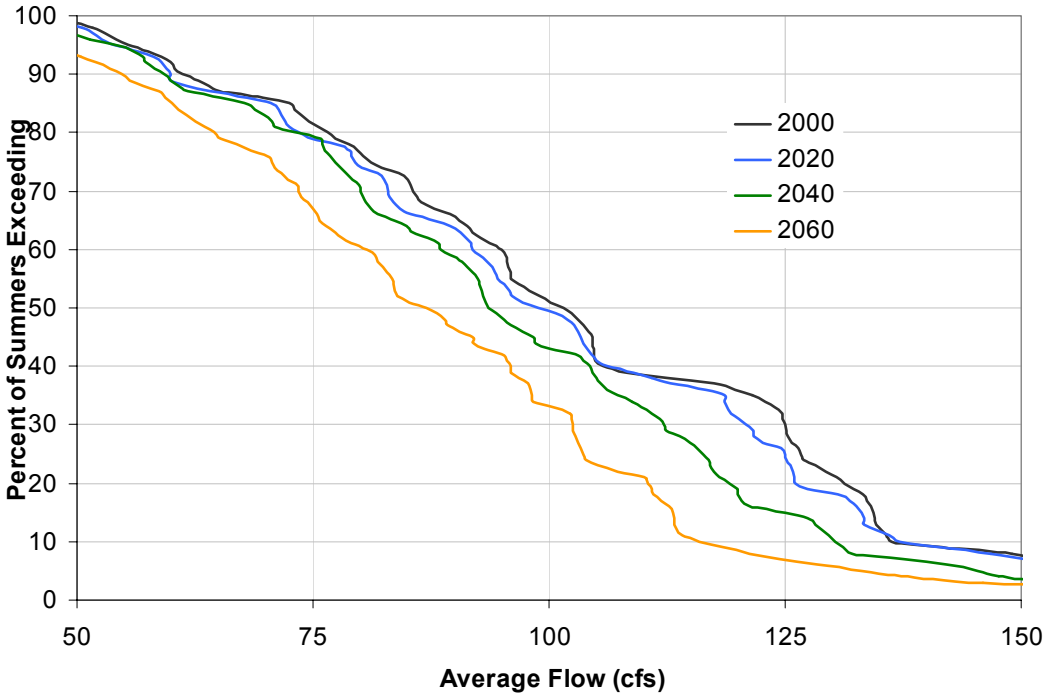


**Figure 3** – July-October exceedance curves of mean flows at Dilley on the Tualatin River for 2000, 2020, 2040, and 2060 climate periods.

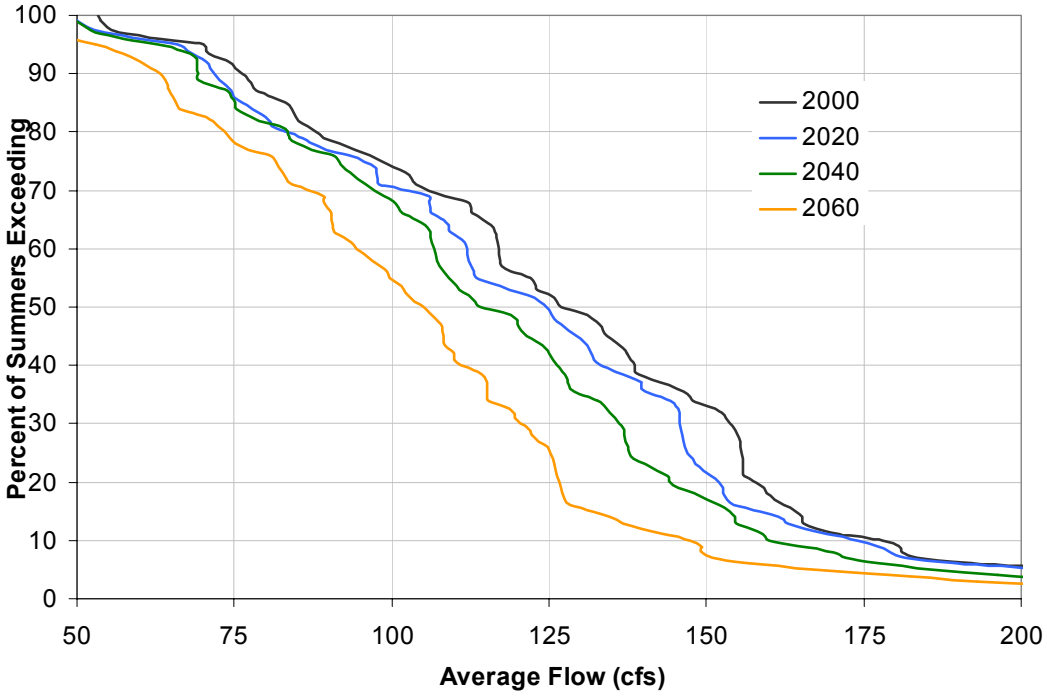


**Figure 4** – July-October exceedance curves of mean flows at the mouth of Dairy Creek for 2000, 2020, 2040, and 2060 climate periods.

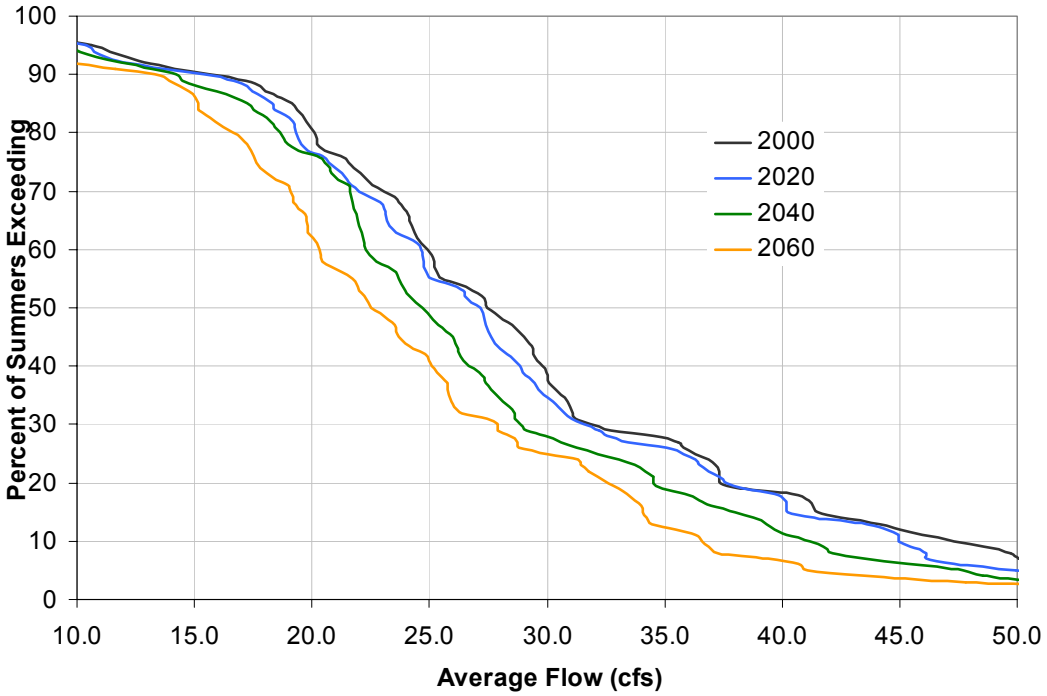


**Figure 5** – July-October exceedance curves of mean flows at the mouth of Rock Creek for 2000, 2020, 2040, and 2060 climate periods.

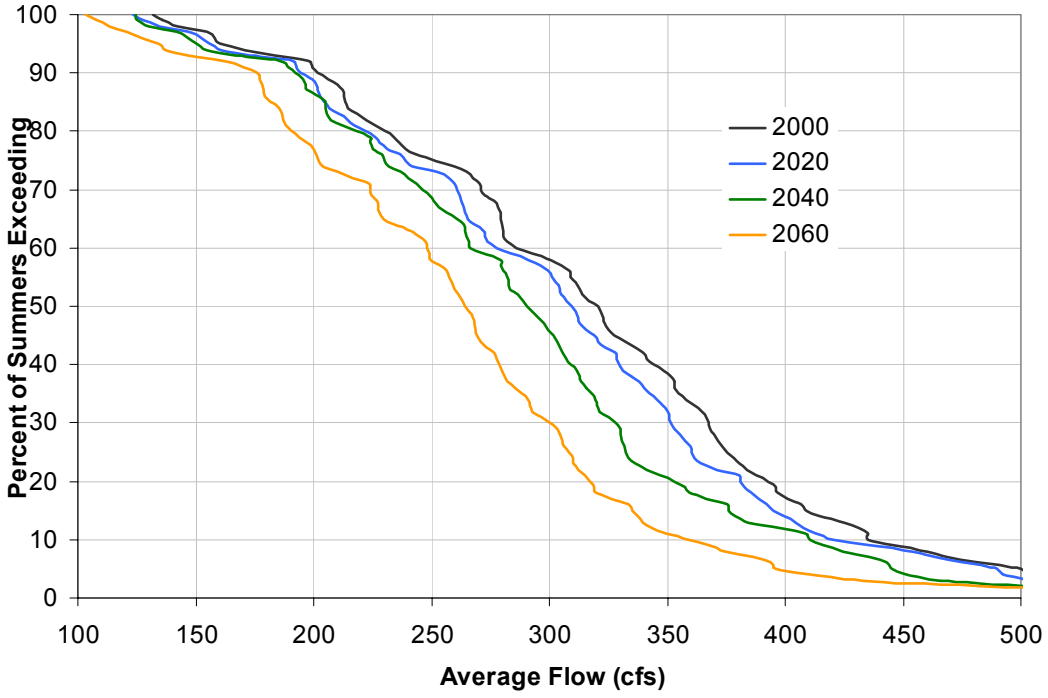


**Figure 6** – July-October exceedance curves of mean flows at the Tualatin River at Highway 10 for 2000, 2020, 2040, and 2060 climate periods.

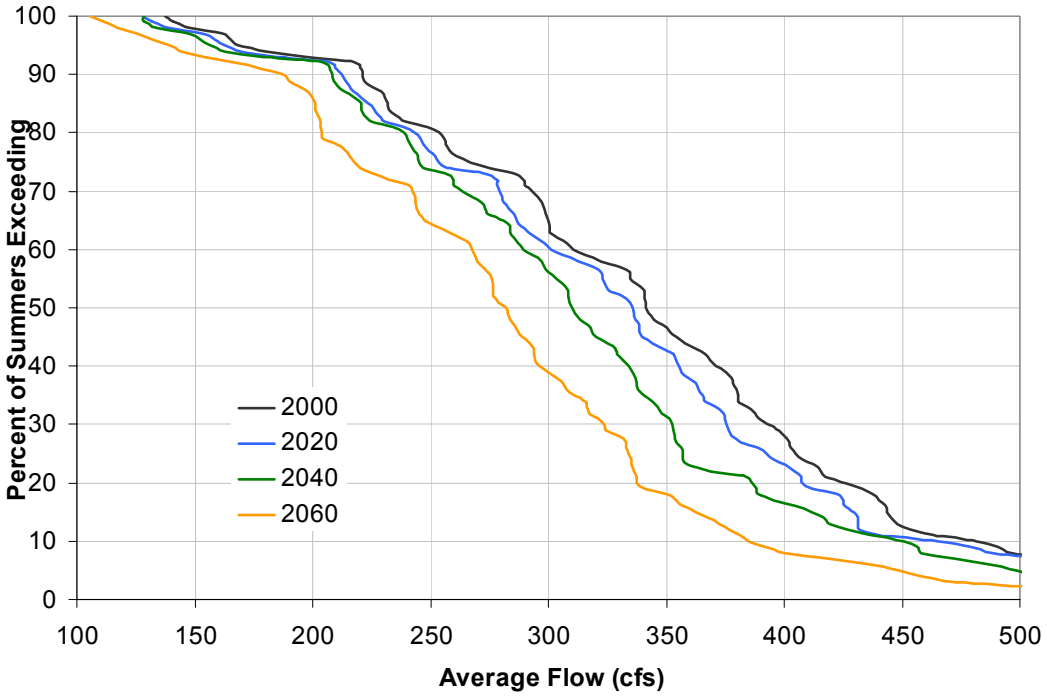


**Figure 7** – July-October exceedance curves of mean flows at the Tualatin River-Fanno Creek confluence for 2000, 2020, 2040, and 2060 climate periods.

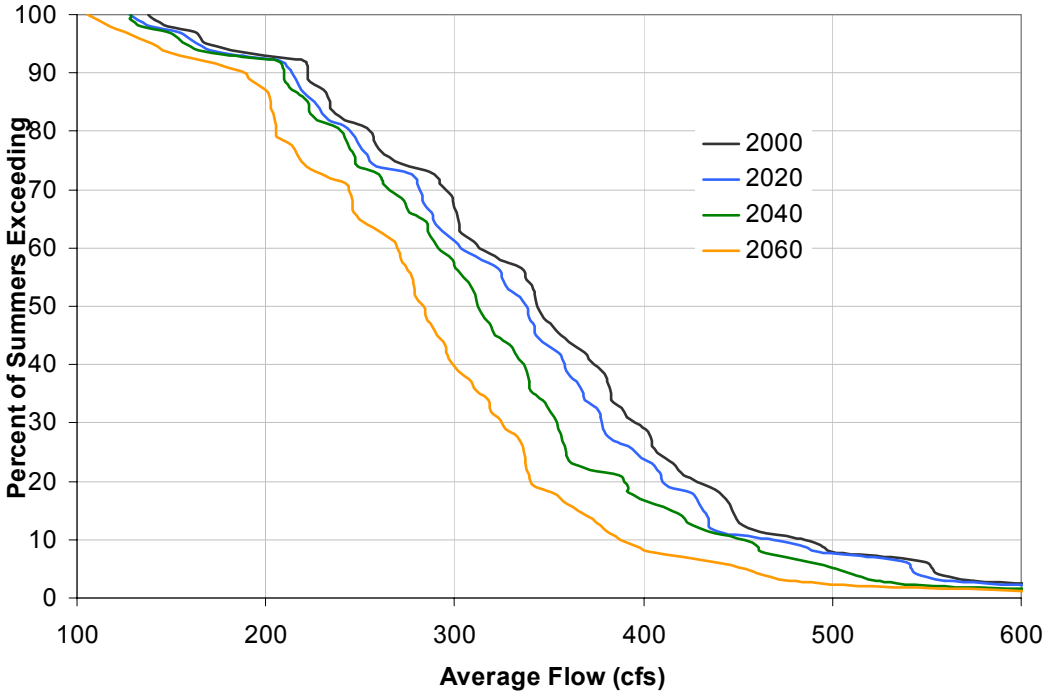


**Figure 8** – July-October exceedance curves of mean flows at the Tualatin River south of Lake Oswego for 2000, 2020, 2040, and 2060 climate periods.

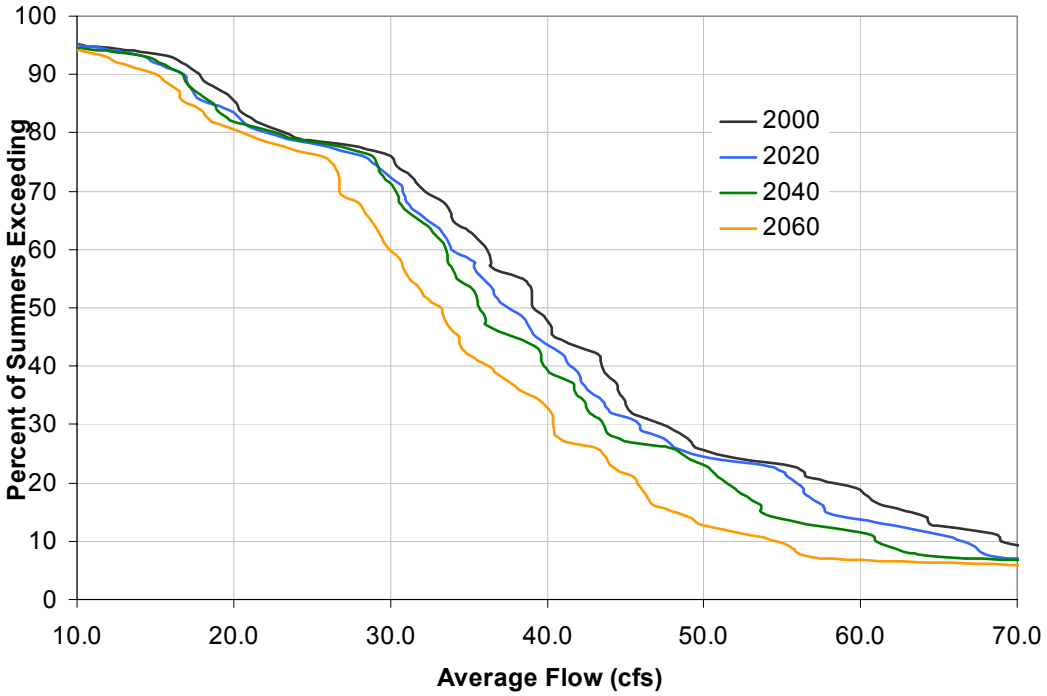


**Figure 9** – July-October exceedance curves of mean flows at the mouth of Gales Creek for 2000, 2020, 2040, and 2060 climate periods.

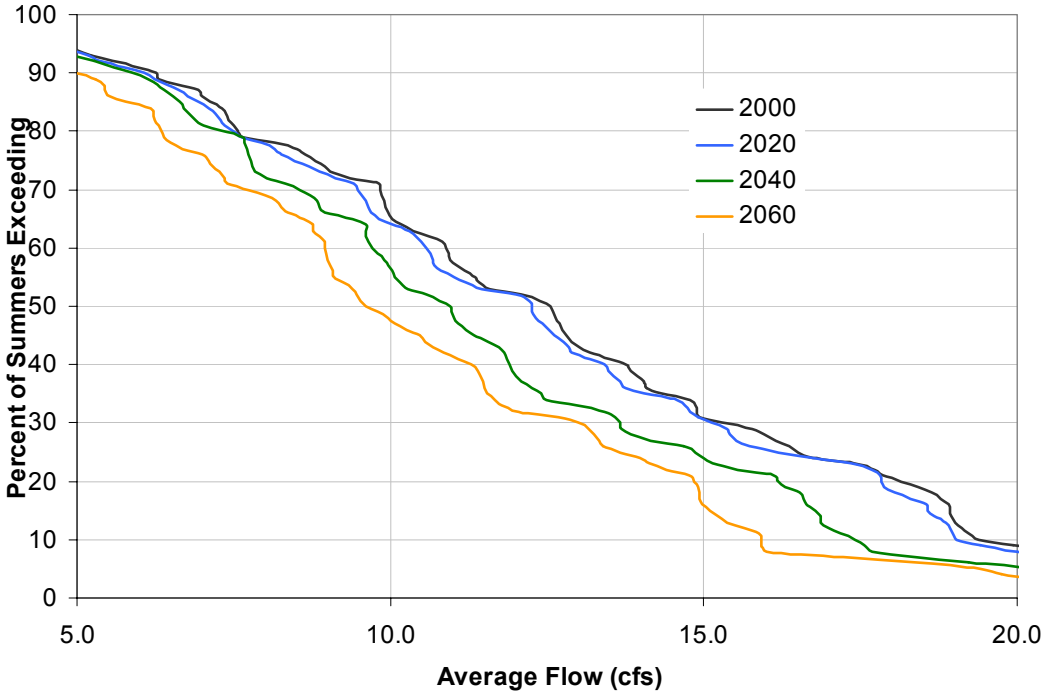


**Figure 10** – July-October exceedance curves of mean flows at the mouth of Fanno Creek for 2000, 2020, 2040, and 2060 climate periods.

# Appendix B

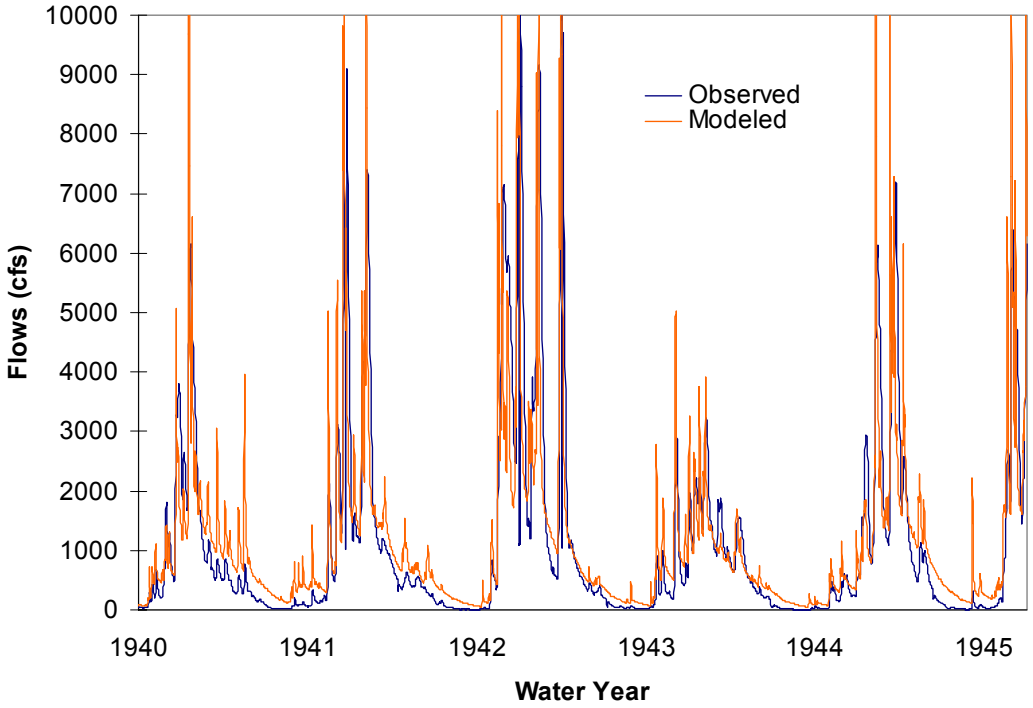


**Figure 1** - Observed (USGS gage 14207500) and BASINS calibrated flows at the mouth of the Tualatin River.

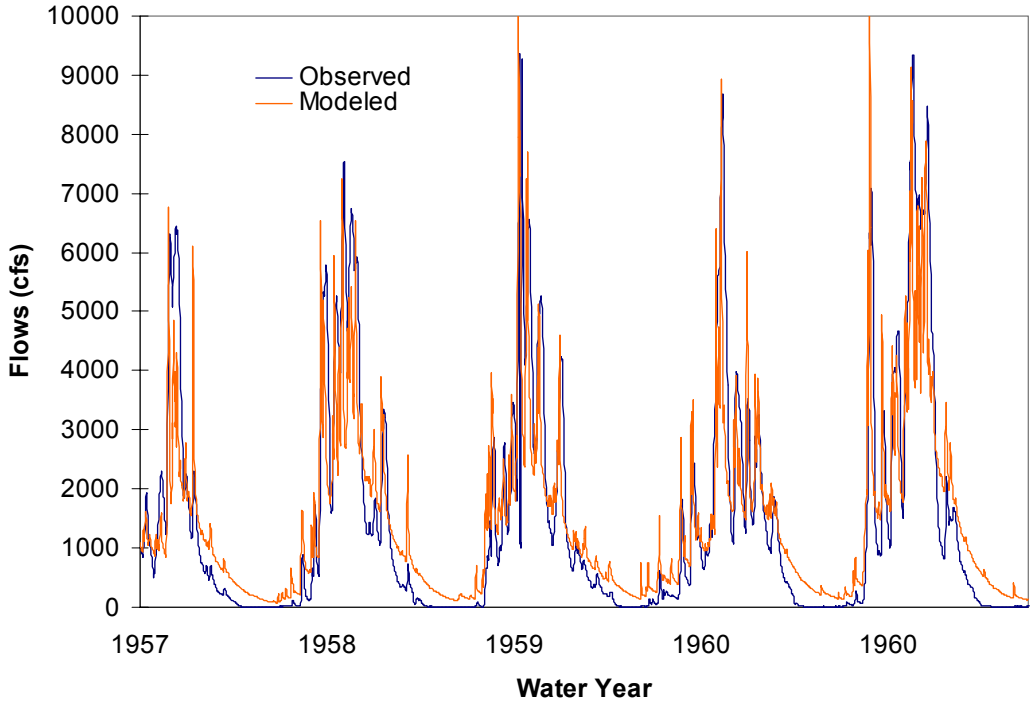


**Figure 2** - Observed (USGS gage 14207500) and BASINS validated flows at the mouth of the Tualatin River.

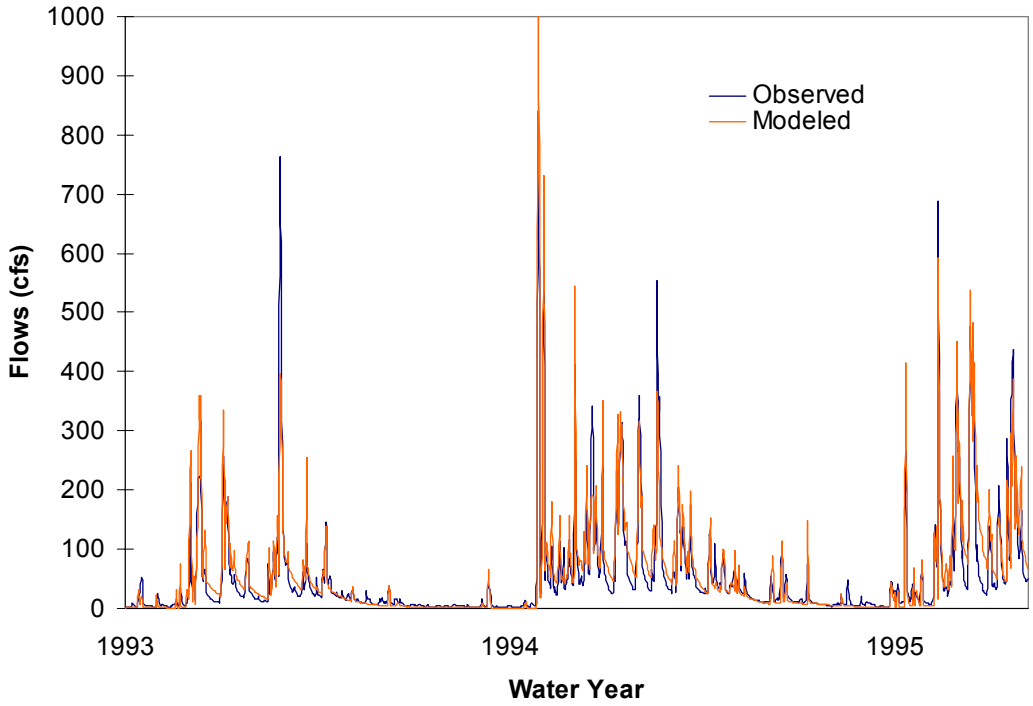


**Figure 3** - Observed (USGS gage 14206950) and BASINS calibrated flows at Fanno Creek.

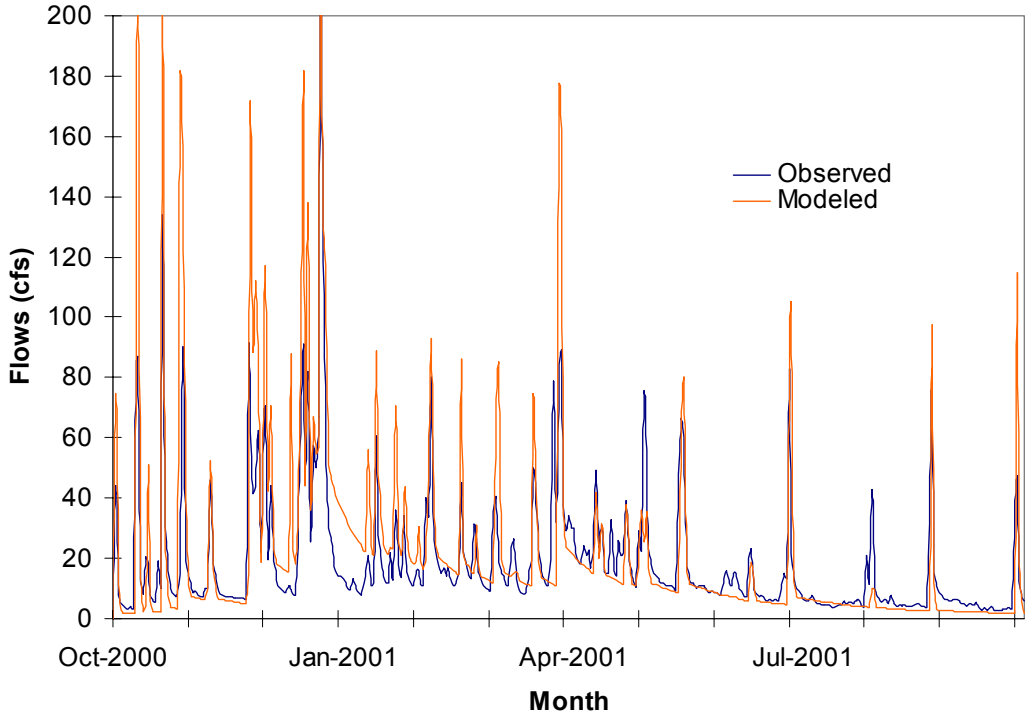


**Figure 4** - Observed (USGS gage 14206950) and BASINS validated flows at Fanno Creek.

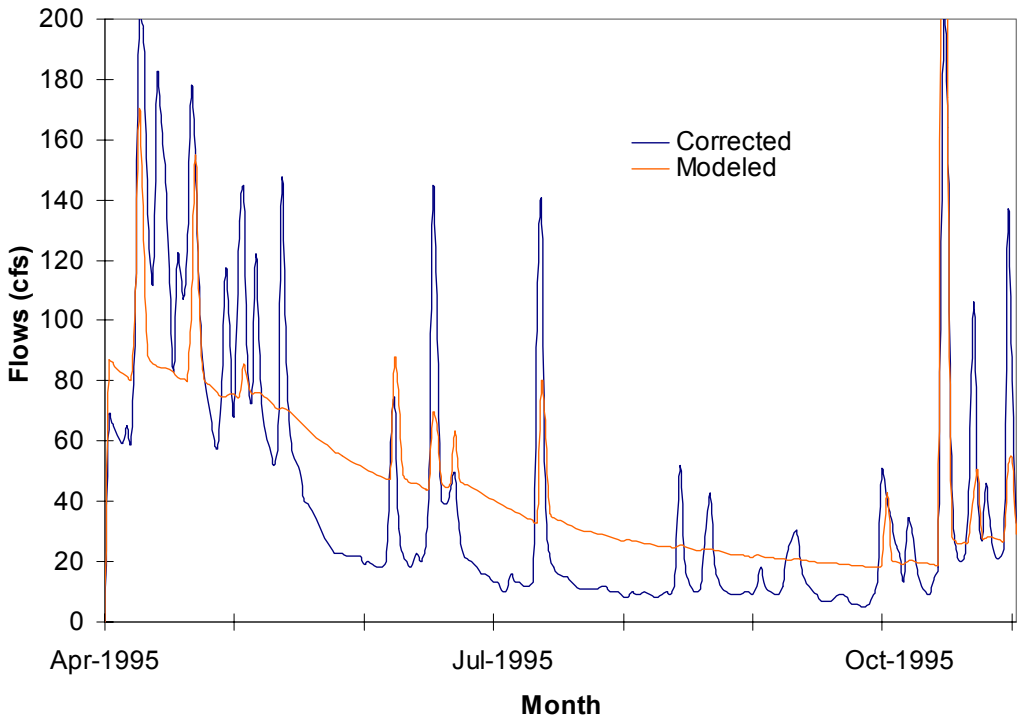


**Figure 5** - Observed (Watermaster gage 14206450) and BASINS calibrated flows at Rock Creek. A correction factor was added to measured summer flow levels to account for upstream diversions.

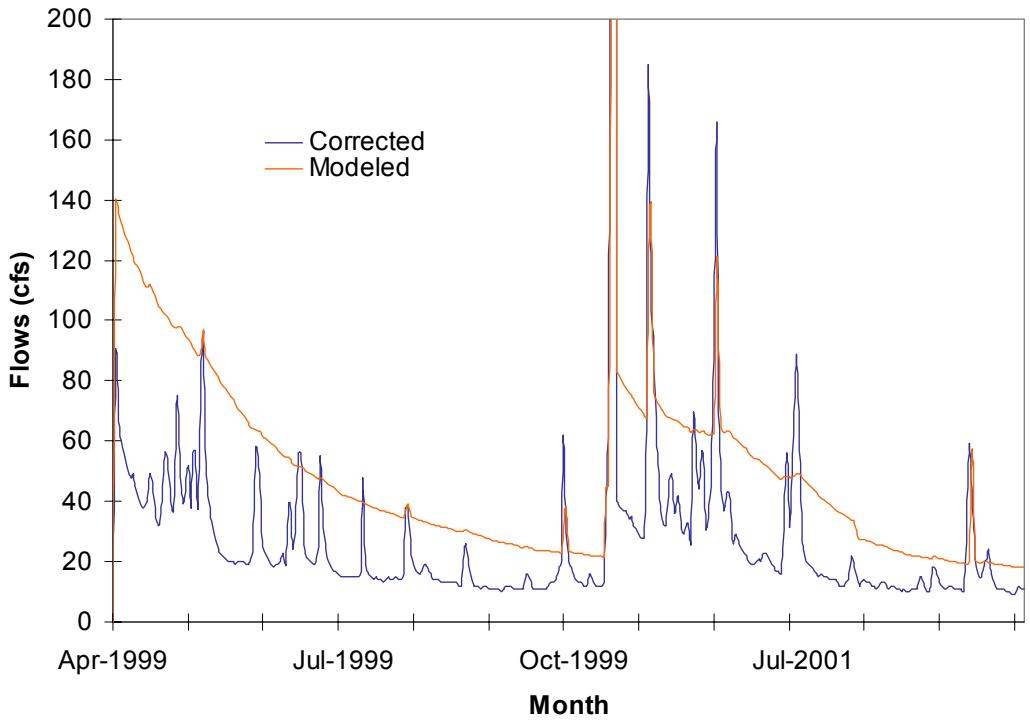


**Figure 6** - Observed (Watermaster gage 14206450) and BASINS validated flows at Rock Creek. A correction factor was added to measured summer flow levels to account for upstream diversions.

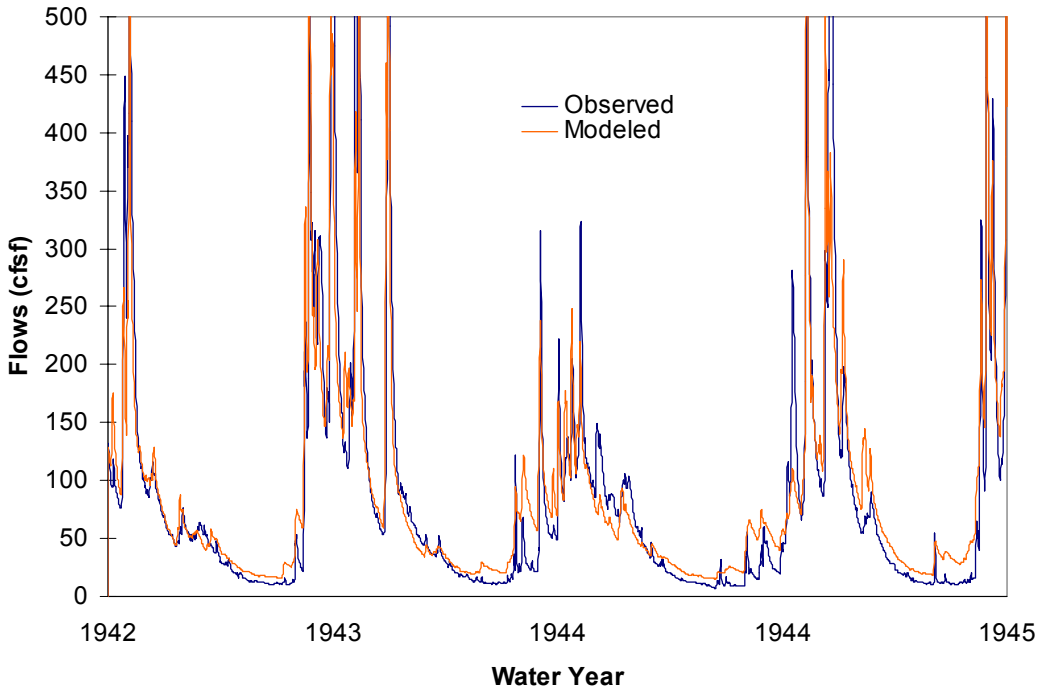


**Figure 7** - Observed (USGS gage 14205500) and BASINS calibrated flows at Dairy Creek.

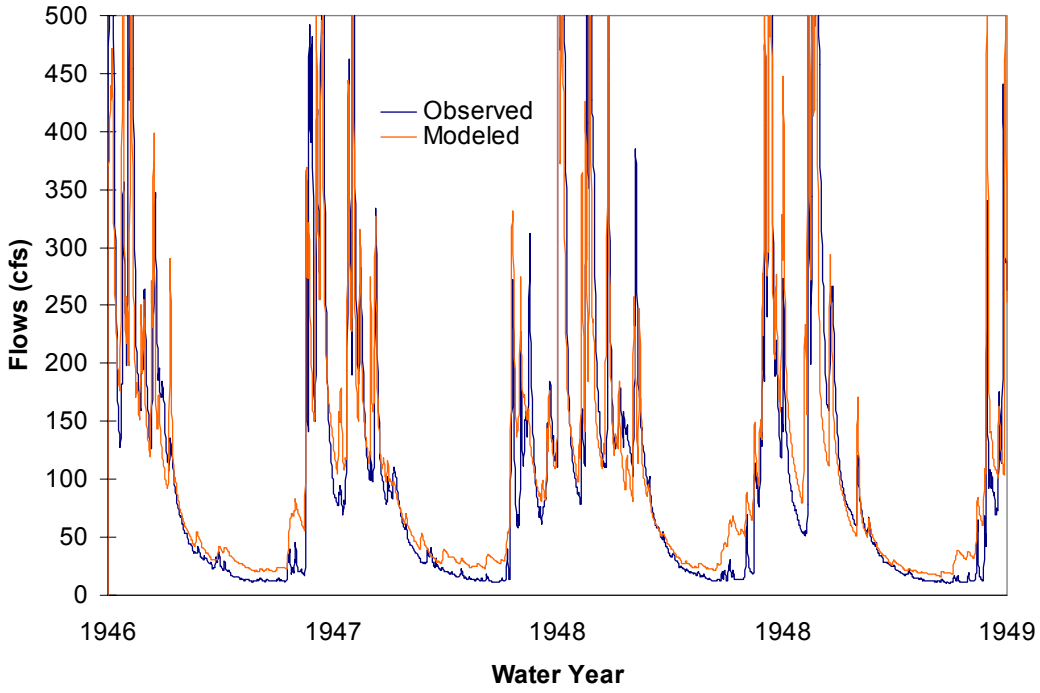


**Figure 8** - Observed (USGS gage 14205500) and BASINS validated flows at Dairy Creek.

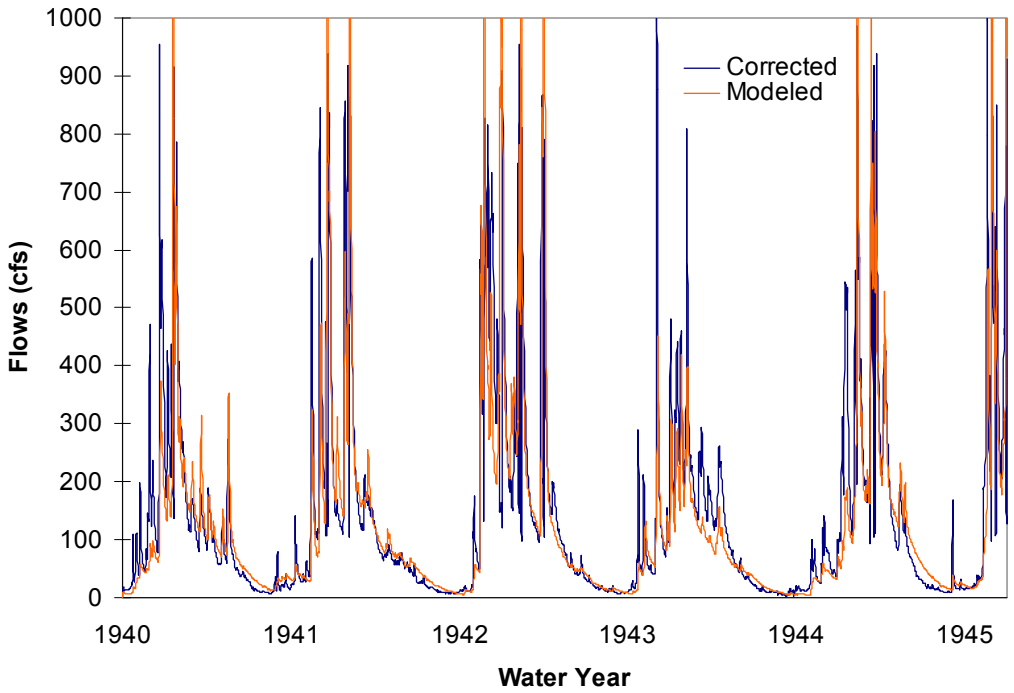


**Figure 9** - Observed (USGS gage 14204500) and BASINS calibrated flows at Gales Creek. A correction factor was added to measured summer flow levels to account for upstream diversions.

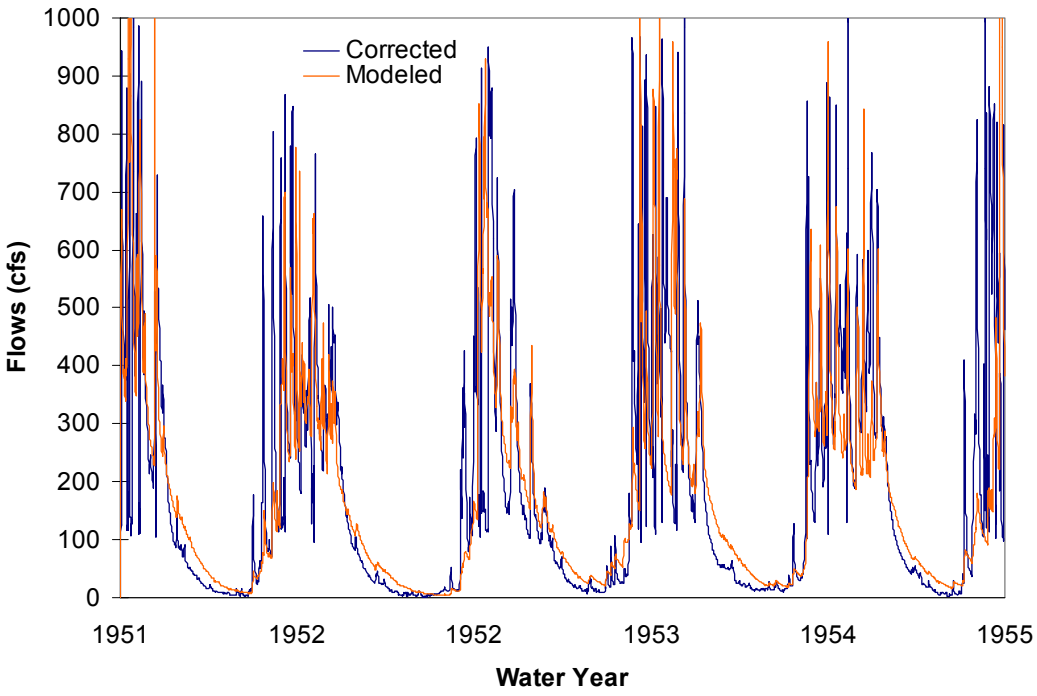


**Figure 10** - Observed (USGS gage 14204500) and BASINS validated flows at Gales Creek. A correction factor was added to measured summer flow levels to account for upstream diversions.

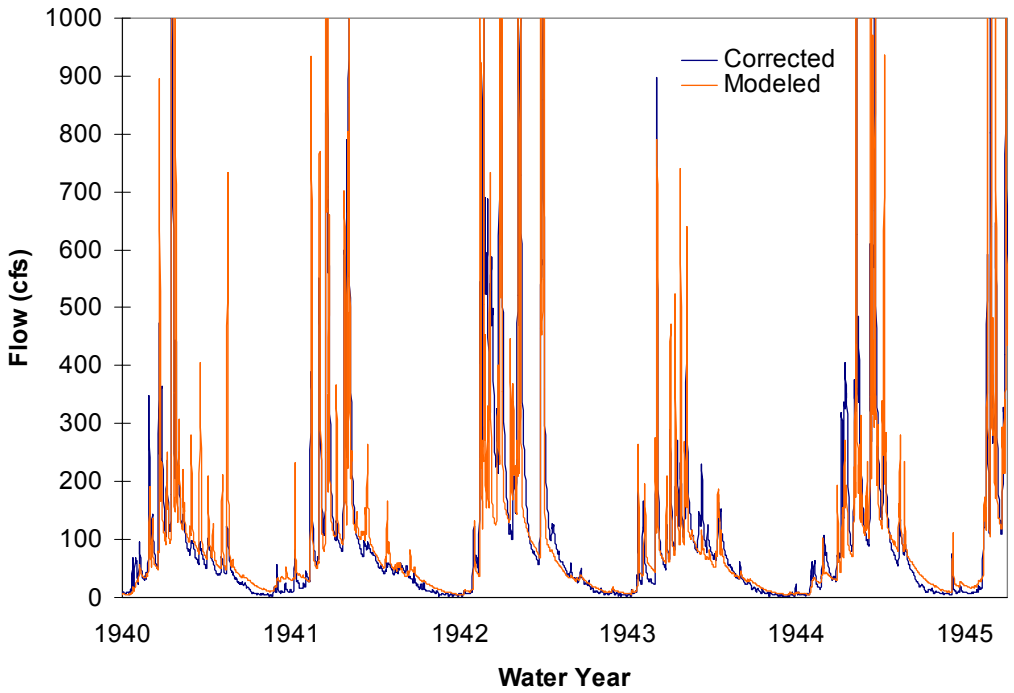


**Figure 11** - Observed (BOR gage SCOO) and BASINS calibrated flows at Scoggins Creek.

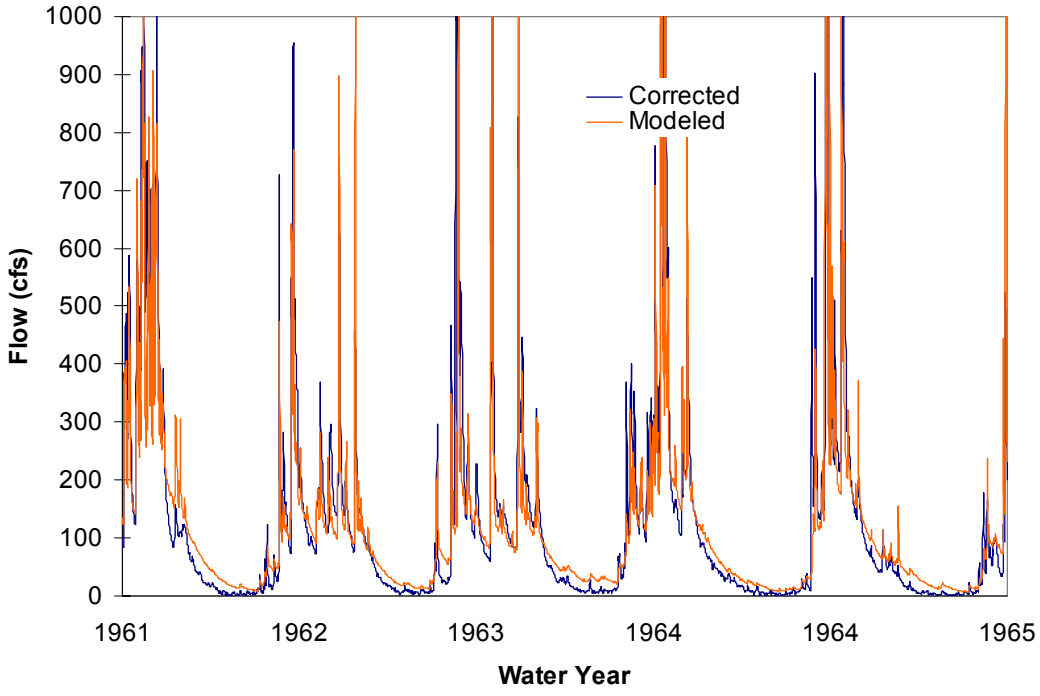


**Figure 12** - Observed (BOR gage SCOO) and BASINS validated flows at Scoggins Creek.

# Appendix C

**Current Storage**

| | 98% Reliable Yield (acre-feet) | | | 97% Reliable Yield (acre-feet) | | |
|---|---|---|---|---|---|---|
| **Demand Scenario** | **Current** | **Contracted** | **2050** | **Current** | **Contracted** | **2050** |
| **Climate Period** | | | | | | |
| 2000 | 36,857 | 36,875 | 19,657 | 37,999 | 37,685 | 35,054 |
| 2020 | 35,428 | 35,659 | 13,760 | 35,999 | 35,659 | 28,502 |
| 2040 | 34,285 | 34,444 | 11,139 | 35,142 | 34,849 | 25,226 |
| 2060 | 33,999 | 34,038 | 9,828 | 34,285 | 34,038 | 24,571 |

| | 95% Reliable Yield (acre-feet) | | | 90% Reliable Yield (acre-feet) | | |
|---|---|---|---|---|---|---|
| **Demand Scenario** | **Current** | **Contracted** | **2050** | **Current** | **Contracted** | **2050** |
| **Climate Period** | | | | | | |
| 2000 | 44,856 | 44,574 | 35,316 | 47,971 | 47,938 | 49,797 |
| 2020 | 43,428 | 42,953 | 32,040 | 46,542 | 46,722 | 48,486 |
| 2040 | 42,571 | 42,143 | 28,764 | 43,399 | 43,480 | 45,800 |
| 2060 | 41,542 | 40,927 | 23,522 | 42,828 | 43,075 | 43,245 |

**20 ft Expansion**

| | 98% Reliable Yield (acre-feet) | | | 97% Reliable Yield (acre-feet) | | |
|---|---|---|---|---|---|---|
| **Demand Scenario** | **Current** | **Contracted** | **2050** | **Current** | **Contracted** | **2050** |
| **Climate Period** | | | | | | |
| 2000 | 58,856 | 58,757 | 58,970 | 59,428 | 59,162 | 59,625 |
| 2020 | 57,428 | 57,946 | 58,315 | 57,428 | 57,298 | 57,790 |
| 2040 | 56,571 | 56,731 | 57,004 | 55,713 | 55,515 | 56,349 |
| 2060 | 54,285 | 51,868 | 55,694 | 54,856 | 54,705 | 54,383 |

| | 95% Reliable Yield (acre-feet) | | | 90% Reliable Yield (acre-feet) | | |
|---|---|---|---|---|---|---|
| **Demand Scenario** | **Current** | **Contracted** | **2050** | **Current** | **Contracted** | **2050** |
| **Climate Period** | | | | | | |
| 2000 | 60,571 | 60,378 | 61,591 | 68,285 | 68,482 | 70,109 |
| 2020 | 58,513 | 58,311 | 59,035 | 64,770 | 65,159 | 67,488 |
| 2040 | 57,142 | 56,731 | 58,118 | 64,828 | 65,038 | 67,291 |
| 2060 | 56,571 | 56,326 | 56,808 | 65,628 | 66,010 | 68,339 |

**40 ft Expansion**

| | 98% Reliable Yield (acre-feet) | | | 97% Reliable Yield (acre-feet) | | |
|---|---|---|---|---|---|---|
| **Demand Scenario** | **Current** | **Contracted** | **2050** | **Current** | **Contracted** | **2050** |
| **Climate Period** | | | | | | |
| 2000 | 73,256 | 72,940 | 73,647 | 73,342 | 73,345 | 73,974 |
| 2020 | 69,828 | 69,698 | 70,305 | 70,770 | 71,076 | 72,009 |
| 2040 | 69,542 | 69,698 | 70,305 | 70,628 | 70,792 | 71,222 |
| 2060 | 71,085 | 71,035 | 71,616 | 70,970 | 71,116 | 72,533 |

| | 95% Reliable Yield (acre-feet) | | | 90% Reliable Yield (acre-feet) | | |
|---|---|---|---|---|---|---|
| **Demand Scenario** | **Current** | **Contracted** | **2050** | **Current** | **Contracted** | **2050** |
| **Climate Period** | | | | | | |
| 2000 | 74,570 | 74,763 | 75,186 | 76,227 | 76,181 | 76,661 |
| 2020 | 71,428 | 71,400 | 71,779 | 73,170 | 73,142 | 73,778 |
| 2040 | 71,085 | 71,076 | 71,517 | 72,685 | 72,656 | 73,319 |
| 2060 | 72,570 | 72,453 | 72,959 | 73,856 | 73,547 | 73,974 |

**Current Storage + Sain Creek Tunnel Scenario**

| | 98% Reliable Yield (acre-feet) | | | 97% Reliable Yield (acre-feet) | | |
|---|---|---|---|---|---|---|
| **Demand Scenario** | **Current** | **Contracted** | **2050** | **Current** | **Contracted** | **2050** |
| **Climate Period** | | | | | | |
| 2000 | 31,428 | | | 36,857 | | |
| 2020 | 30,571 | | | 36,285 | | |
| 2040 | 30,857 | | | 36,571 | | |
| 2060 | 30,571 | | | 36,571 | | |

| | 95% Reliable Yield (acre-feet) | | | 90% Reliable Yield (acre-feet) | | |
|---|---|---|---|---|---|---|
| **Demand Scenario** | **Current** | **Contracted** | **2050** | **Current** | **Contracted** | **2050** |
| **Climate Period** | | | | | | |
| 2000 | 37,142 | | | 45,142 | | |
| 2020 | 35,999 | | | 43,999 | | |
| 2040 | 34,571 | | | 43,428 | | |
| 2060 | 34,571 | | | 38,857 | | |

**20 ft Storage Expansion + Sain Creek Tunnel Scenario**

| | 98% Reliable Yield (acre-feet) | | | 97% Reliable Yield (acre-feet) | | |
|---|---|---|---|---|---|---|
| **Demand Scenario** | **Current** | **Contracted** | **2050** | **Current** | **Contracted** | **2050** |
| **Climate Period** | | | | | | |
| 2000 | 58,571 | | | 58,856 | | |
| 2020 | 57,428 | | | 56,571 | | |
| 2040 | 56,571 | | | 55,142 | | |
| 2060 | 53,142 | | | 54,285 | | |

| | 95% Reliable Yield (acre-feet) | | | 90% Reliable Yield (acre-feet) | | |
|---|---|---|---|---|---|---|
| **Demand Scenario** | **Current** | **Contracted** | **2050** | **Current** | **Contracted** | **2050** |
| **Climate Period** | | | | | | |
| 2000 | 59,428 | | | 67,713 | | |
| 2020 | 57,142 | | | 64,370 | | |
| 2040 | 55,999 | | | 64,228 | | |
| 2060 | 55,428 | | | 65,028 | | |

**40 ft Storage Expansion + Sain Creek Tunnel Scenario**

| | 98% Reliable Yield (acre-feet) | | | 97% Reliable Yield (acre-feet) | | |
|---|---|---|---|---|---|---|
| **Demand Scenario** | **Current** | **Contracted** | **2050** | **Current** | **Contracted** | **2050** |
| **Climate Period** | | | | | | |
| 2000 | 72,285 | | | 73,142 | | |
| 2020 | 68,913 | | | 70,570 | | |
| 2040 | 68,856 | | | 70,370 | | |
| 2060 | 70,085 | | | 70,770 | | |

| | 95% Reliable Yield (acre-feet) | | | 90% Reliable Yield (acre-feet) | | |
|---|---|---|---|---|---|---|
| **Demand Scenario** | **Current** | **Contracted** | **2050** | **Current** | **Contracted** | **2050** |
| **Climate Period** | | | | | | |
| 2000 | 74,570 | | | 75,999 | | |
| 2020 | 71,428 | | | 72,942 | | |
| 2040 | 71,085 | | | 72,456 | | |
| 2060 | 72,285 | | | 73,627 | | |